

# “Clustering and Conquer” Procedures for Parallel Large-Scale Ranking and Selection

Zishi Zhang

Guanghua School of Management, Peking University, Beijing, China, zishizhang@stu.pku.edu.cn

Yijie Peng

Guanghua School of Management, Peking University, Beijing, China, pengyijie@gsm.pku.edu.cn

This work breaks the sample efficiency bottleneck in parallel large-scale ranking and selection (R&S) problem by leveraging correlation information. We modify the commonly used “divide and conquer” framework in parallel computing by adding a correlation-based clustering step, transforming it into “clustering and conquer”. This seemingly simple modification can achieve an  $\mathcal{O}(p)$  sample complexity reduction rate, which represents the maximum attainable reduction for the class of sample-optimal R&S methods. Our approach enjoys two key advantages: 1) it does not require highly accurate correlation estimation or precise clustering, and 2) it allows for seamless integration with various existing R&S method, while achieving optimal sample complexity. Theoretically, we develop a novel gradient analysis framework to analyze sample efficiency and guide the design of large-scale R&S procedures. Building upon this framework, we propose a gradient-based budget allocation policy. We also introduce a new clustering algorithm, selection policy, and precision criterion tailored for large-scale scenarios. Finally, in large-scale AI applications such as neural architecture search, our methods demonstrate superior performance.

*Key words:* simulation, ranking and selection, parallel computing

---

## 1. Introduction

Ranking and selection (R&S) aims to identify the best design from a finite set of alternatives, through conducting simulation and learning about their performances (Bechhofer 1954). It is typically framed into two main formulations: fixed-precision and fixed-budget. Fixed-precision R&S methods terminate the simulation once a pre-specified level of precision is achieved. Notable examples include the stage-wise method of Rinott (1978) and the KN family (Kim and Nelson 2001, Hong and Nelson 2005, Jeff Hong 2006), among others. In contrast, fixed-budget R&S methods stop the simulation once a predetermined total simulation budget is exhausted, with the goal of optimizing precision. This category includes methods such as OCBA (Chen et al. 2000, Fu et al. 2007), large-deviation-based approaches (Glynn and Juneja 2004), and methods proposed by Chick and Inoue (2001) and Frazier et al. (2008). For a more comprehensive review of the R&S literature, please refer to Chen et al. (2015) and Hong et al. (2021).

In recent years, R&S methods have found significant applications in AI-related problems, such as Reinforcement Learning (Li et al. 2023, Zhu et al. 2024) and Monte Carlo Tree Search (Li et al. 2021, Liu et al. 2024), as well as in other large-scale industrial problems (Xu et al. 2016, Chen et al. 2023). This growing body of work has led to a shift in research focus toward large-scale R&S problem, especially in parallel computing environments (Hunter and Nelson 2017). Here, “large-scale” refers to a large number of alternatives, denoted by  $p$ . The literature on large-scale R&S can generally be divided into two branches. One branch focuses on addressing the challenges related to parallel computing implementation, such as information communication, synchronization, and workload balancing. Notable works in this branch include Luo et al. (2015) and Ni et al. (2017). The other branch focuses on improving sample efficiency. Recent efforts in this branch primarily aim to modify the inefficient all-pairwise comparison paradigm of classic fully-sequential R&S methods such as the KN family. For example, Zhong and Hong (2022) introduce a Knockout Tournament (KT) paradigm (and its fixed-budget version, FBKT (Hong et al. 2022)), which restricts comparisons to “matches” involving only two alternatives at a time. The PASS paradigm of Pei et al. (2022) compares each alternative against a common standard to avoid exhaustive pairwise comparisons.

However, existing R&S methods typically assume independence among alternatives and discard the valuable structural information (Eckman and Henderson 2022). As a result, current large-scale R&S methods appear to have reached a bottleneck in terms of sample efficiency, leaving limited room for further improvement through the design of new comparison paradigms under independence (for instance, the KT paradigm has been proven to achieve the lowest rate of sample complexity (Zhong and Hong 2022, Hong et al. 2022)). Notably, in real-world large-scale R&S problems, a large number of alternatives are often systematically generated through decision combinations or the discretization of continuous decision spaces, which results in abundant internal information that can be exploited. Consider the following motivational example from the AI field.

***Neural Architecture Search (NAS):** a key challenge in deep learning, aims to identify the best-performing neural network architecture design for a specific task, given that evaluating a neural architecture on a test dataset is computationally expensive. The number of alternatives is exponentially large, as the search space includes combinations of multiple decisions, such as the number of layers, types of activation functions, and types of operations. Consequently, many of these alternatives share common structural components, and state-of-the-art algorithms (Guo et al. 2020, Mellor et al. 2021) typically leverage this shared information using techniques such as weight sharing and clustering.*

Inspired by this practical example, leveraging shared information among alternatives is a promising avenue for pushing the boundaries of sample efficiency, yet this remains a gap in the large-scale R&S literature. Existing efforts in utilizing shared information can be broadly categorized into

two streams. The first involves using additional contextual or covariate information (L. Salemi et al. 2019, Shen et al. 2021, Du et al. 2024). However, this approach relies on specific problem structures and is not applicable for general-purpose use. The second stream focuses on exploiting correlation and other similarity information (Fu et al. 2007, Frazier et al. 2009, Qu et al. 2015, Zhou et al. 2023). However, none of these methods is fully suitable for large-scale problems, as they typically require precise estimation of correlation parameters. Furthermore, despite showing promising experimental results, these methods lack rigorous mathematical analysis to elucidate and quantify the benefits derived from integrating similarity information, and they do not provide theoretical guarantees of their performance in large-scale settings.

Before introducing our method, we first provide some necessary background: most prominent parallel R&S methods adopt the *divide and conquer* framework (Ni et al. 2017, Zhong and Hong 2022), where alternatives are randomly distributed across processors, then the local best is selected from each processor, and the global best is selected from these local bests. This framework is widely adopted, not only in parallel R&S but also in various other parallel computing problems. In our work, we extend the traditional *divide and conquer* framework by adding a correlation-based clustering step. This modified approach, termed the *Parallel Correlation Clustering and Conquer* (P3C) procedure, clusters alternatives based on their correlation and assigns alternatives from the same cluster to a single processor, rather than distributing them randomly. Both theoretical and empirical evidence show that this simple modification significantly improves sample efficiency. Moreover, P3C enjoys the advantage of not requiring precise estimation of the correlation parameter, as it is sufficient to merely identify which alternatives are highly correlated. Additionally, P3C is a ready-to-use tool that can be directly integrated with any existing fixed-precision or fixed-budget R&S methods.

The intuition behind P3C is that, *clustering highly correlated alternatives together can effectively cancel out stochastic fluctuations in the same direction*. To be more specific, the reason why R&S requires a large number of samples is due to the random simulation outputs, which occasionally leads to undesirable situations where “good” alternatives may unexpectedly perform worse than “bad” ones. If highly correlated alternatives are grouped together for comparison, their fluctuations tend to align in the same direction to some extent. When a “good” alternative occasionally performs poorly, the “bad” alternatives are likely to show similar declines; conversely, when a “bad” alternative performs better than expected, the “good” alternatives tend to exceed expectations as well. This way, the true ranking is preserved, enabling us to identify the true best alternative with fewer simulations. This concept is similar to the common random number (CRN) technique in the simulation literature (L’Ecuyer 1990, Glasserman and Yao 1992, Nelson and Matejckik 1995, Chen

et al. 2012), which introduces positive correlation artificially to reduce variance and expedite pairwise comparisons. However, it is important to note that our theoretical analysis is fundamentally different from CRN, as we focus on the global impact of correlation information: for instance, one interesting conclusion from our analysis is that increasing the correlation between a pair of alternatives can increase the probability of selecting other “good” alternatives that are *not* directly related to this pair. Moreover, this work studies a general case, where correlations between the simulation outputs of alternatives may arise from a variety of sources, not necessarily from the intentionally introduced CRN. For instance, correlations may result from spatial dependencies (Chen et al. 2012, Ding and Zhang 2024), inherent similarities (Qu et al. 2015, Frazier et al. 2009), or from common latent factors (see the drug discovery example in the experiment section of this paper). Finally, it is worth mentioning that this work is not the first to apply clustering techniques in R&S. A related study by Li et al. (2022) uses Gaussian Mixture Models (GMM), a clustering algorithm based on mean performance, to extract shared information in *non*-parallel settings. However, in parallel R&S, clustering alternatives with similar mean performance on the same processor can be detrimental due to the increased challenge of differentiating them. This work does not assume any additional covariate or contextual structure in the output distribution, meaning that highly correlated alternatives do not necessarily share similar means.

To formalize the intuition of P3C, we develop a novel gradient analysis framework. In the literature, the probability of correct selection (PCS) is commonly used as a measure of the precision of R&S methods. It is defined as the probability that the sample average of the “true best” alternative is higher than that of the others. We generalize the classical PCS by replacing the “true best” with any alternative  $\tau$ , termed as the individual PCS( $\tau$ ), which serves as a probabilistic criterion for assessing the performance of alternative  $\tau$ . We then analyze the derivative of individual PCS with respect to correlation information to explore the novel “**mean-covariance**” interaction, as opposed to the widely discussed “mean-variance” tradeoff. The analysis shows that, increasing correlation between alternatives induces an interesting “separation” effect, which probabilistically amplifies good alternatives while suppressing the bad ones. These theoretical insights explain why P3C can enhance sample efficiency thorough correlation-based clustering. Furthermore, by performing gradient analysis with respect to the sample size, we quantify the reduction in sample complexity that correlation-based clustering can bring in parallel computing environments. The gradient analysis established in this paper provides a fundamental framework for studying the sample efficiency and guiding the design of large-scale R&S procedures. Similarly, a related work by Peng et al. (2017) also explores gradient analysis in R&S, but it investigates the impact of “induced correlation”, which is induced by variance under the independent assumption, rather than the actual correlation

existing between alternatives. Additionally, other works exploring gradient analysis in R&S include Peng et al. (2015), Zhang et al. (2023), and others.

In recent literature, analyzing the asymptotic behavior of the required total sample size as  $p \rightarrow \infty$  has become a critical approach for assessing the sample efficiency of large-scale R&S algorithms (Zhong and Hong 2022, Hong et al. 2022, Li et al. 2024). As  $p \rightarrow \infty$ , the theoretical lowest growth rate of the required total sample size to achieve non-zero precision asymptotically is  $\mathcal{O}(p)$ , and a R&S procedure that achieves this  $\mathcal{O}(p)$  sample complexity is referred to as *sample-optimal*. To our best knowledge, known sample-optimal R&S methods in the literature include the median elimination (ME) procedure (Even-Dar et al. 2006), the KT procedure and its fixed-budget version FBKT, as well as the simple greedy procedure in Li et al. (2024). As  $p$  grows large, the proposed P3C performs multiple rounds of “clustering and conquer”, which closely resembles the knockout tournament scheme in Zhong and Hong (2022) and Hong et al. (2022). Similarly, we prove that by appropriately setting the size of clusters, P3C combined with commonly used fixed-precision or fixed-budget R&S methods, can also achieve sample optimality. This significantly expands the spectrum of sample-optimal R&S methods. Moreover, the reduction in sample complexity achieved by P3C is  $\mathcal{O}(p)$ , which represents the maximum reduction rate attainable for the class of sample-optimal R&S methods. This implies that, although sample-optimal R&S methods already achieve the lowest  $\mathcal{O}(p)$  growth rate in complexity, P3C can further reduce the slope, thereby breaking the bottleneck.

A consensus in large-scale R&S literature is that there may exist a large number of acceptably *good* alternatives with means lying within a  $\delta$  range around the best one (Ni et al. 2017, Pei et al. 2022). In such “low-confidence scenarios” (Peng et al. 2016, 2017) characterized by similar means and finite sample sizes, the traditional PCS becomes very low, rendering it practically meaningless. However, we observe an interesting phenomenon: for some alternatives  $\tau$ , the individual PCS can be much higher than the traditional PCS by even several orders of magnitude. This indicates that some alternatives have a much higher probability of being the best than the one with maximum mean. From a gradient analysis perspective, we find that this is due to the influence of correlation information, which becomes a critical factor in determining PCS in low-confidence scenarios. Therefore, we propose a new selection policy, which selects the alternative that maximizes the individual PCS, termed *probabilistic optimal selection* (PrOS), instead of simply choosing the largest sample mean. Similar probability-based selection policies are often adopted in the Bayesian framework (Peng et al. 2016, Russo 2020, Kim et al. 2022), and the integration of similarity information into selection policies is explored in Zhou et al. (2023). Correspondingly, the individual PCS of the PrOS is termed moPCS (the most optimistic probability of correct selection), which becomes a

new precision criterion suitable for large-scale R&S. Additionally, we propose a new gradient-based simulation budget allocation (GBA) policy, tailored for moPCS.

Similar to moPCS, in order to address the limitations of traditional PCS in large-scale settings, works such as Ni et al. (2017) and Zhong and Hong (2022) also adopt a relaxed criterion known as the probability of good selection (PGS). PGS is defined as the probability that an alternative, whose performance lies within a  $\delta$  range of the true best, is selected. In addition to PGS, other commonly used precision criteria include the Expected Opportunity Cost (EOC) (Gao et al. 2017, Chick and Wu 2005), and the Expected Value of Information (EVI) (Chick et al. 2010). A review of these criteria can be found in (Branke et al. 2007) and (Eckman and Henderson 2022).

The main contributions of this paper can be summarized as follows.

- We propose the sample-optimal P3C procedure for large-scale R&S problems, which expands the class of sample-optimal R&S methods.
- We develop a novel gradient analysis framework for studying sample efficiency and guiding the design of large-scale R&S procedures. This framework uncovers the “mean-covariance” interaction in R&S and shows that correlation-based clustering in P3C can achieve rate-optimal reductions in sample complexity.
- We introduce a new selection policy, PrOS, and a new precision criterion, moPCS, for large-scale R&S. Correspondingly, we propose a GBA sampling policy tailored to this new criterion.
- We propose a parallelizable few-shot alternative clustering algorithm, denoted as  $\mathcal{AC}^+$ , which effectively addresses the challenges of large-scale clustering. Additionally, we introduce the *probability of correct clustering* (PCC) as a metric to quantify the quality of the clustering.

## 2. Problem Formulation

Let  $\mathcal{P} = \{1, 2, \dots, p\}$  denote the index set for all  $p$  alternatives. We adopt a Frequentist framework, and the output of alternative  $i \in \mathcal{P}$  is a random variable  $X_i$ . We assume that the population distribution of the random vector  $(X_1, X_2, \dots, X_p)$  is multivariate normal  $N(\boldsymbol{\mu}, \Sigma_{p \times p})$ , where  $\boldsymbol{\mu} = (\mu_1, \dots, \mu_p)$  is the mean vector and  $\Sigma_{p \times p}$  is the covariance matrix. Let  $x_{ij}$  denote the  $j$ th simulation observation of alternative  $i$ . The observation vectors  $(x_{1j}, x_{2j}, \dots, x_{pj}) \sim N(\boldsymbol{\mu}, \Sigma_{p \times p})$  are independently and identically distributed. We assume

$$\text{cov}(x_{im}, x_{jn}) = \begin{cases} 0 & m \neq n \\ \text{cov}(X_i, X_j) & m = n \end{cases},$$

where  $\text{cov}(X, Y)$  represents the covariance between random variables  $X$  and  $Y$ . Let  $N_i$  denote the individual sample size allocated to alternative  $i$  and  $\bar{x}_i$  be the sample average, then  $\text{cov}(\bar{x}_i, \bar{x}_j) = \frac{\text{cov}(X_i, X_j)}{N_{i,j}}$ , where  $N_{i,j} \triangleq \max(N_i, N_j)$ . Let  $[m]$  denote the index of the alternative with  $m$ -largest

mean, i.e.  $\mu_{[1]} > \mu_{[2]} > \dots > \mu_{[p]}$ . The objective of R&S is to identify the true best alternative  $[1] = \arg \max_{i \in \mathcal{P}} \mu_i$ , under either a fixed budget constraint or a fixed precision constraint (with the definition of precision detailed in Section 3.2).

Suppose the  $p$  alternatives come from  $k$  non-overlapping clusters based on correlation:  $\mathcal{G}_1, \dots, \mathcal{G}_k$ , with cardinality  $|\mathcal{G}_j| = p_j$  ( $\sum_{j=1}^k p_j = p$ ).  $G$  is a mapping from  $\mathcal{P}$  to  $\{1, 2, \dots, k\}$ , where  $G(i) = j$  if alternative  $i$  belongs to  $\mathcal{G}_j$ .  $\Pi = (G(1), G(2), \dots, G(p)) \in \mathbb{R}^p$  represents the true cluster partition (unknown) of  $p$  alternatives and we need sampling to recover it. Alternatives within the same cluster are highly correlated, whereas alternatives from different clusters are less correlated. Let  $r_{ij}$  denote the Pearson correlation coefficient between  $X_i$  and  $X_j$ . We assume that the correlation coefficient between any two alternatives belonging to the same cluster exceeds that between any two alternatives from different clusters. The independent case is also included by setting  $p = k$ .

ASSUMPTION 1.  $r_{ij} > r_{mn}$  for all  $i, j, m, n \in \mathcal{P}$  such that  $G(i) = G(j)$  and  $G(m) \neq G(n)$ , and  $0 < r_{ij} < 1$ .

The clustering algorithms adopted in this paper satisfy this assumption. It is important to note that, this work does not assume any additional structure in the performance of alternatives, such as a covariate or contextual structure. As a result, the correlations between alternatives are independent of their means, meaning that highly correlated alternatives do not necessarily have similar means.

Recently, analyzing the asymptotic behavior as  $p \rightarrow \infty$  has emerged as a critical approach for assessing the theoretical performance of large-scale R&S algorithms (Zhong and Hong 2022, Hong et al. 2022, Li et al. 2024). As  $p \rightarrow \infty$ , the theoretical lowest growth rate of the required total sample size to deliver a non-zero precision asymptotically is  $\mathcal{O}(p)$ . A R&S procedure that achieves this  $\mathcal{O}(p)$  sample complexity is referred to as *sample-optimal* in this paper. When examining the asymptotic behavior as  $p \rightarrow \infty$ , we assume the same regime as Li et al. (2024): the index of the true best  $[1]$  remains unchanged, and the difference between  $[1]$  and  $[2]$  remains above a positive constant and the covariance between any two alternatives is upper bounded by a constant.

### 3. The Framework of P3C

#### 3.1. From “Divide and Conquer” to “Clustering and Conquer”

“Divide and conquer” has long served as the foundational framework for many mainstream parallel R&S methods (Ni et al. 2017, Zhong and Hong 2022). In this approach, alternatives are distributed across different processors, where each processor selects its local best alternative, and the global best is selected from these local bests. We extend this framework by introducing a “clustering and conquer” strategy, formally termed Parallel Correlation Clustering and Conquer (P3C). The key distinction in P3C is an additional step of correlation-based clustering, which assigns alternatives from the same cluster to a single processor, as opposed to random assignment. This simple modification leads to a significant improvement in sample efficiency.

Specifically, as outlined in Procedure 1 and Figure 1, P3C starts with an initialization Stage 0. Then, in Stage 1, we continue sampling and then cluster alternatives based on estimated correlations. The sample size can be determined in advance based on the required clustering accuracy. Additionally, the novel few-shot clustering algorithm  $\mathcal{AC}^+$ , detailed in Section 6, enables the effective parallelization of both Stage 0 and Stage 1 in large-scale problems. Upon completion of Stage 1, the alternatives of the same cluster are sent to a single processor. During Stage 2, we perform R&S to select the *local best* within each cluster. Here, the choice of R&S method is flexible and depends on the specific problem formulation and selection policies. For example, the KT or KN family (Kim and Nelson 2001, Hong and Nelson 2005, Jeff Hong 2006) can be applied in the fixed-precision P3C. Additionally, for the fixed-budget formulation, we propose a new gradient-based allocation strategy, GBA (see Section 5). In Stage 3, we continue R&S within these remaining *local bests* to select the final winner. Note that this paper focuses on analyzing the sample efficiency of the P3C, while many challenges in parallel implementation, such as master-worker task coordination, synchronization, and workload balancing, are beyond our scope. For comprehensive solutions to these issues, readers are encouraged to refer to the prior works of Luo et al. (2015) and Ni et al. (2017).

Next, we consider the asymptotic behavior of P3C as  $p \rightarrow \infty$ . When  $p$  is large, the number of remaining *local bests* after Stage 2 may still be substantial. In such cases, the original P3C requires some modification. Specifically, P3C employs repeated rounds of “clustering and conquer” (i.e., Stages 1 and 2) until the number of remaining alternatives becomes manageable for a single processor (in practice, the maximum number of alternatives  $p_m \geq 2$  that can be handled by a single processor is specified). This multi-round structure closely resembles the knockout tournament paradigm of Zhong and Hong (2022) and Hong et al. (2022), and consequently, it can be expected that P3C achieves sample optimality as well. **In fixed-precision R&S**, let the final desired precision be  $1 - \alpha$ , where  $\alpha$  is the desired false elimination probability (FEP). The FEP  $\alpha_2^r$  for each processor in the  $r$ -th round of “clustering and conquer”, and the FEP  $\alpha_3$  of the Stage 3 in P3C must satisfy  $\sum_r \alpha_2^r + \alpha_3 = \alpha$ . We set  $\alpha_2^r = \frac{\alpha - \alpha_3}{2^r}$ , as done in Zhong and Hong (2022). Our analysis shows that, as long as the number of alternatives within each cluster is upper bounded by a  $p_m < \infty$ , P3C combined with KT or KN family is sample-optimal (see Section 5). This finding expands the class of sample-optimal R&S methods. **In fixed-budget R&S**, P3C also adopts a multi-round structure when  $p \rightarrow \infty$ . We prove that fixed-budget P3C can also achieve sample optimality. The main body of this paper focuses on the fixed-precision setting, so we defer the detailed discussion of fixed-budget P3C to Appendix EC.5.

---

**Procedure 1** Parallel Correlation Clustering and Conquer (P3C)

---

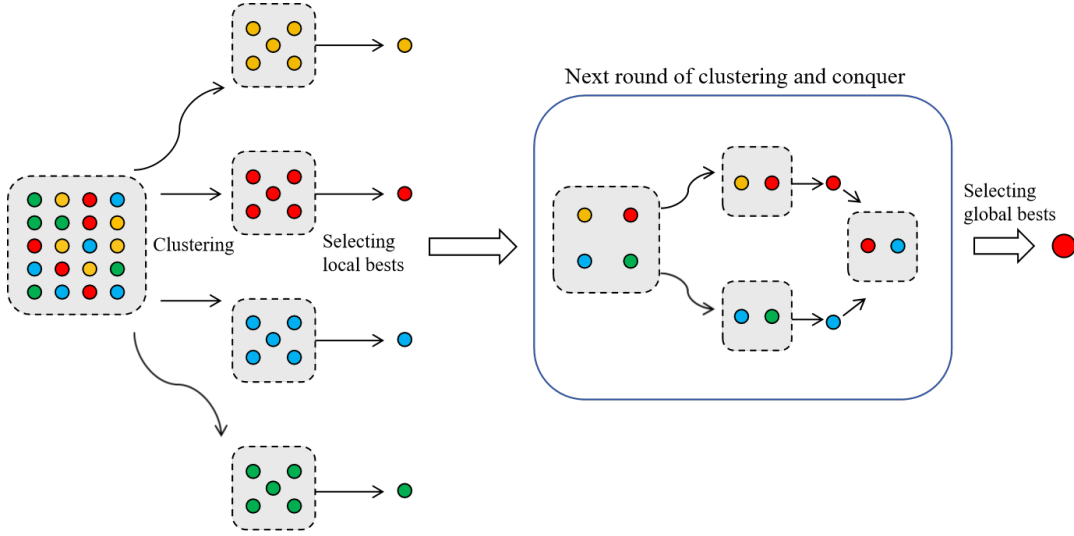


Figure 1 Parallel correlation clustering and conquer.

**Stage 0 (Initialization).** Simulate each alternative for  $n_0 \geq 3$  times and estimate  $\Sigma$ .

**Stage 1 (Clustering).** Continue sampling. Apply the correlation-based clustering algorithm  $\mathcal{AC}^+$  to partition all alternatives into several clusters. Subsequently, assign all alternatives within the same cluster to a single processor.

**Stage 2 (Conquer).** Perform R&S within each cluster to select the local best.

**Stage 3 (Final Comparison).** If the number of remaining alternatives in contention  $\leq p_m$ , perform R&S on the remaining alternatives to select the global optimal alternative. Otherwise, repeat Stage 1 and Stage 2 for the remaining alternatives.

### 3.2. Probabilistic Optimal Selection Policy

Another innovation of this paper is proposing a new selection policy, along with a new probability criterion for measuring the precision of R&S. In traditional R&S procedures, the selection policy is specified as  $\tau^m = \arg \max_{i \in \mathcal{P}} \bar{x}_i$ , and the corresponding probability guarantee is the traditional PCS, defined as  $\text{PCS}_{\text{trad}} \triangleq P(\bar{x}_{[1]} > \bar{x}_j, j \neq [1])$ . For any alternative  $\tau \in \mathcal{P}$ , we define the individual PCS of  $\tau$  as

$$\text{PCS}(\tau) \triangleq P(\bar{x}_\tau > \bar{x}_j, j \neq \tau).$$

This is a natural generalization of traditional PCS as  $\text{PCS}_{\text{trad}} = \text{PCS}([1])$ . According to Hong et al. (2021), the statistical meaning of  $\text{PCS}(\tau)$  is the probability of rejecting the null hypothesis that “ $\tau$  is *not* the true best”, making it a metric to evaluate the performance of  $\tau$ . Then we define the PrOS (Probabilistic Optimal Selection) as the alternative maximizing  $\text{PCS}(\tau)$ :

$$\tau^* \triangleq \arg \max_{\tau \in \mathcal{P}} \text{PCS}(\tau).$$

In practice,  $\text{PCS}(\tau)$  and  $\tau^*$  are calculated by plugging in parameters estimated with samples collected so far. Naturally, the PrOS policy corresponds to a new criterion:  $\text{PCS}(\tau^*)$ , referred to as *the most optimistic probability of correct selection* (moPCS). The moPCS provides a relaxed probability guarantee, as  $\text{moPCS} \geq \text{PCS}_{\text{trad}}$ . In large-scale R&S, the means of many alternatives may become very close to the true best, known as the low-confidence scenario (Peng et al. 2016, 2017). In such cases,  $\text{PCS}_{\text{trad}}$  could become close to zero and meaningless. However, our large-scale experiments show that moPCS can be several tens of times higher than  $\text{PCS}_{\text{trad}}$ , reaching a desirable confidence level. This implies that, compared to the alternative  $\tau^m$  with the maximum sample mean,  $\tau^*$  has a much higher probability of being the best. This phenomenon is theoretically explained in Section 4.1.2, which may be attributed to the influence of correlation information. Finally, note that the theoretical analysis in this paper is built upon  $\text{PCS}(\tau)$ , which is more general and can encompass both  $\text{PCS}_{\text{trad}}$  (by letting  $\tau = [1]$ ) and moPCS (by letting  $\tau = \tau^*$ ).

#### 4. Theoretical Analysis: Understanding Mean-Correlation Interactions

In this section, we present a comprehensive analysis of P3C from a novel gradient analysis perspective. Viewing  $\text{PCS}(\tau; \boldsymbol{\mu}, \Sigma, \{N_i\}_{i \in \mathcal{P}})$  as a function of mean, covariance and the allocation of sample sizes, we analyze its derivatives to gain insights for designing large-scale R&S procedures. In Section 4.1, we show how mean and correlation interact to influence  $\text{PCS}(\tau)$ . Specifically, Subsection 4.1.1 shows that  $\text{PCS}(\tau)$  prioritizes mean information; Subsection 4.1.2 highlights the impact of correlation information in low-confidence scenarios; and Subsections 4.1.3 and 4.1.4 reveal an interesting “separation” effect, which clarifies why correlation-based clustering in P3C leads to improved sample efficiency. In Section 4.2, we quantify the sample complexity reduction brought about by P3C and show that it leads to an optimal sample complexity reduction for the class of *sample-optimal* R&S methods.

##### 4.1. Interaction and Impact of Mean and Correlation on PCS

First, we introduce additional notations. Let  $\sigma_i^2$  denote the variance of  $X_i$ . For any alternative  $\tau \in \mathcal{P}$ ,  $\text{PCS}(\tau)$  can be rewritten as  $P(y_1^\tau > -d_1^\tau, \dots, y_p^\tau > -d_p^\tau)$ , where  $y_i^\tau = \frac{\bar{x}_\tau - \bar{x}_i - (\mu_\tau - \mu_i)}{\sqrt{\lambda_i^\tau}}$ ,  $d_i^\tau = \frac{\mu_\tau - \mu_i}{\sqrt{\lambda_i^\tau}}$ ,  $\lambda_i^\tau = \text{var}(\bar{x}_\tau - \bar{x}_i) = \frac{\sigma_\tau^2}{N_\tau} + \frac{\sigma_i^2}{N_i} - 2\frac{\text{cov}(X_\tau, X_i)}{N_{\tau,i}}$ ,  $i \in \mathcal{P} \setminus \{\tau\}$ . The vector  $\mathbf{y}^\tau = (y_1^\tau, \dots, y_{\tau-1}^\tau, y_{\tau+1}^\tau, \dots, y_p^\tau)$  follows distribution  $N(0, \Phi^\tau)$ , with the covariance matrix  $\Phi^\tau = (\tilde{r}_{i,j}^\tau)_{(p-1) \times (p-1)}$  where  $i, j \in \mathcal{P} \setminus \{\tau\}$ . The diagonal elements of  $\Phi^\tau$  is 1 and  $|\tilde{r}_{i,j}^\tau| \leq 1$ . We further note that the theoretical results are highly technical and involve intricate interactions between sample allocation and distribution parameters. To provide more concise results and clearer insights, we introduce only a mild assumption that  $\tilde{r}_{i,j}^\tau$  is bounded.

**ASSUMPTION 2 (Moderate Correlation).**  $\forall i, j \in \mathcal{P} \setminus \{\tau\}$ , (a)  $\tilde{r}_{i,j}^\tau > R_{i,j}^a = -\sin(1) \approx -0.84$ ; (b)  $|\tilde{r}_{i,j}^\tau| < R_{i,j}^b \triangleq \left| \frac{d_j^\tau}{d_i^\tau} \right|$ ; (c)  $\tilde{r}_{i,j}^\tau < R_{i,j}^c \triangleq \sin\left(\frac{(d_j^\tau)^2}{(d_i^\tau)^2}\right)$ .

Different theorems may incorporate one or more of the above assumptions as needed. In Appendix EC.2, we show that these assumptions are readily satisfied for prominent R&S methods, as long as the correlations between alternatives are not extremely large (including the case of independence).

**4.1.1. Priority of mean information** The following fundamental properties justify the use of the new PrOS policy. First,  $\text{PCS}(\tau)$  is a reasonable criterion for evaluating the performance of  $\tau$ , as  $\text{PCS}(\tau)$  prioritizes mean information and increases monotonically with respect to the mean  $\mu_\tau$  under any correlation configuration. Second, the PrOS is consistent, that is, it converges to the true best as the sample size tends to infinity. See the proof in Appendix EC.1.

**THEOREM 1.** (a)  $\text{PCS}(\tau)$  is differentiable with respect to  $\boldsymbol{\mu} = (\mu_1, \dots, \mu_p)$  and  $\frac{\partial \text{PCS}(\tau)}{\partial \mu_\tau} > 0$ ;  
 (b)  $\tau^*$  converges to [1] almost surely as  $N_i \rightarrow \infty$  for  $\forall i \in \mathcal{P}$ .

**4.1.2. Impact of correlation information** If an alternative’s mean is distinctly prominent, it is highly likely to be selected as the PrOS. However, in the low-confidence scenario where the sample size is *finite* and numerous alternatives have similar means, correlation information may become the dominant factor in individual PCS. In that case, PrOS may not necessarily be the alternative [1], and consequently,  $\text{moPCS} > \text{PCS}_{\text{trad}}$  strictly. The following result demonstrates such a scenario. See the proof in Appendix EC.1.

**PROPOSITION 1.** Suppose that  $N_i$  is finite for all  $i \in \mathcal{P}$  and there exists  $\tau_0 \in \mathcal{P}$  such that  $\tilde{r}_{i,j}^{\tau_0} > \tilde{r}_{i,j}^\tau$  for all  $\tau \in \mathcal{P} \setminus \{\tau_0\}$  and all  $i, j \in \mathcal{P}$ , then there exists  $\delta > 0$  such that if  $|\mu_i - \mu_{\tau_0}| < \delta$  holds for all  $i \in \mathcal{P} \setminus \{\tau_0\}$ , we have  $\tau^* = \tau_0$ . Furthermore, if  $\tau_0 \neq [1]$ , then  $\text{moPCS} > \text{PCS}_{\text{trad}}$  strictly.

Although the scenario discussed in Proposition 1 does not cover all possibilities, its proof helps us understand how correlation information dominates individual PCS in low-confidence scenarios. The proof can be interpreted from a sensitivity analysis perspective. When all alternatives are identical, with the same means and covariance parameters, their individual PCS values are equal. If small perturbations are introduced to the means within a range of  $\delta$ , while significantly perturbing the correlation configuration, the mean value theorem suggests that the small changes in the means have a limited impact. In contrast, the correlation parameters predominantly determine which alternative has the highest individual PCS.

**4.1.3. The derivative of PCS with respect to correlation information.** We now delve into a more refined interaction effect between the mean and correlation through gradient analysis. We first present the technical results in Section 4.1.3, and then, in Section 4.1.4, we intuitively explain the underlying “separation” effect and show how P3C leverages this insight to accelerate R&S process. The proof of the technical results in Section 4.1.3 and Section 4.1.4 is provided in Appendix EC.2.

**THEOREM 2.** Let  $\tau = [m]$ , we define  $\mathcal{I}^+(\tau) \triangleq \{[i] : i < m\}$  and  $\mathcal{I}^-(\tau) \triangleq \{[i] : i > m\}$ , which are the index sets of the alternatives with larger and smaller mean than  $\tau$ , respectively. We denote the sign of a real number as  $\text{sign}(\cdot)$ . Then  $\forall i \in \mathcal{P} \setminus \{\tau\}$ ,

$$\frac{\partial PCS(\tau)}{\partial r_{\tau i}} = D_i^\tau + I_i^\tau,$$

where

$$D_i^\tau \triangleq \frac{\partial PCS(\tau)}{\partial d_i^\tau} \frac{\partial d_i^\tau}{\partial r_{\tau i}},$$

$$I_i^\tau = \sum_{j \in \{1, \dots, p\} \setminus \{i, \tau\}} I_i^{\tau, j} \triangleq \sum_{j \in \{1, \dots, p\} \setminus \{i, \tau\}} 2 \frac{\partial PCS(\tau)}{\partial \tilde{r}_{i, j}^\tau} \frac{\partial \tilde{r}_{i, j}^\tau}{\partial r_{\tau i}}.$$

(a)  $D_i^\tau > 0$  for  $i \in \mathcal{I}^-(\tau)$  and  $D_i^\tau < 0$  for  $i \in \mathcal{I}^+(\tau)$ ;

(b)  $\text{sign}(I_i^{\tau, j}) = \text{sign}(-\sigma_i^2(N_i)^{-1} + r_{\tau, i} \sigma_\tau \sigma_i (N_{\tau, i})^{-1} - r_{\tau, j} \sigma_\tau \sigma_j (N_{\tau, j})^{-1} + r_{i, j} \sigma_i \sigma_j (N_{i, j})^{-1})$ .

**REMARK 1.** The specific expressions of these terms can be found in the appendix. The analysis presented in this section does not specify the computation of these terms but can help gain insights through the magnitude and sign of each term. To complete the analysis of the ‘‘mean-covariance’’ interaction, we also present the impact of variance information in the appendix.

As shown in Theorem 2, the derivative  $\frac{\partial PCS(\tau)}{\partial r_{i\tau}}$  is composed of two parts: the *mean-determined* (MD) term  $D_i^\tau$  and the *mean-independent* (MI) term  $I_i^\tau$ . The sign of the  $D_i^\tau$  depends on whether the mean  $\mu_i$  is larger or smaller than  $\mu_\tau$ , whereas the sign of  $I_i^\tau$  is independent of the mean. Determining the sign of  $I_i^\tau$  is generally complex and unclear. Therefore, before proceeding, it is necessary to establish the magnitudes of  $D_i^\tau$  and  $I_i^\tau$  terms to ascertain which term dominates. For a given vector  $\mathbf{d}$  and an index set  $S$ , we write  $\mathbf{d}_S$  the vector composed of the components from  $\mathbf{d}$  with indices  $S$ . Similar notations  $\Sigma_S$  are used for submatrices of matrix  $\Sigma$ . Let  $N$  denote the total sample size, i.e.,  $N = \sum_{i \in \mathcal{P}} N_i$ .

**ASSUMPTION 3 (Non-vanishing Individual Sample Size).**  $N_i \sim \mathcal{O}(N_j)$  as  $N \rightarrow \infty$ ,  $\forall i, j \in \mathcal{P}$ .

**COROLLARY 1.**  $\forall i \in \mathcal{P} \setminus \{\tau\}$ , we define  $\mathcal{S}_{-i}^+(\tau) \triangleq \{j \in \mathcal{P} \setminus \{i, \tau\} \mid -\tilde{d}_j^\tau > 0\}$ ,  $-\tilde{d}_j^\tau \triangleq -d_j^\tau + d_i^\tau \tilde{r}_{i, j}^\tau$ ,  $j \in \mathcal{P} \setminus \{\tau, i\}$ . If Assumption 2(a) and Assumption 3 hold, then

(a)

$$|D_i^\tau| \sim \mathcal{O}(e^{-\mathcal{J}_i^\tau N}) \triangleq \mathcal{O}\left(\exp\left(-\frac{(d_i^\tau)^2 + Q_S^\tau}{2}\right)\right), \quad (1)$$

$$|I_i^\tau| \sim \mathcal{O}(e^{-\mathcal{J}_i^\tau N}) \triangleq \mathcal{O}\left(\exp\left(-\min_{j \neq i} \frac{(d_i^\tau)^2 + (d_j^\tau)^2}{2(1 + \arcsin(\tilde{r}_{i, j}^\tau))}\right)\right), \quad (2)$$

as  $N \rightarrow \infty$ , where  $Q_S^\tau \triangleq \min_{\mathbf{x} \geq \mathbf{d}_{\mathcal{S}_{-i}^+(\tau)}} \langle \mathbf{x}, (\Sigma_{\mathcal{S}_{-i}^+(\tau)}^Z)^{-1} \mathbf{x} \rangle$ ,  $\mathbf{x} = (x_1, \dots, x_{|\mathcal{S}_{-i}^+(\tau)|}) \in \mathbb{R}^{|\mathcal{S}_{-i}^+(\tau)|}$ ,  $\mathbf{d} = (-\tilde{d}_1^\tau, \dots, -\tilde{d}_p^\tau) \in \mathbb{R}^{p-2}$  and  $\Sigma^Z$  is a covariance matrix of  $p$  transformed variables which are given

in the appendix;

(b) When  $\tau = [1]$ , if Assumption 2(b) and 2(c) hold, then  $\mathcal{D}_i^\tau < \mathcal{I}_i^\tau$ ;

(c) Let  $\mathcal{D}_i^\tau(m)$  and  $\mathcal{I}_i^\tau(m)$  denote the asymptotic decay rates of  $D_i^\tau$  and  $I_i^\tau$  when  $\tau = [m]$ . Suppose only the ranking  $m$  of  $\tau$  changes, while all other parameters (covariance matrix, sample sizes, and the absolute value of pairwise mean differences) remain fixed. If Assumption 2(b) holds,  $\mathcal{D}_i^\tau(m)$  is non-decreasing as  $m$  increases, while  $\mathcal{I}_i^\tau(m)$  remains constant for all  $m$ .

Some key observations follow. First, both the MD and MI terms will decrease exponentially to 0 as the total sample size  $N$  increases. Whether the MD terms or MI terms dominate depends on the relative magnitudes of decay rates  $\mathcal{D}_i^\tau$  and  $\mathcal{I}_i^\tau$ . Second, combining Corollary 1(b) and Corollary 1(c), let  $\tau = [m]$ . When  $m = 1$ , the MD term is dominant. As the ranking  $m$  increases, the MI term gradually surpasses the MD term. While the exact ranking  $m$  at which the MI term becomes the dominant component is unclear, we can at least confirm that there exists a subset  $\mathcal{P}' \subseteq \mathcal{P}$ , critically containing  $[1]$ , where the MD term remains dominant for all  $i \in \mathcal{P}'$  (i.e.,  $\mathcal{D}_i^\tau < \mathcal{I}_i^\tau$ ). The alternatives in  $\mathcal{P}'$  are top-ranked “good” alternatives, and in practice, users are typically only interested in the individual  $\text{PCS}(\tau)$  of a “good” alternative  $\tau$ . For example, if the  $\text{PCS}_{\text{trad}}$  criterion is adopted,  $\tau = [1]$ , and if moPCS is used,  $\tau = \tau^*$ . Therefore, in the intuitive analysis in Section 4.1.4, we assume that the MD term dominates for any alternative under consideration (this assumption is used exclusively in the intuitive analysis below). Moreover, when analyzing  $\text{PCS}_{\text{trad}}$  in the subsequent sections, since  $[1] \in \mathcal{P}'$ , we can be certain that the MD term dominates.

**4.1.4. “Separation” effect** Base on the aforementioned technical results, we are now ready to show the underlying insight. According to the Theorem 2(a), focusing solely on the MD term, the correlations between  $\tau$  and alternatives in  $\mathcal{I}^-(\tau)$  impose a cumulative positive effect on  $\text{PCS}(\tau)$ , and conversely, correlations between  $\tau$  and those alternatives in  $\mathcal{I}^+(\tau)$  impose a cumulative negative effect. Consequently, the impact of correlation on  $\text{PCS}(\tau)$  hinges on the ranking of  $\tau$ . If  $\tau$  is near the top, the number of alternatives in  $\mathcal{I}^-(\tau)$  dominates, and then the cumulative positive effects surpass the cumulative negative effects. Increasing the correlations  $\{r_{\tau i}\}_{i \in \mathcal{P} \setminus \{\tau\}}$  is more likely to improve  $\text{PCS}(\tau)$  (specifically, when  $\tau = [1]$  and  $\mathcal{I}^+(\tau) = \emptyset$ , then increasing the correlation will certainly improve  $\text{PCS}(\tau)$ ). On the contrary, if the alternative  $\tau$ 's mean performance is poor, the influence of correlation is reversed, and increasing the correlation around  $\tau$  will decrease  $\text{PCS}(\tau)$ .

In summary, as shown in regions I and IV of Figure 2, increasing the correlation level among the alternatives can induce a “separation” effect, which may “amplify” good alternatives and “suppress” bad alternatives in terms of individual PCS. This makes the distinction between good and bad alternatives more pronounced, thereby accelerating the R&S procedure. This phenomenon

is analogous to the electrophoresis technique in chemistry, where an electric field propels particles with positive and negative charges in different directions to separate the mixture. Conversely, decreasing the overall correlation leads to an undesirable aggregation phenomenon (regions II and III). In practice, we cannot directly modify the correlation parameters within the true distribution of alternatives. However, in a parallel computing environment, we can enhance the local correlation level in each processor using clustering techniques. This is the rationale behind P3C’s use of correlation-based clustering to enhance sample efficiency.

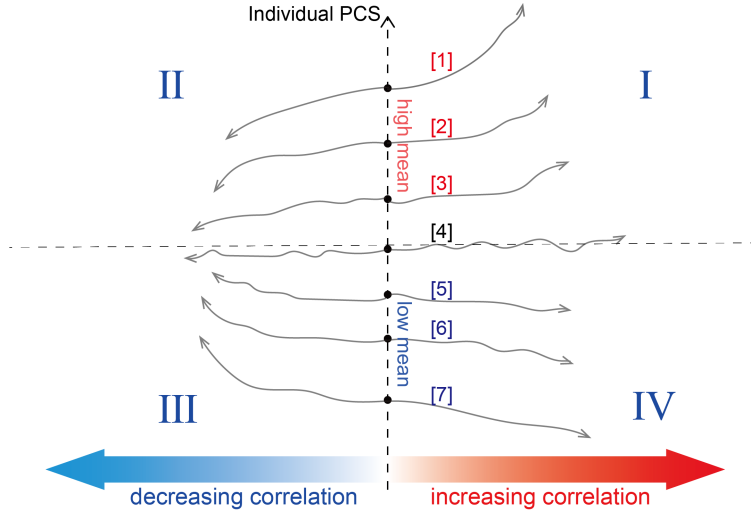


**Figure 2** An illustrative example with 7 alternatives, where the top 3 alternatives [1], [2] and [3] exhibit high mean performances, and [5], [6] and [7] exhibit low mean performances.

Before concluding this section, we present the following lemma, which will be used in the next section as a supplement to Theorem 2.

LEMMA 1.  $\forall i, j \in \mathcal{P} \setminus \{\tau\}$ ,  $\frac{\partial PCS(\tau)}{\partial r_{ij}} \geq 0$ . If  $\mathcal{D}_i^\tau < \mathcal{I}_i^\tau$ , then  $\frac{\partial PCS(\tau)}{\partial r_{ij}} \sim o\left(\left|\frac{\partial PCS(\tau)}{\partial r_{i\tau}}\right|\right)$ .

This lemma characterizes the impact of correlations  $\{r_{ij}\}_{i,j \in \mathcal{P} \setminus \{\tau\}}$ , which are *not* directly associated with  $\tau$ . These correlations in the surrounding environment always have a non-negative impact on  $PCS(\tau)$ , regardless of mean information. This further complements the argument that clustering correlated alternatives can accelerate the R&S procedure. Additionally, if  $\tau$  is a “good” alternative within  $\mathcal{P}'$ , meaning that  $\mathcal{D}_i^\tau < \mathcal{I}_i^\tau$ , the impact of  $\{r_{ij}\}_{i,j \in \mathcal{P} \setminus \{\tau\}}$  is negligible compared to  $\{r_{\tau i}\}_{i \in \mathcal{P} \setminus \{\tau\}}$ , so it will not affect the aforementioned “separation” phenomenon induced by  $\{r_{\tau i}\}_{i \in \mathcal{P} \setminus \{\tau\}}$ .

#### 4.2. Rate-Optimal Sample Complexity Reduction

After understanding how P3C utilizes correlation-based clustering to accelerate the R&S process, we now proceed to quantify the reduced sample complexity in fixed-precision R&S. In a parallel computing environment, we compare two distinct strategies: ( $\mathcal{R}$ ) randomly assigning an equal

number of alternatives to each processor, as in traditional “divide and conquer” procedures; and (C) adopting a correlation-based clustering approach, assigning each cluster to a single processor, as in P3C. Since the PrOS dynamically changes with sampling, we adopt the  $\text{PCS}_{\text{trad}}$  criterion in this section.

We consider a scenario with  $k$  clusters ( $k \ll p$ ) and  $k$  available parallel processors. Each cluster  $\mathcal{G}_j$  ( $j = 1, \dots, k$ ) contains one local best alternative  $\tau_j$ , which has the highest mean, along with  $\frac{p}{k}$  suboptimal alternatives. The true clustering label is unknown, but we assume knowledge of the indices of the local bests  $\{\tau_j\}_{j=1, \dots, k}$ . Each local best is placed on a dedicated processor and remains fixed, without being relocated to another processor in either strategy  $\mathcal{R}$  or  $\mathcal{C}$ . All  $k$  local bests share the same mean and variance. The remaining  $p$  suboptimal alternatives, which also have identical means and variances, are distributed across processors according to strategy  $\mathcal{R}$  or  $\mathcal{C}$ . Then, samples are simulated until each processor achieves  $\text{PCS}_{\text{trad}} > 1 - \alpha$ . The required total sample sizes in strategies  $\mathcal{R}$  and  $\mathcal{C}$  are denoted as  $N_R$  and  $N_C$ , respectively. Correlation coefficients within the same cluster are  $R$ , while those between different clusters are  $r$ , with a difference of  $\Delta r = R - r$ .

Due to the limited number of samples used for learning correlation information, the clustering accuracy in strategy  $\mathcal{C}$  may be less than 1. Given the randomness of simulation outputs, we introduce *probability of correct clustering* (PCC) to measure the statistical guarantee of clustering quality, defined as

$$\text{PCC} \triangleq P(\Pi_n = \Pi),$$

where  $\Pi_n = (G_n(1), \dots, G_n(p)) \in \mathbb{R}^p$  is the partition result obtained by the employed clustering algorithm after processing  $n$  samples, with  $G_n(i)$  denoting the cluster assignment of alternative  $i$ . Finally, Theorem 3 quantifies the sample complexity reduction brought about by correlation-based clustering.

ASSUMPTION 4.  $\text{PCS}_{\text{trad}}$  is a monotonically increasing, differentiable and concave function with respect to the total sample size  $N$ .

THEOREM 3. Assume that in the  $j$ -th processor ( $j = 1, \dots, k$ ), Assumptions 3 and 4 hold, and that Assumptions 2(b) and 2(c) are satisfied for the local best  $\tau_j$ . Then, there exist  $\xi \in (0, 1)$  such that:

$$\mathbb{E}(N_R - N_C) \geq \gamma \Delta r \left( \text{PCC} - \frac{1}{k} \right) p, \quad (3)$$

where  $\gamma = \frac{\partial \text{PCS}_{\text{trad}}^1(\Sigma', N_\xi)}{\partial r_{i_0, \tau}} \left( \frac{\partial \text{PCS}_{\text{trad}}^1(\Sigma, N_\xi)}{\partial N} \right)^{-1}$ ,  $N_\xi = N_0 + \xi(N_C - N_0)$ , with  $\text{PCS}_{\text{trad}}^1$  being the local  $\text{PCS}_{\text{trad}}$  of the first processor,  $\Sigma$  and  $\Sigma'$  being two covariance matrices,  $i_0 \in \mathcal{G}_1 \setminus \{\tau_1\}$  and  $N_0$  being the initialization sample size.

REMARK 2. Assumption 4 means the use of a sensible sampling policy, which ensures that  $\text{PCS}_{\text{trad}}$  improves as the total sample size increases. The concavity assumption means that as the sample size increases, the marginal improvement in  $\text{PCS}_{\text{trad}}$  (which is upper bounded by 1) gradually diminishes. This assumption can be removed, yielding similar but less concise results. Theorem 3 holds universally without the need for specifying the sampling method. The employed sampling method is reflected in the denominator of  $\gamma$  (i.e.,  $\frac{\partial \text{PCS}_{\text{trad}}}{\partial N}$ ), influencing how fast  $\text{PCS}_{\text{trad}}$  grows with the total sample size.

Some key observations of Theorem 3 follow. First, correlation-based clustering guarantees a positive reduction in sample complexity as long as  $\text{PCC} > \frac{1}{k}$ . Second, for the class of *sample-optimal* R&S methods which achieve a sample complexity of  $\mathcal{O}(p)$ , the reduction attained by correlation-based clustering is also  $\mathcal{O}(p)$ , since  $\gamma$  has been proven to be at least  $\mathcal{O}(1)$  for this class (see Appendix EC.3 for the proof). Notably, this represents the maximum achievable reduction rate for this class of R&S methods; any further reduction would violate the theoretical lower bound of  $\mathcal{O}(p)$  sample complexity. This implies that, although *sample-optimal* R&S methods already achieve the lowest linear growth rate, P3C can further break the bottleneck by reducing the slope of the line. Third, the amount of sample complexity reduction also depends on the gap  $\Delta r$  between intra-cluster correlations and inter-cluster correlations. If all alternatives are independent, i.e.,  $\Delta r = 0$ , clustering would not yield any improvement.

The proof of Theorem 3 is provided in Appendix EC.3. The intuition of the proof is summarized by the following informal equation, which is established within each processor:

$$\Delta \text{PCS}_{\text{trad}} = \underbrace{\frac{\partial \text{PCS}_{\text{trad}}}{\partial N}(N_R - N_0)}_{\text{Strategy } \mathcal{R}} = \overbrace{\frac{\partial \text{PCS}_{\text{trad}}}{\partial \Sigma}(\Sigma' - \Sigma)}^{\text{Sample Complexity Reduction}} + \underbrace{\frac{\partial \text{PCS}_{\text{trad}}}{\partial N}(N_C - N_0)}_{\text{Strategy } \mathcal{C}}. \quad (4)$$

Equation (4) is derived using the mean value theorem, and we omit the exact evaluation points for the derivatives  $\frac{\partial \text{PCS}_{\text{trad}}(\cdot)}{\partial N}$  and  $\frac{\partial \text{PCS}_{\text{trad}}(\cdot)}{\partial \Sigma}$ , though it is worth noting that these points differ between terms. The term  $\frac{\partial \text{PCS}_{\text{trad}}}{\partial \Sigma}$  is used here as an intuitive representation of the sensitivity to changes in correlation structure, as described in Theorem 2 and Lemma 1. This equation implies that, both increasing the sample size and adjusting the correlation structure contribute to the improvement in  $\text{PCS}_{\text{trad}}$ . Strategy  $\mathcal{R}$  directly increases the sample size from  $N_0$  to  $N_R$ , resulting in an improvement of  $\Delta \text{PCS}_{\text{trad}}$ . In contrast, Strategy  $\mathcal{C}$  first modifies the correlation structure from  $\Sigma$  to  $\Sigma'$  through a clustering step, which immediately improves  $\text{PCS}_{\text{trad}}$ . Consequently, a smaller sample size  $N_C$  is sufficient to achieve the same precision as Strategy  $\mathcal{R}$ . The improvement contributed by changes in the correlation structure directly accounts for the reduction in sample complexity.

## 5. Gradient-based Budget Allocation

In Sections 4.1.1, 4.1.2 and the subsequent experimental Section 7, we justify the use of the new PrOS policy and the moPCS criterion. A natural question arises: do existing R&S methods remain effective under the new criterion and within the P3C framework? This section analyzes this question under both fixed-precision and fixed-budget formulations, and further proposes a new budget allocation policy tailored to the moPCS criterion.

For fixed-precision R&S, since  $\text{moPCS} \geq \text{PCS}_{\text{trad}}$ , existing R&S methods such as the KN family and KT, which ensure  $\text{PCS}_{\text{trad}} > 1 - \alpha$ , remain valid under the moPCS criterion. Furthermore, employing the KN family or KT within the P3C framework (denoted as P3C-KN and P3C-KT, respectively) is sufficiently effective, as it achieves sample-optimality in rate, provided that the number of alternatives within each cluster is bounded by  $p_m < \infty$ , as shown in the following proposition. The proof is provided in Appendix EC.5.

**PROPOSITION 2 (Sample Optimality of P3C-KN and P3C-KT).** *Let  $N_{KN}$  and  $N_{KT}$  denote the required total sample sizes to achieve  $\text{moPCS} \geq \text{PCS}_{\text{trad}} \geq 1 - \alpha$  using P3C-KN and P3C-KT, respectively. If the number of alternatives within each cluster is upper bounded by a constant  $p_m < \infty$ , then  $\mathbb{E}(N_{KN}) \sim \mathbb{E}(N_{KT}) \sim \mathcal{O}(p)$  as  $p \rightarrow \infty$ .*

However, for the fixed-budget R&S problem, traditional methods may become ineffective or even counterproductive under the moPCS criterion. For instance, in the celebrated OCBA algorithm (Chen et al. 2000), a large proportion of samples is often allocated to [1] and other “good” alternatives with high means. Nevertheless, as shown in the following proposition (by letting  $\tau = \tau^*$ ), allocating samples to “good” alternatives in  $\mathcal{I}^+(\tau^*)$  may unexpectedly reduce the moPCS in certain scenarios (see the proof in Appendix EC.4). Therefore, it is necessary to design new simulation budget allocation strategies tailored to the moPCS criterion.

**PROPOSITION 3 (Negative Effect of Sample Size).** (a) *The gradient of  $\text{PCS}(\tau)$  with respect to  $N_i$  is*

$$\frac{\partial \text{PCS}(\tau)}{\partial N_i} = \tilde{D}_i^\tau + \tilde{I}_i^\tau, \quad \forall i \in \mathcal{P}, \quad (5)$$

where  $|\tilde{D}_i^\tau| \sim \mathcal{O}(e^{-\mathcal{D}_i^\tau N})$  and  $|\tilde{I}_i^\tau| \sim \mathcal{O}(e^{-\mathcal{J}_i^\tau N})$ . For  $i \in \mathcal{P} \setminus \{\tau\}$ ,  $\mathcal{D}_i^\tau$  and  $\mathcal{J}_i^\tau$  are given by (1) and (2), respectively, and  $\mathcal{D}_\tau^\tau = \min_{i \in \mathcal{P} \setminus \{\tau\}} \mathcal{D}_i^\tau$ ,  $\mathcal{J}_\tau^\tau = \min_{i \in \mathcal{P} \setminus \{\tau\}} \mathcal{J}_i^\tau$ .

(b)  $\forall i \in \mathcal{I}^+(\tau)$ , if “ $N_\tau \geq N_i$ ”, or if “ $N_\tau < N_i$  and  $r_{\tau i} < \frac{\sigma_i}{2\sigma_\tau}$ ”, then it follows that  $\tilde{D}_i^\tau < 0$ .

This result of Proposition 3(b) is similar to Peng et al. (2015), but the latter is restricted to  $\text{PCS}_{\text{trad}}$  under the independence assumption. Although Proposition 3(b) lists some cases, it does not exhaustively cover all possible scenarios where additional sampling may have a negative effect. Additionally, the impact of sample size on moPCS may vary dynamically as the sampling process

progresses. Therefore, to ensure that moPCS consistently grows in a positive direction, we follow the gradient analysis perspective of this paper and propose an adaptive gradient-based budget allocation (GBA) policy (see Algorithm 1). GBA is a myopic method with the objective of achieving the highest marginal improvement at each step. Specifically, in each iteration, a sample batch of size  $N_B$  is allocated to the alternative  $i$  that has the largest (or top- $m$ ) derivative of the moPCS with respect to the sample size, until the total budget is exhausted. That is,

$$\tau_{\text{GBA}} = \arg \max_{i \in \mathcal{P}} \frac{\partial \text{moPCS}}{\partial N_i} = \arg \max_{i \in \mathcal{P}} \frac{\partial \text{PCS}(\tau^*)}{\partial N_i}.$$

The intuition of GBA is similar to the myopic policy in Chick et al. (2010), the expected improvement (EI) method in (Ryzhov 2016), the gradient-based policy in Peng et al. (2017) and the heuristic policy in Chen and Ryzhov (2023). The sample optimality of using GBA within the P3C framework (denoted as P3C-GBA) is discussed in the Appendix EC.5. In our large-scale experiments, P3C-GBA demonstrates remarkable performance under both  $\text{PCS}_{\text{trad}}$  and the moPCS criterion.

Regarding the computation of  $\frac{\partial \text{moPCS}}{\partial N_i}$ , which equals  $\tilde{D}_i^{\tau^*} + \tilde{I}_i^{\tau^*}$  as shown in equation (5), we employ different calculation methods at the beginning of each iteration depending on the relative magnitudes of  $\mathcal{D}_i^{\tau^*}$  and  $\mathcal{I}_i^{\tau^*}$ .

**Case (a):** If  $\mathcal{D}_i^{\tau^*} < \mathcal{I}_i^{\tau^*}$ , the term  $\tilde{D}_i^{\tau^*}$  dominates over  $\tilde{I}_i^{\tau^*}$ , and  $\frac{\partial \text{moPCS}}{\partial N_i} \approx \tilde{D}_i^{\tau^*}$ . Although the  $\tilde{D}_i^{\tau^*}$  terms can be computed analytically, it requires calculating a  $(p-1)$ -dimensional integral, which is computationally intractable in large-scale problems. Therefore, we adopt a cheap Bonferroni lower bound  $\text{moPCS}_B$  as an approximation of moPCS.

$$\text{moPCS} \geq \text{moPCS}_B \triangleq \sum_{i \in \mathcal{P} \setminus \{\tau^*\}} \Phi(d_i^{\tau^*}) - (p-2). \quad (6)$$

The other two commonly used calculation methods, the Slepian lower bound (Branke et al. 2007) and the equivalent one-dimensional integral (Peng et al. 2016), may not be applicable in our work due to the correlation among alternatives. For further computational considerations, please refer to Eckman and Henderson (2022). In Case (a), the Bonferroni approximation is a good approximation in the sense that it surprisingly preserves the sign of the true gradient, as shown in Proposition 4. This property allows us to reliably determine whether sampling a specific alternative is beneficial or detrimental, ensuring growth in the positive direction. Moreover, the derivative  $\frac{\partial \text{moPCS}_B}{\partial N_i}$  has a simple closed-form expression, which is provided in Appendix EC.4.

**PROPOSITION 4.**  $\text{sign}(\frac{\partial \text{moPCS}_B}{\partial N_i}) = \text{sign}(\tilde{D}_i^{\tau^*}), \forall i \in \mathcal{P} \setminus \{\tau^*\}$ .

**Case (b):** If  $\mathcal{D}_i^{\tau^*} \geq \mathcal{I}_i^{\tau^*}$ , then the  $\tilde{I}_i^{\tau^*}$  term dominates.  $\frac{\partial \text{moPCS}}{\partial N_i} \approx \tilde{I}_i^{\tau^*}$ . Calculating the  $\tilde{I}_i^{\tau^*}$  term is computationally straightforward, as it has a closed-form expression (see Appendix EC.4).

---

**Algorithm 1** Gradient-based Budget Allocation (GBA)

---

**Input:** Batch size  $N_B$ , initialization samples, total budget  $N$ ,  $m$  (optional)**Step 0:** Calculate the PrOS  $\tau^*$  and estimate the covariance using the initialization samples.**Step 1:** For any  $i \in \mathcal{P}$ , calculate  $\frac{\partial \text{moPCS}}{\partial N_i}$ . Perform additional  $N_B$  simulations for the alternative  $\tau_{\text{GBA}} = \arg \max_{i \in \mathcal{P}} \frac{\partial \text{moPCS}}{\partial N_i}$  (optional: top  $m$  alternatives with the highest gradients).**Step 3:** Update estimators of means, covariance matrix, and  $\tau^*$ . If total number of samples  $> N$ , stop; otherwise, update  $\tau^*$  and go to Step 1.

---

## 6. Large-Scale Alternative Clustering

While PCC does not directly determine the final statistical precision of R&S, a higher PCC, as shown in Theorem 3, can facilitate greater sample savings. Nevertheless, clustering in large-scale problems presents challenges, both computationally and statistically. To address these challenges and strive for a high PCC, inspired by a well-known few-shot learning approach in the deep learning literature, namely, Prototypical Networks (Snell et al. 2017), we propose a parallel alternative clustering algorithm  $\mathcal{AC}^+$ . Following this, we detail the methodology for calculating the PCC.

### 6.1. Few-shot Alternative Clustering

In P3C, we cluster alternatives instead of their simulation outputs, a concept known as variable clustering in statistical literature. A commonly used algorithm for this purpose is the hierarchical clustering algorithm (Jolliffe 1972), denoted as  $\mathcal{AC}$  (see pseudocode in the Appendix EC.6). The framework of  $\mathcal{AC}$  is as follows. Suppose the number of clusters  $k$  is known. Initially, each alternative is treated as an individual group. In each iteration, the two groups with the maximum similarity  $R$  are merged until  $k$  groups remain. The (empirical) similarity between two groups of alternatives,  $G^1$  and  $G^2$ , is quantified by  $R(G^1, G^2) = \max_{i \in G^1, j \in G^2} \hat{r}_{ij}^n$ , where  $\hat{r}_{ij}^n$  denotes the estimated  $r_{ij}$  using  $n$  samples. It is important to note that the conventional estimator of  $r_{ij}$ , the sample correlation coefficient  $\bar{r}_{ij}^n$ , may suffer from poor statistical properties and computational efficiency for large  $p$  (Fan et al. 2020). Therefore, an easy-to-compute large-dimensional covariance estimator from (Ledoit and Wolf 2020) is provided in Appendix EC.6. Nonetheless,  $\mathcal{AC}$  still requires estimating the entire  $p \times p$  correlation matrix, which necessitates a large sample size, and more importantly, cannot be parallelized.

The few-shot  $\mathcal{AC}^+$  algorithm resolves the above issues. As shown in Algorithm 2, initially,  $\mathcal{P}$  is split into two sets: the support set  $\mathcal{P}_s$  and the query set  $\mathcal{P}_q$ , with sizes  $p_s$  and  $p_q$  respectively.  $p_s$  is set to be greater than  $k$  but much smaller than  $p$ . Next, alternatives in  $\mathcal{P}_s$  are grouped into  $k$  clusters using the  $\mathcal{AC}$  algorithm, which can be efficiently handled on a single processor due to the moderate size of  $p_s$ . In each cluster  $\mathcal{G}_j$  ( $j = 1, 2, \dots, k$ ), one *representative* alternative  $\tau_j$  is chosen as the “prototype” of the cluster. Finally, each alternative in the query set  $\mathcal{P}_q$  is assigned

to an existing cluster by identifying the most correlated prototype. This matching process can be parallelized by sending a copy of the  $k$  prototypes to each processor and then randomly assigning alternatives in  $\mathcal{P}_q$  to different processors. Given that  $k \ll p$  typically, the additional simulation cost for these copies is negligible.  $\mathcal{AC}^+$  eliminates the need for estimating the entire correlation matrix and only requires estimating a small submatrix.

As for the selection of the “prototype” within each cluster  $\mathcal{G}_j$ , the process is as follows. (i) Apply principal component analysis (PCA) to the cluster  $\mathcal{G}_j$  to identify the first principal component  $PC_{\mathcal{G}_j}$ , which is a synthetic variable given by  $PC_{\mathcal{G}_j} = \sum_{i \in \mathcal{G}_j} k_{ij} X_i$ . Detailed calculations can be found in standard machine learning textbooks. In variable clustering literature,  $PC_{\mathcal{G}_j}$  is often termed as the “latent component” of  $\mathcal{G}_j$ , proven to be the linear combination that maximizes the sum of squared correlations with the alternatives located in  $\mathcal{G}_j$  (Vigneau and Qannari 2003). The loading  $k_{ij}$  measures the correlation between the alternative  $i$  and  $PC_{\mathcal{G}_j}$ . (ii) Select the alternative with the largest loading  $k_{ij}$  as the *representative* “prototype” of  $\mathcal{G}_j$  (Al-Kandari and Jolliffe 2001):

$$\tau_j = \arg \max_{i \in \mathcal{G}_j} k_{ij}. \quad (7)$$

Moreover, as shown in Proposition 2, bounding the number of alternatives within each cluster is essential for asymptotic sample optimality and for balancing computational load across different processors (Ni et al. 2017). Fortunately, the hierarchical structure of the  $\mathcal{AC}$  and  $\mathcal{AC}^+$  algorithms makes it straightforward to satisfy this requirement. We set an upper limit,  $p_m$ , on the size of each cluster. Once a cluster reaches this limit, no new alternatives are added, and the new alternatives are assigned to the second closest cluster. This also naturally guides our choice of  $k$ , which, in practice, can be set to approximately 2 to 3 times  $\frac{p}{p_m}$ .

---

**Algorithm 2** Few-shot Alternative Clustering  $\mathcal{AC}^+$ 


---

Input: sample size  $n$ , the number of clusters  $k$ ,  $p_s$ ,  $p_q$ .

**Step 1:** Randomly split the set  $\mathcal{P}$  into two sets,  $\mathcal{P}_s$  and  $\mathcal{P}_q$ , with sizes  $p_s$  and  $p_q$ , respectively.

**Step 2 (Selecting Prototypes):** On a single processor, simulate  $n$  samples for each alternative in  $\mathcal{P}_s$  and calculate the estimated covariance matrix  $\hat{\Sigma}_n^{\mathcal{P}_s}$  with (EC.6.1). Input  $\hat{\Sigma}_n^{\mathcal{P}_s}$  into the algorithm  $\mathcal{AC}$  and output the clustering result  $\Pi_n^{\mathcal{P}_s}$ . Within  $\mathcal{P}_s$ , calculate the *prototype*  $\tau_j$  of cluster  $\mathcal{G}_j$  with (7),  $\forall j \in \{1, 2, \dots, k\}$ . Let  $\mathcal{P}_p = \{\tau_1, \dots, \tau_k\}$ .

**Step 3 (Matching):** Send a copy of  $\mathcal{P}_p$  to each processor. Randomly and equally allocate  $\mathcal{P}_q$  to each processor. For any  $j \in \mathcal{P}_q$ , simulate alternative  $j$  for  $n$  times and calculate  $\hat{r}_{\tau_i, j}^n$  for any  $i \in \{1, 2, \dots, k\}$ .  $G_n(j) = \arg \max_{i \in \{1, 2, \dots, k\}} \hat{r}_{\tau_i, j}^n$ .

Return the partition  $\Pi_n$ .

---

## 6.2. Computation of PCC

Next, we establish a computable lower bound for  $\text{PCC}_{\mathcal{AC}^+}$ , the statistical guarantee of  $\mathcal{AC}^+$ . Let  $\Gamma \triangleq \{(ab, ac) | G(a) = G(b), G(a) \neq G(c), a, b, c \in \mathcal{P}, a \neq b\}$  be the collection of pairs of overlapping intra-cluster and inter-cluster correlations.  $\Gamma_s \triangleq \{(ab, ac) \in \Gamma | a, b, c \in \mathcal{P}_s\}$  and  $\Gamma_q \triangleq \{(a\tau_i, a\tau_j) \in \Gamma | a \in \mathcal{P}_q, i = G(a), j \in \{1, 2, \dots, k\} \setminus \{i\}\}$  are two subsets of  $\Gamma$ . Fisher's  $z$  transformation of correlation coefficients, defined as  $z(r) \triangleq \frac{1}{2} \ln \frac{1+r}{1-r}$ , is monotonically increasing in  $(0, 1)$ . Therefore, according to Assumption 1,  $z(r_{ab}) > z(r_{ac})$  for any pair  $(ab, ac) \in \Gamma$ . Borrowing the idea of indifference zone in R&S literature, in the following proposition we strengthen Assumption 1 by introducing a correlation indifference parameter  $\delta_c > 0$  and assume  $z(r_{ab}) > z(r_{ac}) + \delta_c$ .

PROPOSITION 5. *If Assumption 1 holds and all clusters have equal sizes, then*

$$\text{PCC}_{\mathcal{AC}^+} \geq (1 - k(1 - 1/k)^{p_s}) P\left(\bigcap_{(ab, ac) \in \Gamma_s} \{\hat{r}_{ab}^n > \hat{r}_{ac}^n\}\right) P\left(\bigcap_{(ab, ac) \in \Gamma_q} \{\hat{r}_{ab}^n > \hat{r}_{ac}^n\}\right). \quad (8)$$

Let  $\Gamma_\star$  be either  $\Gamma_s$  or  $\Gamma_q$ . If  $z(r_{ab}) > z(r_{ac}) + \delta_c$  for any  $(ab, ac) \in \Gamma_\star$ , then

$$P\left(\bigcap_{(ab, ac) \in \Gamma_\star} \{\hat{r}_{ab}^n > \hat{r}_{ac}^n\}\right) \geq \sum_{(ab, ac) \in \Gamma_\star} \Phi\left(\frac{\delta_c}{\sqrt{\frac{2(1-\bar{r}_{bc}^n)h(a,b,c)}{n-3}}}\right) - (|\Gamma_\star| - 1), \quad (9)$$

where  $h(a, b, c) = \frac{1-f \cdot \bar{R}^2}{1-\bar{R}^2}$ , with  $\bar{R}^2(a, b, c) = \frac{(\bar{r}_{ab}^n)^2 + (\bar{r}_{bc}^n)^2}{2}$  and  $f(a, b, c) = \frac{1-\bar{r}_{bc}^n}{2(1-\bar{R}^2)}$ .

Additionally, the computation of  $\text{PCC}_{\mathcal{AC}^+}$  when cluster sizes are **unequal**, as well as the computation of  $\text{PCC}_{\mathcal{AC}}$  can be found in Appendix EC.6. As  $n \rightarrow \infty$ , the lower bound of  $\text{PCC}_{\mathcal{AC}^+}$  converges to  $1 - k(1 - 1/k)^{p_s}$ , approaching 1 in large-scale problems where  $p_s$  is in the hundreds or thousands, and  $k$  is significantly smaller than  $p_s$ . In practice, an excessively high PCC is not necessary. As long as the accuracy surpasses that of random clustering, an improvement in R&S sample efficiency can be ensured. This highlights the unique advantage of P3C over other R&S methods leveraging correlation information, as it does not rely on precise clustering or accurate correlation estimation. Moreover, with the computable lower bound of PCC in Proposition 5, one can determine the required sample size to achieve a given clustering precision (the calculation of this sample size is provided in Appendix EC.6).

## 7. Numerical Experiments

In Section 7.1, we provide a simple example to illustrate some key theoretical results of this paper, including the mean-correlation interaction (Theorem 2, Corollary 1 and Lemma 1) and the negative effect of sample size (Proposition 3). In Section 7.2, we test the performance of P3C under fixed-precision constraints and the  $\text{PCS}_{\text{trad}}$  metric. In Section 7.3, we test the performance of P3C under fixed-budget constraints, emphasizing the advantages of using the PrOS policy, the moPCS metric, and the GBA sampling policy.

### 7.1. Illustrative Example

Consider a group of 5 alternatives:  $(X_1, X_2, X_3, X_4, X_5)$ , each following a normal distribution. The mean and covariance parameters are given by  $\boldsymbol{\mu} = (\mu_1, \mu_2, \mu_3, \mu_4, \mu_5) = (2.1, 2.0, 1.95, 1.9, 1.9)$  and

$$\Sigma = \begin{pmatrix} 0.1 & x & x & x & x \\ x & 0.1 & 0.01 & 0.01 & y \\ x & 0.01 & 0.1 & 0.01 & y \\ x & 0.01 & 0.01 & 0.1 & y \\ x & y & y & y & 0.1 \end{pmatrix}.$$

All alternatives share the same variance. Alternative 1 has the highest mean, and its covariance with other alternatives is  $x$  ( $0 \leq x < 0.1$ ). Alternative 5 is the poorest performer, and its covariance with alternatives 2, 3 and 4 is  $y$  ( $0 \leq y < 0.1$ ). To illustrate the proposed mean-correlation interaction theory (Theorem 2, Corollary 1 and Lemma 1), we calculate PCS(1) and PCS(5) with different  $x$  and  $y$ , keeping the mean and variance parameters constant. The sample size for each alternative is 10 (total sample size  $N = 50$ ). Table 1 presents the values of PCS(1) and PCS(5) when  $x$  takes on the values of 0.01, 0.02, 0.03, and 0.05, and  $y$  takes on the values of 0, 0.02, 0.04, and 0.06, respectively (there is no value in the table for  $(x = 0.05, y = 0.06)$  because  $\Sigma$  is not positive definite). The actual values of individual PCS are calculated using Monte Carlo numerical integration. The experimental results align with our theory of mean-correlation interaction: increasing correlation promotes alternatives with high means while suppressing those with low means. When  $y$  is held constant, PCS(1) increases as  $x$  increases, consistent with Theorem 2 and Corollary 1. When  $x$  is fixed, PCS(1) also increases with the growth of  $y$ , where  $y$  represents correlations between alternative 5 and alternatives 2-4, not directly associated with alternative 1. This result is consistent with Lemma 1. On the contrary, PCS(5) decreases as  $x$  (or  $y$ ) increases.

**Table 1** PCS(1) and PCS(5) with Different  $x$  and  $y$  ( $N = 50$ ).

	$y = 0$		$y = 0.02$		$y = 0.04$		$y = 0.06$	
	PCS(1)	PCS(5)	PCS(1)	PCS(5)	PCS(1)	PCS(5)	PCS(1)	PCS(5)
$x = 0.01$	0.6707	0.0349	0.6741	0.0269	0.6875	0.1777	0.6879	0.0051
$x = 0.02$	0.6852	0.0331	0.6904	0.0255	0.7003	0.0168	0.7018	0.0050
$x = 0.03$	0.6979	0.0288	0.7141	0.0233	0.7171	0.0154	0.7274	0.0048
$x = 0.05$	0.7506	0.0197	0.7662	0.0166	0.7690	0.0119		

Next, we illustrate the negative effect of sample size on moPCS in low-confidence scenarios. We set  $x = 0.05$ ,  $y = 0.01$ , and the sample sizes for alternatives 1-5 are  $N_1, 10, 5, 5,$  and  $5$  respectively. The aforementioned mean parameter configuration  $\boldsymbol{\mu}$  represents a high-confidence scenario, where the mean of alternative 1 is noticeably higher than that of the other alternatives. Therefore, as

shown in the “high confidence scenario” row of Table 2, alternative 1 maximizes individual PCS and is selected as the PrOS. Below, to construct a low-confidence scenario, we reduce the mean of alternative 1 and modify the parameter configuration to  $\boldsymbol{\mu}' = (2.01, 2.0, 1.95, 1.9, 1.9)$ . In this low-confidence scenario, the correlation parameter becomes the dominant factor. Alternative 2 maximizes individual PCS and is selected as the PrOS. Alternative 1 has a higher mean than the PrOS and thus belongs to the set  $\mathcal{I}^+(\tau^*)$ . The individual PCS, moPCS, PCS<sub>trad</sub> and PrOS for  $N_1$  values of 5, 6, 7, 8, 9, and 10 are presented in Table 2. Consistent with Proposition 3, increasing the sample sizes of “good” alternatives in  $\mathcal{I}^+(\tau^*)$  may lead to a decrease in moPCS.

**Table 2** PrOS and Various Metrics in Different Scenarios and with Different  $N_1$ .

Scenario		PCS(1)	PCS(2)	PCS(5)	PCS <sub>trad</sub>	moPCS	PrOS
High confidence scenario	$N_1 = 5$	<b>0.6010</b>	0.1913	0.0512	0.6010	0.6010	alt. 1
Low confidence scenario	$N_1 = 5$	0.2900	<b>0.3168</b>	0.1042	0.2900	0.3168	alt. 2
	$N_1 = 6$	0.2762	<b>0.3113</b>	0.1074	0.2762	0.3113	
	$N_1 = 7$	0.2672	<b>0.3068</b>	0.1122	0.2672	0.3068	
	$N_1 = 8$	0.2580	<b>0.3036</b>	0.1179	0.2580	0.3036	
	$N_1 = 9$	0.2516	<b>0.3005</b>	0.1205	0.2516	0.3005	
	$N_1 = 10$	0.2461	<b>0.2976</b>	0.1198	0.2461	0.2976	

## 7.2. Fixed-precision R&S: Drug Discovery

In this section, we test the performance of P3C in the context of the narcotic analgesics drug discovery problem introduced in Negoescu et al. (2011). It studies a set of 6,7-Benzomorphans, which have 5 sites where substituents can be attached (see Figure 3(a)). Specifically, there are 11, 8, 5, 6, and 11 possible substituents for sites 1 to 5, respectively. Additionally, each compound can be positively, negatively, or neutrally charged. Consequently, there are  $11 \times 8 \times 5 \times 6 \times 11 \times 3 \approx 10^5$  available alternative drugs in this large-scale R&S problem. Many structurally similar drugs are governed by common latent factors, leading to a high degree of correlation in their performance. As illustrated in Figure 3(b), a clear pattern of correlation-based clustering emerges in an example comprising 128 drugs. Simulation data are generated based on the Free-Wilson model (Free and Wilson 1964): *the value of the drug = value of the base molecule + value of atom at site 1 + ... + value of atom at site 5*, where the value of each atom is assumed to be an independent normal random variable (latent factor). The mean parameter of each atom is estimated through regression on experimental data from Katz et al. (1977), and the variance is randomly generated from a normal distribution  $N(0, 0.1)$  (excluding negative values). We adopt the fixed-precision formulation of R&S. Our objective is to identify the best drug and ensure a precision of  $1 - \alpha = 0.9$ . We set

$p_m = 1000$  and  $k = 104$ , so only a single round of “clustering and conquer” is required in P3C. The desired FEP for Stage 2 is set to  $\alpha_2 = 0.09$ , and for Stage 3, it is set to  $\alpha_3 = 0.01$  ( $\alpha_2 + \alpha_3 = \alpha$ ).

We incorporate KN (Kim and Nelson 2001) and KT (Zhong and Hong 2022) into the P3C framework, denoting them as P3C-KN and P3C-KT, respectively. P3C-KN and P3C-KT are compared against the traditional stage-wise procedure from Rinott (1978), the Good Selection Procedure (GSP) from Ni et al. (2017) and the standard KT and KN without P3C. However, these benchmarks are based on  $\text{PCS}_{\text{trad}}$  and do not accommodate the newly proposed PrOS policy and moPCS metric. Therefore, in this subsection, we focus on evaluating P3C’s performance under the classical  $\text{PCS}_{\text{trad}}$  metric. The screening methods used in KN and KT rely on the indifference zone assumption, whereas GSP’s screening method does not. To ensure a fair comparison, we replace the screening method in GSP with one based on the indifference zone assumption from Jeff Hong (2006). We set the indifference zone parameter as  $\delta = 0.1$ . Moreover, we set the initialization sample size as  $N_0 = 20$ , and the correlation estimation and clustering in P3C are exclusively based on the initialization samples, without requiring any additional sampling for this purpose.

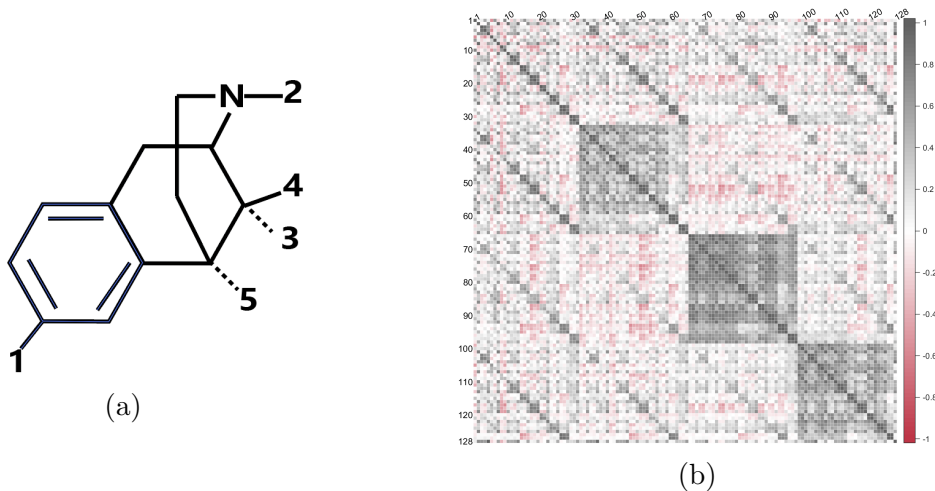


**Figure 3 (a) 5 substituent locations. (b) Clustering phenomenon in drug correlations. Black points represent highly correlated drugs.**

We conduct experiments on a commercial cloud platform and set up a computing cluster with 104 processors. The experiments are conducted under the parallel computing environment of the MATLAB *Parallel Computing Toolbox*, which automatically coordinates workload assignment and information exchange among processors. Additionally, for fairness, Rinott, GSP, standard KT, and standard KN are all implemented within the same parallel environment as P3C using traditional “divide and conquer” strategy. The experiments are repeated 20 times, and averages are taken. Figure 4 presents the required sample sizes for P3C-KT, P3C-KN, KT, KN, Rinott and GSP methods across different  $p$ . Table 3 provides the values at several selected points.

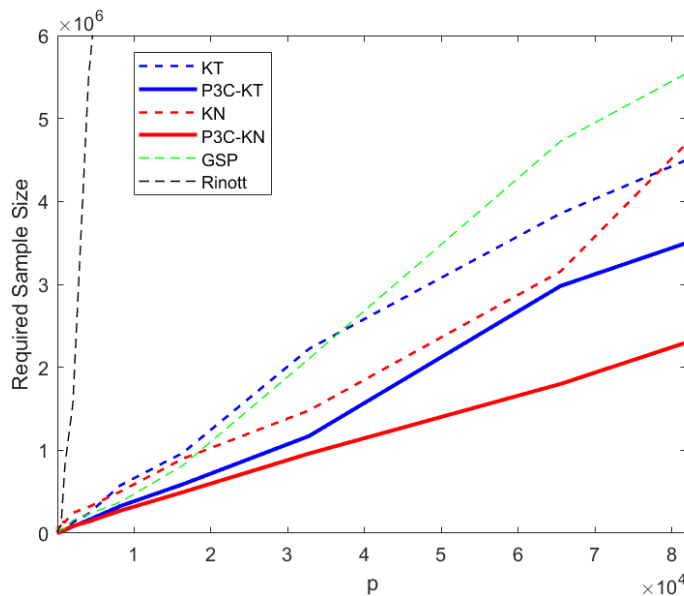


Figure 4 The required total sample size with different number of alternatives  $p$ .

Table 3 The Required Sample Size ( $\times 10^4$ ) with Different Number of Alternatives

$p$	$2^7$	$2^9$	$2^{11}$	$2^{13}$	$2^{14}$	$2^{15}$	$2^{16}$
<b>KT</b>	0.73	3.77	13.04	57.44	96.97	222.12	385.57
<b>KT-P3C</b>	0.48	1.99	8.04	32.57	59.05	117.05	298.14
<b>KN</b>	4.70	13.36	24.46	50.08	89.86	147.96	315.74
<b>KN-P3C</b>	0.52	2.23	8.70	27.03	49.51	96.01	182.00
<b>GSP</b>	0.96	4.88	15.50	37.29	81.87	210.31	472.67
<b>Rinott</b>	2.23	9.26	156	945	2718	6268	15519

In the experiment, P3C-KN and P3C-KT are the top two performers, with P3C-KN performing best in large-scale scenarios. The required total sample sizes for both P3C-KN and P3C-KT increase linearly with  $p$ , indicating that both methods achieve the optimal  $\mathcal{O}(p)$  sample complexity, as predicted by Proposition 2. Moreover, on average, P3C-KN requires only 46% of the sample size needed by the standard KN, while P3C-KT requires only 68% of the sample size needed by the standard KT. These results validate the analysis in Section 4, which explains how correlation-based clustering reduces the sample complexity of parallel R&S methods. It can be observed from Figure 4 that the slope of the line representing KT decreases after applying P3C. This indicates a reduction in sample complexity of  $\mathcal{O}(p)$ , consistent with Theorem 3. In contrast, the classical stage-wise Rinott method requires significantly greater computational resources, necessitating 30 to 50 times the sample size of the other 5 fully-sequential methods in this experiment. This highlights the superior sample efficiency of fully-sequential methods in large-scale fixed-precision R&S problems.

Additionally, we present the wall-clock time of the experiments in Table 4. Compared to the standard “divide-and-conquer” framework, P3C introduces only one additional clustering step. Therefore, the extra time consumption caused by using P3C is primarily attributed to the clustering time. Table 4 also reports the clustering time using the  $\mathcal{AC}^+$  algorithm, with  $p_s$  set to one-tenth of the total number of alternatives. Our experiments show that, even when  $p$  reaches  $2^{16}$ , the clustering step, facilitated by the parallel  $\mathcal{AC}^+$  algorithm, takes only 11.714 seconds. This time is negligible compared to other components, such as simulation time and communication time, which are mainly determined by the sample complexity of the algorithm. Since P3C has been proven to reduce sample complexity, these components require less time. As shown in the table 4, the wall-clock time for KT-P3C and KN-P3C is significantly lower than their counterparts without P3C.

**Table 4 Wall Clock Time (Seconds) with Different Number of Alternatives**

$p$	$2^7$	$2^9$	$2^{11}$	$2^{13}$	$2^{14}$	$2^{15}$	$2^{16}$
<b>Clustering Time</b>	<b>0.009</b>	<b>0.060</b>	<b>0.086</b>	<b>0.208</b>	<b>0.610</b>	<b>2.438</b>	<b>11.714</b>
<b>KT</b>	0.460	0.713	2.213	9.379	20.483	47.708	129.790
<b>KT-P3C</b>	0.389	0.755	1.288	3.306	7.064	18.188	48.830
<b>KN</b>	0.243	0.499	3.708	12.057	27.159	65.770	168.114
<b>KN-P3C</b>	0.202	1.271	8.123	17.803	21.654	37.573	89.200
<b>GSP</b>	0.481	1.038	2.646	6.686	17.956	71.556	278.306

According to Theorem 3, PCC significantly influences the performance of P3C. Employing the  $\mathcal{AC}^+$  algorithm, we investigate  $PCC_{\mathcal{AC}^+}$  under different sample sizes and different sizes of the support set ( $p_s = 25, 50, 75, 100, 150$ ). We focus on the first 1024 drugs and set the cluster number to  $k = 8$ . The result is shown in Figure 5. As the sample size approaches infinity, consistent with Proposition 5,  $PCC_{\mathcal{AC}^+}$  converges to  $1 - k(1 - 1/k)^{p_s}$  (denoted as  $P(D)$ ), which is less than 1. Larger  $p_s$  values lead to a larger  $P(D)$ . At  $p_s = 25$ , the PCC is notably constrained by the  $P(D)$  term and cannot exceed 0.3. As  $p_s$  increases to 50, PCC approaches acceptably close to 1. Although the maximum PCC value of  $\mathcal{AC}^+$  with  $p_s = 50$  is lower compared to that of larger  $p_s$ , the growth rate of  $\mathcal{AC}^+$  with  $p_s = 50$  is the fastest till convergence. This could be attributed to the less efficient  $\mathcal{AC}$  algorithm used for clustering in the support set. As the size of the support set  $p_s$  increases, it significantly hampers overall PCC.

### 7.3. Fixed-budget R&S: Neural Architecture Search

The general NAS problem can be divided into two phases: architecture search (including search space and search strategy) and architecture performance estimation. However, training and evaluating neural networks on test datasets can often be resource-intensive. Suppose that we have

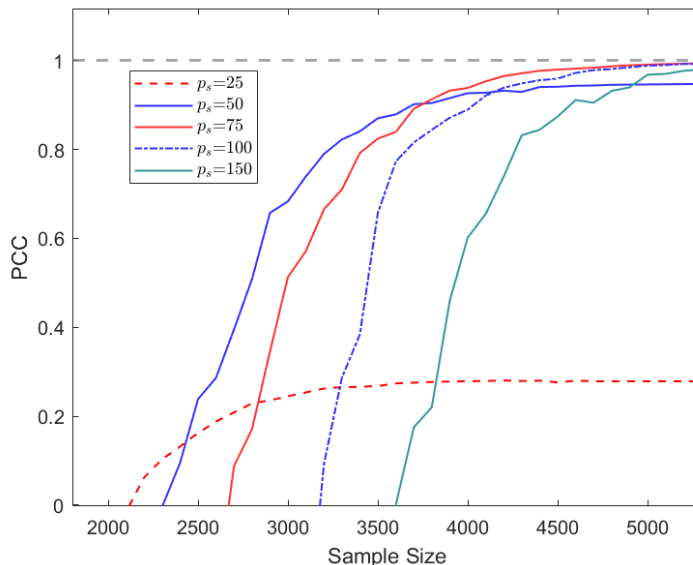


**Figure 5** Comparison of  $PCC_{AC+}$  with different support set sizes  $p_s$ .

already obtained a set  $\mathcal{P}$  of  $p$  alternative architectures through certain search methods, the best architecture is defined as the one that maximizes generalization accuracy:

$$[1] \triangleq \arg \max_{i \in \mathcal{P}} \mathbb{E}(\text{ACC}_i), \quad (10)$$

where  $\text{ACC}_i$  is the accuracy of alternative  $i$  and the expectation is computed over the probability space of all of the unseen data points. It is impossible to calculate the expectation in (10) exactly, so we estimate it using Monte Carlo over the test dataset. Therefore, NAS can be viewed as a discrete simulation optimization problem, where the simulation model is a neural network. Testing one architecture on a batch of test data corresponds to one simulation run, and the accuracy is the simulation output. Given the limited size of the test dataset, which corresponds to a finite amount of simulation resources, we formulate NAS as a fixed-budget R&S problem. To separately evaluate the improvements brought by GBA and P3C, we compare the following methods: standard GBA, the CBA method of Fu et al. (2007) (which can be viewed as an extension of OCBA that accounts for correlations between alternatives), the GBA and CBA methods combined with P3C, denoted as P3C-GBA and P3C-CBA, FBKT from Hong et al. (2022) and the naive equal allocation (EA). Additionally, standard GBA, CBA, FBKT, EA are also implemented in a parallel computing environment using traditional “divide and conquer” strategy: In Stage 1, alternatives are randomly and equally partitioned into several groups of the same size and allocated to different processors; In Stage 2, a local best is selected from each processor; and in Stage 3, these selected local best alternatives are compared to determine the ultimate best.

*Performance metric and selection policy.* We conduct experiments under two metrics, i.e., moPCS and  $\text{PCS}_{\text{trad}}$ . The former adopts the PrOS policy. The latter adopts the  $\tau^m$  selection policy.

*Dataset.* This experiment is performed on the *CIFAR-10* dataset, which is used for image classification tasks. The dataset is divided into two parts: 10000 images for the test set and the remaining 50000 images for the training set.

*Search Phase.* The search phase is implemented in PyTorch using the *Single-Path One-Shot* (SPOS) method (Guo et al. 2020), a state-of-the-art NAS algorithm. The search space is a single-path supernet composed of 20 choice blocks connected in series, each with 4 choices. Thus, the search space size is  $4^{20}$ . In Zhong and Hong (2022), the problem dimension reaches  $10^6$ , but the architecture search phase at this scale is estimated to take over 500 hours in a virtual machine with a RTX 3090 (24GB) GPU. Therefore, in our experiment, we set the number of alternative architectures to be  $p = 10^5$  (the extensive time consumption is attributed to the search algorithm, not P3C itself).

*Ranking and selection.* The R&S phase is conducted under the same parallel computing environment as described in Section 7.2. After obtaining  $10^5$  alternative architectures, we use P3C-GBA, GBA, P3C-CBA, CBA, FBKT and EA to allocate computational resources for performance evaluation and select the best one. In GBA, we perform only one round of “clustering and conquer”. One simulation observation corresponds to testing an architecture on a batch of 32 images. Therefore, the maximum sample size for each alternative is  $\frac{10000}{32} \approx 312$ . This experiment does not involve intentional use of CRN, and the initialization sample size  $N_0 = 20$ . The moPCS (or  $\text{PCS}_{\text{trad}}$ ) values are directly estimated based on 1000 independent macro replications. The true best [1] (invisible to the users and used solely for the final  $\text{PCS}_{\text{trad}}$  calculation) is estimated by selecting the alternative with the highest accuracy on the entire test set. Moreover, in the Stage 2 of “divide and conquer” and P3C, the moPCS (or  $\text{PCS}_{\text{trad}}$ ) values vary across different processors. The overall moPCS (or  $\text{PCS}_{\text{trad}}$ ) for Stage 2 is approximated by a weighted average based on the number of alternatives on each processor.

The experimental results under moPCS metric and PrOS policy are depicted in Figure 6(a), and the results under  $\text{PCS}_{\text{trad}}$  metric and  $\tau^m$  selection policy are depicted in Figure 6(b). This experiment is a low-confidence scenario, where 95% of the alternatives’ mean performances fall within the interval (0.878, 0.889). As shown in the Figure 6(b),  $\text{PCS}_{\text{trad}}$  is extremely low under several existing benchmark sampling strategies. Comparing Figures 6(a) and (b), under the same sampling strategy, moPCS is found to achieve values tens of times higher than  $\text{PCS}_{\text{trad}}$  using only about  $\frac{1}{10}$  of the budget. This indicates that in low-confidence scenarios, the maximum mean and the maximum individual PCS are often inconsistent, as analyzed in Section 4.1.2. Employing the PrOS policy along with the moPCS metric is advantageous in such a case. Otherwise, the traditional

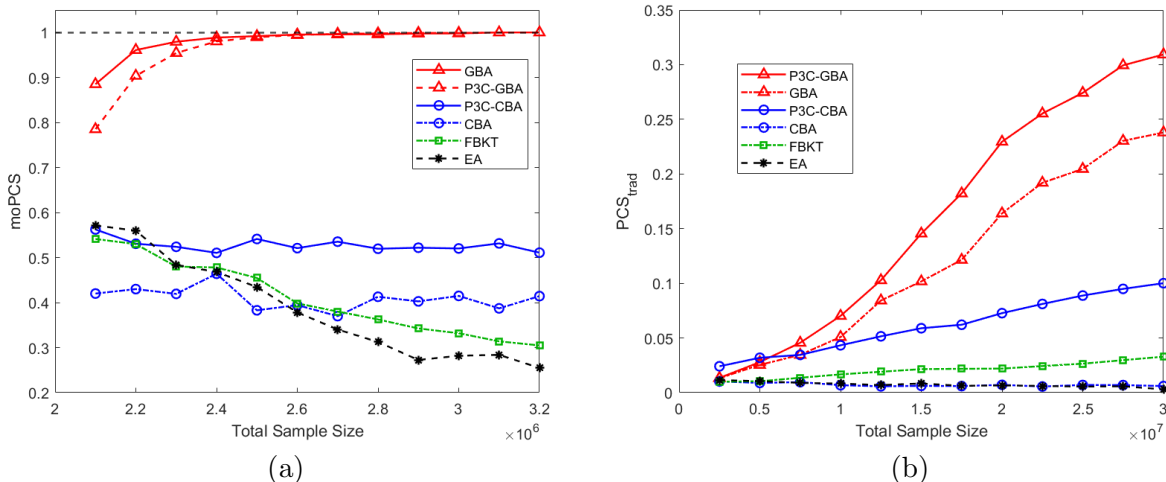


**Figure 6** (a) Comparison of different R&S procedures under moPCS metric (b) Comparison of different R&S procedures under  $PCS_{\text{trad}}$  metric. Since the initialization sample size is  $N_0 = 20$ , the curves do not start from “Total Sample Size = 0”.

$\tau^m$  selection policy and  $PCS_{\text{trad}}$  metric would overlook many alternatives that have a much higher probability of being the best.

As shown in Figure 6(a), P3C-GBA and GBA significantly outperform the other methods under the moPCS metric, quickly converging to 1 with a relatively small sample size. P3C-GBA slightly exceeds GBA in the early stages. The improvement brought by P3C is even more evident in CBA, where the average moPCS of P3C-CBA is 41% higher than that of CBA. Additionally, existing methods such as CBA, FBKT, and EA show a decline in moPCS as the total sample size increases, which aligns with the negative effect of sample size described in Proposition 3.

Under the  $PCS_{\text{trad}}$  metric, as shown in Figure 6(b), P3C-GBA and GBA still significantly outperform the other methods, with P3C-GBA exceeding GBA by 30%. For EA and standard CBA, due to the large problem size and the low-confidence scenario, the  $PCS_{\text{trad}}$  metric does not show significant growth as the total sample size increases from  $0.25 \times 10^7$  to  $3 \times 10^7$ . With FBKT, the  $PCS_{\text{trad}}$  metric increases but remains below 0.05. However, when combined with P3C, CBA surprisingly improves by a factor of 8.5, surpassing FBKT, which further supports the effectiveness of P3C in large-scale fixed-budget R&S.

## 8. Concluding Remarks

This paper shows that the class of rate-optimal R&S methods is relatively broad. Many traditional methods, when integrated with the multi-round mechanism of P3C, or even some simple greedy strategies, can achieve linear growth rate in sample size. However, their performance may still be suboptimal, as the slope of the growth curve may remain relatively steep. Consequently,

there exists considerable potential for further enhancement of rate-optimal R&S methods, particularly in reducing the slope of the growth rate. In this paper, both theoretical and empirical evidence suggest that leveraging correlation information is a viable path to overcoming the sample efficiency bottleneck in large-scale R&S problems. However, in large-scale scenarios, correlation parameters are often imprecisely estimated, making fine-tuned allocation strategies that rely on accurate parameter estimation ineffective. In contrast, the P3C procedure presented in this paper is a ready-to-use tool that achieves significant improvements without requiring excessively high clustering accuracy; it only needs to identify which alternatives are highly correlated.

## References

- Al-Kandari NM, Jolliffe IT (2001) Variable selection and interpretation of covariance principal components. *Communications in Statistics-Simulation and Computation* 30(2):339–354.
- Bechhofer RE (1954) A single-sample multiple decision procedure for ranking means of normal populations with known variances. *The Annals of Mathematical Statistics* 16–39.
- Branke J, Chick SE, Schmidt C (2007) Selecting a selection procedure. *Management Science* 53(12):1916–1932.
- Chen CH, Chick SE, Lee LH, Pujowidianto NA (2015) Ranking and selection: Efficient simulation budget allocation. *Handbook of Simulation Optimization* 45–80.
- Chen CH, Lin J, Yücesan E, Chick SE (2000) Simulation budget allocation for further enhancing the efficiency of ordinal optimization. *Discrete Event Dynamic Systems* 10:251–270.
- Chen W, Gao S, Chen W, Du J (2023) Optimizing resource allocation in service systems via simulation: A bayesian formulation. *Production and Operations Management* 32(1):65–81.
- Chen X, Ankenman BE, Nelson BL (2012) The effects of common random numbers on stochastic kriging metamodels. *ACM Transactions on Modeling and Computer Simulation (TOMACS)* 22(2):1–20.
- Chen Y, Ryzhov IO (2023) Balancing optimal large deviations in sequential selection. *Management Science* 69(6):3457–3473.
- Chick SE, Branke J, Schmidt C (2010) Sequential sampling to myopically maximize the expected value of information. *INFORMS Journal on Computing* 22(1):71–80.
- Chick SE, Inoue K (2001) New two-stage and sequential procedures for selecting the best simulated system. *Operations Research* 49(5):732–743.
- Chick SE, Wu Y (2005) Selection procedures with frequentist expected opportunity cost bounds. *Operations Research* 53(5):867–878.
- Ding L, Zhang X (2024) Sample and computationally efficient stochastic kriging in high dimensions. *Operations Research* 72(2):660–683.

- Du J, Gao S, Chen CH (2024) A contextual ranking and selection method for personalized medicine. *Manufacturing & Service Operations Management* 26(1):167–181.
- Eckman DJ, Henderson SG (2022) Posterior-based stopping rules for bayesian ranking-and-selection procedures. *INFORMS Journal on Computing* 34(3):1711–1728.
- Even-Dar E, Mannor S, Mansour Y, Mahadevan S (2006) Action elimination and stopping conditions for the multi-armed bandit and reinforcement learning problems. *Journal of machine learning research* 7(6).
- Fan J, Li R, Zhang CH, Zou H (2020) *Statistical foundations of data science* (CRC press).
- Frazier P, Powell W, Dayanik S (2009) The knowledge-gradient policy for correlated normal beliefs. *INFORMS journal on Computing* 21(4):599–613.
- Frazier PI, Powell WB, Dayanik S (2008) A knowledge-gradient policy for sequential information collection. *SIAM Journal on Control and Optimization* 47(5):2410–2439.
- Free SM, Wilson JW (1964) A mathematical contribution to structure-activity studies. *Journal of medicinal chemistry* 7(4):395–399.
- Fu MC, Hu JQ, Chen CH, Xiong X (2007) Simulation allocation for determining the best design in the presence of correlated sampling. *INFORMS Journal on Computing* 19(1):101–111.
- Gao S, Chen W, Shi L (2017) A new budget allocation framework for the expected opportunity cost. *Operations Research* 65(3):787–803.
- Glasserman P, Yao DD (1992) Some guidelines and guarantees for common random numbers. *Management Science* 38(6):884–908.
- Glynn P, Juneja S (2004) A large deviations perspective on ordinal optimization. *Proceedings of the 2004 Winter Simulation Conference, 2004.*, volume 1 (IEEE).
- Guo Z, Zhang X, Mu H, Heng W, Liu Z, Wei Y, Sun J (2020) Single path one-shot neural architecture search with uniform sampling. *Computer Vision—ECCV 2020: 16th European Conference, Glasgow, UK, August 23–28, 2020, Proceedings, Part XVI 16*, 544–560 (Springer).
- Hong LJ, Fan W, Luo J (2021) Review on ranking and selection: A new perspective. *Frontiers of Engineering Management* 8(3):321–343.
- Hong LJ, Jiang G, Zhong Y (2022) Solving large-scale fixed-budget ranking and selection problems. *INFORMS Journal on Computing* 34(6):2930–2949.
- Hong LJ, Nelson BL (2005) The tradeoff between sampling and switching: New sequential procedures for indifference-zone selection. *IIE Transactions* 37(7):623–634.
- Hunter SR, Nelson BL (2017) Parallel ranking and selection. *Advances in Modeling and Simulation: Seminal Research from 50 Years of Winter Simulation Conferences*, 249–275 (Springer).
- Jeff Hong L (2006) Fully sequential indifference-zone selection procedures with variance-dependent sampling. *Naval Research Logistics (NRL)* 53(5):464–476.

- Jolliffe IT (1972) Discarding variables in a principal component analysis. i: Artificial data. *Journal of the Royal Statistical Society Series C: Applied Statistics* 21(2):160–173.
- Katz R, Osborne SF, Ionescu F (1977) Application of the free-wilson technique to structurally related series of homologs. quantitative structure-activity relationship studies of narcotic analgetics. *Journal of Medicinal Chemistry* 20(11):1413–1419.
- Kim SH, Nelson BL (2001) A fully sequential procedure for indifference-zone selection in simulation. *ACM Transactions on Modeling and Computer Simulation (TOMACS)* 11(3):251–273.
- Kim T, Kim Kk, Song E (2022) Selection of the most probable best. *arXiv preprint arXiv:2207.07533* .
- L Salemi P, Song E, Nelson BL, Staum J (2019) Gaussian markov random fields for discrete optimization via simulation: Framework and algorithms. *Operations Research* 67(1):250–266.
- L’Ecuyer P (1990) Random numbers for simulation. *Communications of the ACM* 33(10):85–97.
- Ledoit O, Wolf M (2020) Analytical nonlinear shrinkage of large-dimensional covariance matrices. *The Annals of Statistics* 48(5):3043–3065.
- Li H, Lam H, Peng Y (2022) Efficient learning for clustering and optimizing context-dependent designs. *Operations Research* .
- Li K, Jin X, Jia QS, Ren D, Xia H (2023) An ocba-based method for efficient sample collection in reinforcement learning. *IEEE Transactions on Automation Science and Engineering* .
- Li Y, Fu MC, Xu J (2021) An optimal computing budget allocation tree policy for monte carlo tree search. *IEEE Transactions on Automatic Control* 67(6):2685–2699.
- Li Z, Fan W, Hong LJ (2024) The (surprising) sample optimality of greedy procedures for large-scale ranking and selection. *Management Science* .
- Liu X, Peng Y, Zhang G, Zhou R (2024) An efficient node selection policy for monte carlo tree search with neural networks. *INFORMS Journal on Computing* .
- Luo J, Hong LJ, Nelson BL, Wu Y (2015) Fully sequential procedures for large-scale ranking-and-selection problems in parallel computing environments. *Operations Research* 63(5):1177–1194.
- Mellor J, Turner J, Storkey A, Crowley EJ (2021) Neural architecture search without training. *International Conference on Machine Learning*, 7588–7598 (PMLR).
- Negoescu DM, Frazier PI, Powell WB (2011) The knowledge-gradient algorithm for sequencing experiments in drug discovery. *INFORMS Journal on Computing* 23(3):346–363.
- Nelson BL, Matejcek FJ (1995) Using common random numbers for indifference-zone selection and multiple comparisons in simulation. *Management Science* 41(12):1935–1945.
- Ni EC, Ciocan DF, Henderson SG, Hunter SR (2017) Efficient ranking and selection in parallel computing environments. *Operations Research* 65(3):821–836.

- Pei L, Nelson BL, Hunter SR (2022) Parallel adaptive survivor selection. *Operations Research* .
- Peng Y, Chen CH, Fu MC, Hu JQ (2015) Non-monotonicity of probability of correct selection. *2015 Winter Simulation Conference (WSC)*, 3678–3689 (IEEE).
- Peng Y, Chen CH, Fu MC, Hu JQ (2016) Dynamic sampling allocation and design selection. *INFORMS Journal on Computing* 28(2):195–208.
- Peng Y, Chen CH, Fu MC, Hu JQ (2017) Gradient-based myopic allocation policy: An efficient sampling procedure in a low-confidence scenario. *IEEE Transactions on Automatic Control* 63(9):3091–3097.
- Qu H, Ryzhov IO, Fu MC, Ding Z (2015) Sequential selection with unknown correlation structures. *Operations Research* 63(4):931–948.
- Rinott Y (1978) On two-stage selection procedures and related probability-inequalities. *Communications in Statistics-Theory and methods* 7(8):799–811.
- Russo D (2020) Simple bayesian algorithms for best-arm identification. *Operations Research* 68(6):1625–1647.
- Ryzhov IO (2016) On the convergence rates of expected improvement methods. *Operations Research* 64(6):1515–1528.
- Shen H, Hong LJ, Zhang X (2021) Ranking and selection with covariates for personalized decision making. *INFORMS Journal on Computing* 33(4):1500–1519.
- Snell J, Swersky K, Zemel R (2017) Prototypical networks for few-shot learning. *Advances in neural information processing systems* 30.
- Vigneau E, Qannari E (2003) Clustering of variables around latent components. *Communications in Statistics-Simulation and Computation* 32(4):1131–1150.
- Xu J, Huang E, Hsieh L, Lee LH, Jia QS, Chen CH (2016) Simulation optimization in the era of industrial 4.0 and the industrial internet. *Journal of Simulation* 10(4):310–320.
- Zhang H, Zheng Z, Lavaei J (2023) Gradient-based algorithms for convex discrete optimization via simulation. *Operations research* 71(5):1815–1834.
- Zhong Y, Hong LJ (2022) Knockout-tournament procedures for large-scale ranking and selection in parallel computing environments. *Operations Research* 70(1):432–453.
- Zhou Y, Fu MC, Ryzhov IO (2023) Sequential learning with a similarity selection index. *Operations Research* .
- Zhu Y, Dong J, Lam H (2024) Uncertainty quantification and exploration for reinforcement learning. *Operations Research* 72(4):1689–1709.

## Online Appendices

Before starting the appendix, we first introduce some notations:  $\text{PCS}(\tau) = P(\bar{x}_\tau - \bar{x}_j > 0, j \neq \tau)$ . The vector  $(\bar{x}_\tau - \bar{x}_1, \dots, \bar{x}_\tau - \bar{x}_p)$  has a joint normal distribution with mean  $(\mu_\tau - \mu_1, \dots, \mu_\tau - \mu_p)$  and covariance matrix  $\Lambda^\tau = [\Lambda_{ij}^\tau]_{(p-1) \times (p-1)}$ , where  $\Lambda_{ij}^\tau = \text{cov}(\bar{x}_\tau - \bar{x}_i, \bar{x}_\tau - \bar{x}_j)$ ,  $i, j \in \mathcal{P} \setminus \{\tau\}$ .  $\text{PCS}(\tau)$  can be rewritten as  $P(y_1^\tau > -d_1^\tau, \dots, y_p^\tau > -d_p^\tau)$ , where  $y_i^\tau = \frac{\bar{x}_\tau - \bar{x}_i - (\mu_\tau - \mu_i)}{\sqrt{\lambda_i^\tau}}$ ,  $d_i^\tau = \frac{\mu_\tau - \mu_i}{\sqrt{\lambda_i^\tau}}$ , and  $\lambda_i^\tau = \text{var}(\bar{x}_\tau - \bar{x}_i) = \frac{\sigma_\tau^2}{N_\tau} + \frac{\sigma_i^2}{N_i} - 2\frac{\text{cov}(X_\tau, X_i)}{N_{\tau,i}}$  ( $i \in \mathcal{P} \setminus \{\tau\}$ ). Then  $\mathbf{y}^\tau = (y_1^\tau, \dots, y_{\tau-1}^\tau, y_{\tau+1}^\tau, \dots, y_p^\tau) \sim N(0, \Phi^\tau)$  with probability density function  $f_{\mathbf{y}^\tau}$ . The covariance matrix is

$$\Phi^\tau = \begin{pmatrix} 1 & \cdots & \tilde{r}_{1,p}^\tau \\ \vdots & \ddots & \vdots \\ \tilde{r}_{p,1}^\tau & \cdots & 1 \end{pmatrix}_{(p-1) \times (p-1)},$$

where  $\tilde{r}_{i,j}^\tau$  is the correlation coefficient between  $(\bar{x}_\tau - \bar{x}_i)$  and  $(\bar{x}_\tau - \bar{x}_j)$ ,  $i, j \in \mathcal{P} \setminus \{\tau\}$ . If Assumption 3 holds and  $p$  is fixed,  $\Lambda_{ij}^\tau = \frac{\sigma_\tau^2}{N_\tau} + \frac{\text{cov}(X_i, X_j)}{N_{i,j}} - \frac{\text{cov}(X_\tau, X_i)}{N_{\tau,i}} - \frac{\text{cov}(X_\tau, X_j)}{N_{\tau,j}} \sim \mathcal{O}(\frac{1}{N})$  and  $\lambda_i^\tau, \lambda_j^\tau \sim \mathcal{O}(\frac{1}{N})$ , then we have  $\tilde{r}_{i,j}^\tau \sim \mathcal{O}(1)$ , meaning that its order does not increase with the growth of  $N$ .

### EC.1. Proofs of Theorem 1 and Proposition 1.

#### EC.1.1. Proofs of Theorem 1

*Proof* (1) The derivative of  $\text{PCS}(\tau)$  with respect to mean  $\mu_\tau$  is given by

$$\begin{aligned} \frac{\partial \text{PCS}(\tau)}{\partial \mu_\tau} &= \frac{\partial}{\partial \mu_\tau} P(y_1^\tau > -d_1^\tau, \dots, y_p^\tau > -d_p^\tau) \\ &= \frac{\partial}{\partial \mu_\tau} d_1^\tau \int_{-d_2^\tau}^\infty \cdots \int_{-d_p^\tau}^\infty f_{\mathbf{y}^\tau}(-d_1^\tau, y_2, \dots, y_p) dy_2 \cdots dy_p + \cdots \\ &\quad + \frac{\partial}{\partial \mu_\tau} d_p^\tau \int_{-d_1^\tau}^\infty \cdots \int_{-d_{p-1}^\tau}^\infty f_{\mathbf{y}^\tau}(y_1, y_2, \dots, -d_p^\tau) dy_1 \cdots dy_{p-1}. \end{aligned} \quad (\text{EC.1.1})$$

Each term in (EC.1.1) is bounded and  $\text{PCS}(\tau)$  is differentiable at any point within the domain of  $\mu_\tau$  because the left and right derivatives are identical. Similarly,  $\text{PCS}(\tau)$  is also differentiable with respect to  $\mu_i$  for  $i \in \mathcal{P} \setminus \{\tau\}$ . Additionally, it is straightforward to verify that the partial derivative  $\frac{\partial \text{PCS}(\tau)}{\partial \mu_i}$  ( $i \in \mathcal{P}$ ) is continuous. Therefore,  $\text{PCS}(\tau)$  is differentiable with respect to  $\boldsymbol{\mu} = (\mu_1, \dots, \mu_p)$ . Since  $\frac{\partial d_i^\tau}{\partial \mu_\tau} > 0$  holds for any  $i \in \mathcal{P} \setminus \{\tau\}$ , we have  $\frac{\partial \text{PCS}(\tau)}{\partial \mu_\tau} > 0$ .

(2) Next, we prove that  $\tau^*$  converges to [1] almost surely as  $N_i \rightarrow \infty$ ,  $\forall i \in \mathcal{P}$ . For any  $\tau \neq [1]$ , there exists  $i_0(\tau) \in \mathcal{P}$ , s.t.  $\mu_\tau - \mu_{i_0} < 0$ . Then  $d_{i_0}^\tau \rightarrow -\infty$  when  $N_i \rightarrow \infty$ ,  $\forall i \in \mathcal{P}$ . Then we have

$$\text{PCS}(\tau) = P(y_1^\tau > -d_1^\tau, \dots, y_p^\tau > -d_p^\tau) \leq P(y_{i_0}^\tau > -d_{i_0}^\tau) \rightarrow 0.$$

Notice that  $d_i^{[1]} \rightarrow +\infty$  for any  $i \in \mathcal{P} \setminus \{[1]\}$  when  $N_i \rightarrow \infty$ . Therefore,  $P(y_i^{[1]} > -d_i^{[1]}) \rightarrow 1$ . Then we have

$$\begin{aligned} \text{PCS}([1]) &= P(y_1^{[1]} > -d_1^{[1]}, \dots, y_p^{[1]} > -d_p^{[1]}) \\ &\geq \sum_{i \in \mathcal{P} \setminus \{[1]\}} P(y_i^{[1]} > -d_i^{[1]}) - (p-2) \rightarrow p-1 - (p-2) = 1. \end{aligned}$$

Since  $\tau^*$  is the one maximizing  $\text{PCS}(\tau)$ ,  $\tau^* \rightarrow [1]$  almost surely.  $\square$

### EC.1.2. Proof of Proposition 1.

*Proof* First, we consider the situation when all means are equal, i.e.,  $\boldsymbol{\mu} = (\mu_1, \dots, \mu_p)$  where  $\mu_1 = \dots = \mu_p$ . Under this parameter figuration, by Slepian normal comparison lemma (Azaïs and Wschebor 2009), for any  $\tau \in \mathcal{P} \setminus \{\tau_0\}$ , we have

$$\begin{aligned} & \text{PCS}(\tau; \boldsymbol{\mu}) - \text{PCS}(\tau_0; \boldsymbol{\mu}) \\ &= P(y_1^\tau > 0, \dots, y_p^\tau > 0) - P(y_1^{\tau_0} > 0, \dots, y_p^{\tau_0} > 0) \\ &\leq \frac{1}{2\pi} \sum_{1 \leq i < j \leq p} (\arcsin \tilde{r}_{i,j}^\tau - \arcsin \tilde{r}_{i,j}^{\tau_0})^+ = 0. \end{aligned}$$

Therefore,  $\text{PCS}(\tau_0)$  is the maximum. According to Theorem 1,  $\text{PCS}(\tau)$  is a continuous function of the mean vector. Therefore, if we modify each  $\mu_\tau (\tau \neq \tau_0)$  slightly by  $\delta_\tau$  to construct a new parameter figuration  $\boldsymbol{\mu}' = (\mu'_1, \dots, \mu'_p)$ , where  $\mu'_\tau = \mu_\tau + \delta_\tau (\tau \neq \tau_0)$  and  $\mu'_{\tau_0} = \mu_{\tau_0}$ , there exists a  $\delta > 0$ , s.t. if  $|\delta_\tau| < \delta$  holds for any  $\tau \neq \tau_0$ , then

$$|\text{PCS}(\tau; \boldsymbol{\mu}') - \text{PCS}(\tau; \boldsymbol{\mu})| < \frac{1}{2}(\text{PCS}(\tau_0; \boldsymbol{\mu}) - \text{PCS}(\tau; \boldsymbol{\mu})),$$

and

$$|\text{PCS}(\tau_0; \boldsymbol{\mu}') - \text{PCS}(\tau_0; \boldsymbol{\mu})| < \frac{1}{2}(\text{PCS}(\tau_0; \boldsymbol{\mu}) - \text{PCS}(\tau; \boldsymbol{\mu})).$$

Then we have

$$\begin{aligned} & \text{PCS}(\tau_0; \boldsymbol{\mu}') - \text{PCS}(\tau; \boldsymbol{\mu}') = \text{PCS}(\tau_0; \boldsymbol{\mu}) + \text{PCS}(\tau_0; \boldsymbol{\mu}') - \text{PCS}(\tau_0; \boldsymbol{\mu}) \\ & \quad - [\text{PCS}(\tau; \boldsymbol{\mu}) + \text{PCS}(\tau; \boldsymbol{\mu}') - \text{PCS}(\tau; \boldsymbol{\mu})] \\ & > \text{PCS}(\tau_0; \boldsymbol{\mu}) - \text{PCS}(\tau; \boldsymbol{\mu}) - 2 \times \frac{1}{2} \times (\text{PCS}(\tau_0; \boldsymbol{\mu}) - \text{PCS}(\tau; \boldsymbol{\mu})) = 0. \end{aligned}$$

$\text{PCS}(\tau_0)$  is still the maximum.  $\tau^* = \tau_0$ .  $\square$

## EC.2. The Gradient Analysis with respect to Correlation Information

### EC.2.1. Proofs of Theorem 2, Corollary 1 and Lemma 1.

Here, we prove a more general result that encompasses not only the derivative of PCS with respect to the correlation information but also the derivative with respect to variance information.

(a)  $\frac{\partial \text{PCS}(\tau)}{\partial \sigma_\tau} = D^+ + D^- + I$ , where  $D^+ = \sum_{i \in \mathcal{I}^+} D_i^\tau$ ,  $D^- = \sum_{i \in \mathcal{I}^-} D_i^\tau$ , and the term  $D_i^\tau > 0$  for  $i \in \mathcal{I}^+(\tau)$ ,  $D_i^\tau < 0$  for  $i \in \mathcal{I}^-(\tau)$ ;

(b) **Theorem 2:**  $\forall i \in \mathcal{P} \setminus \{\tau\}$ ,  $\frac{\partial \text{PCS}(\tau)}{\partial r_{\tau i}} = \tilde{D}_i^\tau + \tilde{I}_i^\tau$ , where  $\tilde{D}_i^\tau > 0$  for  $i \in \mathcal{I}^-(\tau)$  and  $< 0$  for  $i \in \mathcal{I}^+(\tau)$ .

$\tilde{I}_i^\tau = \sum_{j \in \{1, \dots, p\} \setminus \{i, \tau\}} \tilde{I}_i^{\tau, j}$ .  $\text{sign}(\tilde{I}_i^{\tau, j}) = \text{sign}(-\sigma_i^2(N_i)^{-1} + r_{\tau, i} \sigma_\tau \sigma_i (N_{\tau, i})^{-1} - r_{\tau, j} \sigma_\tau \sigma_j (N_{\tau, j})^{-1} + r_{i, j} \sigma_i \sigma_j (N_{i, j})^{-1})$ ;

(c) **Lemma 1:**  $\forall i, j \in \mathcal{P} \setminus \{\tau\}$ ,  $\frac{\partial \text{PCS}(\tau)}{\partial r_{ij}} \geq 0$ . If  $\mathcal{D}_i^\tau < \mathcal{S}_i^\tau$ , then  $\frac{\partial \text{PCS}(\tau)}{\partial r_{ij}} \sim o\left(\left|\frac{\partial \text{PCS}(\tau)}{\partial r_{i\tau}}\right|\right)$ .

The notations in the appendix differ slightly from those in the main text. The symbols  $D_i^\tau$  and

$I_i^\tau$  in the main text correspond to  $\tilde{D}_i^\tau$  and  $\tilde{I}_i^\tau$  here. The proof of Corollary 1 is embedded in (b). Moreover, it is important to note that, in this subsection, when it comes to asymptotic results, we consider the asymptotic regime where sample size  $N$  goes to infinity while keeping  $p$  fixed.

*Proof* (a) The derivative of PCS( $\tau$ ) with respect to the variance of  $\tau$  is given by

$$\begin{aligned}
\frac{\partial \text{PCS}(\tau)}{\partial \sigma_\tau} &= \frac{\partial P(y_1^\tau > -d_1^\tau, \dots, y_p^\tau > -d_p^\tau)}{\partial \sigma_\tau} \\
&= \sum_{i=1, \dots, p, i \neq \tau} \frac{\partial d_i^\tau}{\partial \sigma_\tau} \frac{\partial \text{PCS}(\tau)}{\partial d_i^\tau} + 2 \sum_{1 \leq i < j \leq p, i, j \neq \tau} \frac{\partial \text{PCS}(\tau)}{\partial \tilde{r}_{i,j}^\tau} \frac{\partial \tilde{r}_{i,j}^\tau}{\partial \sigma_\tau} \\
&= \frac{\partial d_1^\tau}{\partial \sigma_\tau} \int_{-d_2}^{\infty} \cdots \int_{-d_p^\tau}^{\infty} f_{y^\tau}(-d_1^\tau, y_2, \dots, y_p) dy_2 \cdots dy_p + \cdots \\
&+ \frac{\partial d_p^\tau}{\partial \sigma_\tau} \int_{-d_1^\tau}^{\infty} \cdots \int_{-d_{p-1}^\tau}^{\infty} f_{y^\tau}(y_1, y_2, \dots, -d_p^\tau) dy_1 \cdots dy_{p-1} \\
&+ 2 \sum_{1 \leq i < j \leq p, i, j \neq \tau} \frac{\partial \text{PCS}(\tau)}{\partial \tilde{r}_{i,j}^\tau} \frac{\partial \tilde{r}_{i,j}^\tau}{\partial \sigma_\tau} \\
&= D^+ - D^- + I,
\end{aligned} \tag{EC.2.1}$$

where

$$D^+ \triangleq \sum_{i \in \mathcal{P} \setminus \{\tau\}} \max\{0, D_i^\tau\},$$

$$D^- \triangleq \sum_{i \in \mathcal{P} \setminus \{\tau\}} \min\{0, D_i^\tau\},$$

$$D_i^\tau \triangleq \frac{\partial d_i^\tau}{\partial \sigma_\tau} \int_{-d_1^\tau}^{\infty} \cdots \int_{-d_{i-1}^\tau}^{\infty} \int_{-d_{i+1}^\tau}^{\infty} \cdots \int_{-d_{\tau-1}^\tau}^{\infty} \int_{-d_{\tau+1}^\tau}^{\infty} \cdots \int_{-d_p^\tau}^{\infty} f_{y^\tau}(y_1, \dots, -d_i^\tau, \dots, y_p) dy_1 \cdots dy_p, \tag{EC.2.2}$$

$$I = 2 \sum_{1 \leq i < j \leq p, i, j \neq \tau} \frac{\partial \text{PCS}(\tau)}{\partial \tilde{r}_{i,j}^\tau} \frac{\partial \tilde{r}_{i,j}^\tau}{\partial \sigma_\tau}. \tag{EC.2.3}$$

$D^+$  is the sum of the positive parts of  $D_i^\tau$  ( $i \in \mathcal{P} \setminus \{\tau\}$ ) and  $D^-$  is the sum of negative parts of them. Notice that  $d_i^\tau = \frac{\mu_\tau - \mu_i}{\sqrt{\lambda_i^\tau}}$  is not necessarily non-negative as  $\mu_\tau$  does not always exceed  $\mu_i$ . If  $i \in \mathcal{I}^+(\tau) \triangleq \{i | \mu_i > \mu_\tau, i \in \mathcal{P} \setminus \{\tau\}\}$ ,  $\frac{\partial d_i^\tau}{\partial \sigma_\tau} > 0$ , the term  $D_i > 0$ , which will only contribute to  $D^+$ . Conversely, if  $i \in \mathcal{I}^-$ , the term  $D_i < 0$  and it is only accounted for in  $D^-$ . This means that  $D^+ = \sum_{i \in \mathcal{I}^+} D_i$  and  $D^- = \sum_{i \in \mathcal{I}^-} |D_i|$ .

In the following part, we will evaluate the growth rate of the terms  $D_i$  and  $I$  as the total sample size  $N$  increases. First, we prove that  $\frac{\partial \text{PCS}(\tau)}{\partial \tilde{r}_{i,j}^\tau}$  is bounded. With Slepian normal comparison lemma, we have

$$\begin{aligned}
0 &\leq \frac{\text{PCS}(\tau; \tilde{r}_{i,j}^\tau + \delta) - \text{PCS}(\tau; \tilde{r}_{i,j}^\tau)}{\delta} \\
&\leq \frac{\arcsin(\tilde{r}_{i,j}^\tau + \delta) - \arcsin(\tilde{r}_{i,j}^\tau)}{2\pi\delta} \times \exp\left(-\frac{(d_i^\tau)^2 + (d_j^\tau)^2}{2(1 + \max\{|\arcsin(\tilde{r}_{i,j}^\tau + \delta)|, \arcsin(\tilde{r}_{i,j}^\tau)\})}\right).
\end{aligned}$$

Let  $\delta \rightarrow 0$ , then

$$0 \leq \frac{\partial \text{PCS}(\tau)}{\partial \tilde{r}_{i,j}^\tau} \leq \frac{1}{2\pi \sqrt{1 - (\tilde{r}_{i,j}^\tau)^2}} \exp\left(-\frac{(d_i^\tau)^2 + (d_j^\tau)^2}{2(1 + \arcsin(\tilde{r}_{i,j}^\tau))}\right). \quad (\text{EC.2.4})$$

According to Assumption 3, we have  $N_i \sim \mathcal{O}(N)$ ,  $\forall i \in \mathcal{P}$  ( $p$  is fixed). Then  $d_i^\tau = \frac{\mu_\tau - \mu_i}{\sqrt{\frac{\sigma_\tau^2}{N_\tau} + \frac{\sigma_i^2}{N_i} - 2\frac{\text{cov}(X_\tau, X_i)}{N_{\tau,i}}}} \sim \mathcal{O}(\sqrt{N})$  and  $\tilde{r}_{i,j}^\tau \sim \mathcal{O}(1)$ . Then

$$\frac{\partial \text{PCS}(\tau)}{\partial \tilde{r}_{i,j}^\tau} \sim \mathcal{O}\left(\exp\left(-\frac{(d_i^\tau)^2 + (d_j^\tau)^2}{2(1 + \arcsin(\tilde{r}_{i,j}^\tau))}\right)\right),$$

and we can introduce a positive constant  $\mathcal{S}_{ij}^\tau$  such that  $\frac{\partial \text{PCS}(\tau)}{\partial \tilde{r}_{i,j}^\tau} \sim \mathcal{O}(e^{-\mathcal{S}_{ij}^\tau N})$ .

We define

$$\begin{aligned} \mathcal{S}_i^\tau &= \min_{j \neq i} \mathcal{S}_{ij}^\tau, \\ \mathcal{S}^\tau &= \min_{i \in \mathcal{P} \setminus \{\tau\}} \mathcal{S}_i^\tau. \end{aligned}$$

It is straightforward to verify that  $\frac{\partial \tilde{r}_{i,j}^\tau}{\partial \sigma_\tau} \sim \mathcal{O}(1)$  by definition. Then with (EC.2.3), we have

$$E \sim \mathcal{O}\left(\exp\left(-\min_{i,j \in \mathcal{P} \setminus \{\tau\}} \frac{(d_i^\tau)^2 + (d_j^\tau)^2}{2(1 + \arcsin(\tilde{r}_{i,j}^\tau))}\right)\right) \sim \mathcal{O}(e^{-\mathcal{S}^\tau N}). \quad (\text{EC.2.5})$$

Then, by definition, we have

$$\frac{\partial d_i^\tau}{\partial \sigma_\tau} \sim \mathcal{O}(\sqrt{N}). \quad (\text{EC.2.6})$$

Next, we will evaluate the following integral for each  $i \in \mathcal{P} \setminus \{\tau\}$ :

$$\begin{aligned} \frac{D_i^\tau}{\frac{\partial d_i^\tau}{\partial \sigma_\tau}} &= \int_{-d_1^\tau}^{\infty} \cdots \int_{-d_{i-1}^\tau}^{\infty} \int_{-d_{i+1}^\tau}^{\infty} \cdots \int_{-d_{\tau-1}^\tau}^{\infty} \int_{-d_{\tau+1}^\tau}^{\infty} \cdots \int_{-d_p^\tau}^{\infty} f_{y^\tau}(y_1, \dots, -d_i^\tau, \dots, y_p) dy_1 \cdots dy_p \\ &= f_{y_i^\tau}(-d_i^\tau) \int_{-d_1^\tau}^{\infty} \cdots \int_{-d_{i-1}^\tau}^{\infty} \int_{-d_{i+1}^\tau}^{\infty} \cdots \int_{-d_{\tau-1}^\tau}^{\infty} \int_{-d_{\tau+1}^\tau}^{\infty} \cdots \int_{-d_p^\tau}^{\infty} f_{y^\tau|y_i^\tau}(y_1, \dots, y_p) dy_1 \cdots dy_p. \end{aligned} \quad (\text{EC.2.7})$$

$f_{y_i^\tau}$  is the marginal density of  $y_i^\tau$ , which is standard normal, and  $f_{y^\tau|y_i^\tau}$  is the conditional density of  $y^\tau$  given  $y_i^\tau$ , which is a multivariate normal distribution  $N(\tilde{\mu}_i, \tilde{\Sigma}_i)$  of dimension  $p-2$  with mean and covariance given by

$$\tilde{\mu}_i = (-d_i^\tau \tilde{r}_{i,1}^\tau, \dots, -d_i^\tau \tilde{r}_{i,p}^\tau), \quad (\text{EC.2.8})$$

$$\tilde{\Sigma}_i = \begin{pmatrix} 1 - (\tilde{r}_{i,1}^\tau)^2 & \tilde{r}_{1,2}^\tau - \tilde{r}_{i,1}^\tau \tilde{r}_{i,2}^\tau & \cdots & \tilde{r}_{1,p}^\tau - \tilde{r}_{i,1}^\tau \tilde{r}_{i,p}^\tau \\ \tilde{r}_{2,1}^\tau - \tilde{r}_{i,2}^\tau \tilde{r}_{i,1}^\tau & 1 - (\tilde{r}_{i,2}^\tau)^2 & \cdots & \tilde{r}_{2,p}^\tau - \tilde{r}_{i,2}^\tau \tilde{r}_{i,p}^\tau \\ \vdots & \vdots & \ddots & \vdots \\ \tilde{r}_{p,1}^\tau - \tilde{r}_{i,p}^\tau \tilde{r}_{i,1}^\tau & \cdots & \cdots & 1 - (\tilde{r}_{i,p}^\tau)^2 \end{pmatrix}_{(p-2) \times (p-2)}. \quad (\text{EC.2.9})$$

By transforming variables, we have

$$\begin{aligned} &\int_{-d_1^\tau}^{\infty} \cdots \int_{-d_p^\tau}^{\infty} f_{y^\tau|y_i^\tau=-d_i^\tau}(y_1, \dots, y_p) dy_1 \cdots dy_p \\ &= \int_{-d_1^\tau}^{\infty} \cdots \int_{-d_p^\tau}^{\infty} f_Z(z_1, \dots, z_p) dz_1 \cdots dz_p, \end{aligned} \quad (\text{EC.2.10})$$

where  $-\tilde{d}_j^\tau = -d_j^\tau + d_i^\tau \tilde{r}_{i,j}^\tau$  and  $f_Z$  is the density of a multivariate normal distribution with zero mean and covariance matrix  $\Sigma^Z = \tilde{\Sigma}_i$ . Then, the integral (EC.2.10) is rewritten as

$$\begin{aligned} & P_Z(z_j > -\tilde{d}_j^\tau, j \in \mathcal{P} \setminus \{i, \tau\}) \\ &= P_Z(\{z_r > -\tilde{d}_r^\tau, r \in \mathcal{S}_{-i}^+(\tau)\} \cap \{z_s > -\tilde{d}_s^\tau, s \in \mathcal{S}_{-i}^-(\tau)\}) \\ &\leq \min\{P_Z(z_r > -\tilde{d}_r^\tau, r \in \mathcal{S}_{-i}^+(\tau)), P_Z(z_s > -\tilde{d}_s^\tau, s \in \mathcal{S}_{-i}^-(\tau))\}, \end{aligned} \quad (\text{EC.2.11})$$

where  $\mathcal{S}_{-i}^+(\tau) \triangleq \{r \in \mathcal{P} \setminus \{i, \tau\} \mid -\tilde{d}_r^\tau > 0\}$  and  $\mathcal{S}_{-i}^-(\tau) \triangleq \{s \in \mathcal{P} \setminus \{i, \tau\} \mid -\tilde{d}_s^\tau < 0\}$ .

Next we evaluate the two terms within the ‘‘min’’ operator respectively. The term

$$P_Z(z_s > -\tilde{d}_s^\tau, s \in \mathcal{S}_{-i}^-(\tau)) \geq P_Z(z_s > 0, s \in \mathcal{S}_{-i}^-(\tau))$$

is lower bounded by a positive value that will not reduce to 0 as  $N$  increases. However, the other term  $P_Z(z_r > -\tilde{d}_r^\tau, r \in \mathcal{S}_{-i}^+(\tau))$  will reduce to 0 as  $N$  grows since  $d_r^\tau \sim \mathcal{O}(\sqrt{N})$ . Next we evaluate the rate of convergence to 0. With Hashorva and Hüsler (2003), there exists a subset  $S$  of  $\mathcal{S}_{-i}^+(\tau)$  such that

$$P_Z(z_r > -\tilde{d}_r^\tau, r \in \mathcal{S}_{-i}^+(\tau)) \sim \mathcal{O}\left(\exp\left(-\frac{Q_S^\tau}{2}\right) \prod_{r \in S} h_r^{-1}\right), \quad (\text{EC.2.12})$$

where  $Q_S^\tau \triangleq \langle \mathbf{d}_S, (\Sigma_S^Z)^{-1} \mathbf{d}_S \rangle = \min_{\mathbf{x} \geq \mathbf{d}_{\mathcal{S}_{-i}^+(\tau)}} \langle \mathbf{x}, (\Sigma_{\mathcal{S}_{-i}^+(\tau)}^Z)^{-1} \mathbf{x} \rangle$ ,  $\mathbf{x} = (x_1, \dots, x_{|\mathcal{S}_{-i}^+(\tau)|}) \in \mathbb{R}^{|\mathcal{S}_{-i}^+(\tau)|}$ ,  $\mathbf{d} = (-\tilde{d}_1^\tau, \dots, -\tilde{d}_p^\tau) \in \mathbb{R}^{p-2}$  and  $h_r \sim \mathcal{O}(\sqrt{N})$  is the  $r$ -th element of  $(\Sigma_S^Z)^{-1} \mathbf{d}_S$ . For simplicity, we omit the polynomial term  $\prod_{r \in S} h_r^{-1}$ , as it does not affect the comparisons of exponentially decaying terms.

Then, with (EC.2.7), (EC.2.11) and (EC.2.12), we have

$$D_i^\tau \sim \mathcal{O}\left(\frac{\partial d_i^\tau}{\partial \sigma_\tau} f_{y_i^\tau}(-d_i^\tau) \exp\left(-\frac{\langle \mathbf{d}_S, (\Sigma_S^Z)^{-1} \mathbf{d}_S \rangle}{2}\right)\right) = \mathcal{O}\left(\exp\left(-\frac{Q_S^\tau + (d_i^\tau)^2}{2}\right)\right).$$

To simplify the form, we rewrite the quadratic form by introducing  $\mathcal{D}_i^\tau > 0$  such that

$$D_i^\tau \sim \mathcal{O}(e^{-\mathcal{D}_i^\tau N}). \quad (\text{EC.2.13})$$

(b) Similar to (a), the derivative of PCS( $\tau$ ) with respect to correlation information  $\{r_{\tau,i}\}_{i \neq \tau}$  is given by

$$\begin{aligned} \frac{\partial \text{PCS}(\tau)}{\partial r_{\tau i}} &= \frac{\partial P(y_1^\tau > -d_1^\tau, \dots, y_p^\tau > -d_p^\tau)}{\partial r_{\tau i}} \\ &= \frac{\partial d_i^\tau}{\partial r_{\tau i}} \frac{\partial \text{PCS}(\tau)}{\partial d_i^\tau} + 2 \sum_{1 \leq i < j \leq p, i, j \neq \tau} \frac{\partial \text{PCS}(\tau)}{\partial \tilde{r}_{i,j}^\tau} \frac{\partial \tilde{r}_{i,j}^\tau}{\partial r_{\tau i}} \\ &= \frac{\partial d_i^\tau}{\partial r_{\tau i}} \int_{-d_1^\tau}^\infty \cdots \int_{-d_{i-1}^\tau}^\infty \int_{-d_{i+1}^\tau}^\infty \cdots \int_{-d_p^\tau}^\infty f_{y^\tau}(y_1, \dots, -d_i^\tau, \dots, y_p) dy_1 \cdots dy_p \\ &+ 2 \sum_{j \in \{1, \dots, p\} \setminus \{i, \tau\}} \frac{\partial \text{PCS}(\tau)}{\partial \tilde{r}_{i,j}^\tau} \frac{\partial \tilde{r}_{i,j}^\tau}{\partial r_{\tau i}} \\ &= \tilde{D}_i^\tau + \tilde{I}_i, \end{aligned} \quad (\text{EC.2.14})$$

where

$$\tilde{D}_i^\tau = \frac{\partial d_i^\tau}{\partial r_{\tau i}} \int_{-d_1^\tau}^\infty \cdots \int_{-d_{i-1}^\tau}^\infty \int_{-d_{i+1}^\tau}^\infty \cdots \int_{-d_p^\tau}^\infty f_{y^\tau}(y_1, \dots, -d_i^\tau, \dots, y_p) dy_1 \cdots dy_p, \quad (\text{EC.2.15})$$

$$\begin{aligned} \tilde{I}_i &= 2 \sum_{j \in \{1, \dots, p\} \setminus \{i, \tau\}} \frac{\partial \text{PCS}(\tau)}{\partial \tilde{r}_{i,j}^\tau} \frac{\partial \tilde{r}_{i,j}^\tau}{\partial r_{\tau i}}, \\ \frac{\partial \tilde{r}_{i,j}^\tau}{\partial r_{\tau i}} &= \frac{\left( -\frac{\sigma_i^2}{N_i} + \frac{r_{\tau,i} \sigma_\tau \sigma_i}{N_{\tau i}} - \frac{r_{\tau,j} \sigma_\tau \sigma_j}{N_{\tau j}} + \frac{r_{i,j} \sigma_i \sigma_j}{N_{ij}} \right) \cdot \frac{\sigma_\tau \sigma_i}{N_{\tau i}}}{\left( \frac{\sigma_\tau^2}{N_\tau} + \frac{\sigma_i^2}{N_i} - 2 \frac{r_{\tau,i} \sigma_\tau \sigma_i}{N_{\tau i}} \right)^{3/2} \left( \frac{\sigma_\tau^2}{N_\tau} + \frac{\sigma_j^2}{N_j} - 2 \frac{r_{\tau,j} \sigma_\tau \sigma_j}{N_{\tau j}} \right)^{1/2}}, \end{aligned} \quad (\text{EC.2.16})$$

where  $N_{\tau i} = \max\{N_\tau, N_i\}$ ,  $N_{\tau j} = \max\{N_\tau, N_j\}$ , and  $N_{ij} = \max\{N_i, N_j\}$ .

Similar to (a), we have

$$\tilde{D}_i^\tau \sim \mathcal{O}\left(\exp\left(-\frac{Q_S^\tau + (d_i^\tau)^2}{2}\right)\right) \sim \mathcal{O}(\sqrt{N} e^{-\mathcal{D}_i^\tau N}),$$

and

$$\begin{aligned} \frac{\partial \tilde{r}_{i,j}^\tau}{\partial r_{\tau i}} &\sim \mathcal{O}(1), \\ \tilde{I}_i &\sim \mathcal{O}\left(\exp\left(-\min_{j \neq i} \frac{(d_i^\tau)^2 + (d_j^\tau)^2}{2(1 + \arcsin(\tilde{r}_{i,j}^\tau))}\right)\right) \sim \mathcal{O}(e^{-\mathcal{I}_i^\tau N}), \end{aligned}$$

which concludes the proof of Corollary 1(a). Next, we prove Corollary 1(b).

If  $\tau = [1]$ , since  $|\tilde{r}_{i,j}^\tau| < |\frac{d_j^\tau}{d_i^\tau}|$  according to the Assumption 2(b), the sign of  $-\tilde{d}_j^\tau$  is the same as  $-d_j^\tau$ . Then  $\mathcal{S}_{-i}^+(\tau) = \{s \in \mathcal{P} \setminus \{i, \tau\} \mid -\tilde{d}_s^\tau > 0\} = \{s \in \mathcal{P} \setminus \{i, \tau\} \mid -d_s^\tau > 0\} = \emptyset$ ,  $\forall i \neq \tau$ . Therefore,  $Q_S^\tau = 0$ , and

$$\frac{Q_S^\tau + (d_i^\tau)^2}{2} = \frac{(d_i^\tau)^2}{2} < \min_{j \neq i} \frac{(d_i^\tau)^2 + (d_j^\tau)^2}{2(1 + \arcsin(\tilde{r}_{i,j}^\tau))}$$

with Assumption 2(c). Then  $\mathcal{D}_i^\tau < \mathcal{I}_i^\tau$ .

Next, we prove Corollary 1(c), which establishes the monotonic non-decreasing property of  $\mathcal{D}_i^\tau(m)$  with respect to the ranking  $m$  of  $\tau$ . We assume that only the ranking  $m$  changes, while all other parameters (covariance matrix, sample sizes, and the absolute value of pairwise mean differences) remain fixed. To prove this, we only need to show that

$$\mathcal{D}_i^\tau(p) \geq \cdots \geq \mathcal{D}_i^\tau(2) \geq \mathcal{D}_i^\tau(1), \quad \forall i \in \mathcal{P} \setminus \{\tau\}.$$

As mentioned earlier,  $\mathcal{S}_{-i}^+(\tau) = \{s \in \mathcal{P} \setminus \{i, \tau\} \mid -d_s^\tau > 0\}$  due to Assumption 2(b), and it is straightforward to conclude that

$$\mathcal{S}_{-i}^+([1]) \subseteq \mathcal{S}_{-i}^+([2]) \subseteq \cdots \subseteq \mathcal{S}_{-i}^+([p]), \quad (\text{EC.2.17})$$

where  $\mathcal{S}_{-i}^+([m])$  denotes the corresponding  $\mathcal{S}_{-i}^+(\tau)$  when  $\tau = [m]$ . This inclusion holds because, as the ranking  $m$  of  $\tau$  increases, more alternatives surpass  $\tau$  in terms of their mean values. Then

$$Q_S^{[p]} \geq \cdots \geq Q_S^{[2]} \geq Q_S^{[1]} \quad (\text{EC.2.18})$$

can be proved by contradiction, where  $Q_S^{[m]}$  denotes the corresponding  $Q_S^{[\tau]}$  when  $\tau = [m]$ . Suppose that there exist  $m < m'$  such that  $Q_S^{[m]} > Q_S^{[m']}$ .

Let

$$\mathbf{x}_* \in \mathbb{R}^{|\mathcal{S}_{-i}^+([m])|} = \arg \min_{\mathbf{x} \geq \mathbf{d}_{\mathcal{S}_{-i}^+([m])}} \langle \mathbf{x}, \Sigma_{\mathcal{S}_{-i}^+([m])}^Z \mathbf{x} \rangle,$$

$$\mathbf{x}'_* \in \mathbb{R}^{|\mathcal{S}_{-i}^+([m'])|} = \arg \min_{\mathbf{x} \geq \mathbf{d}_{\mathcal{S}_{-i}^+([m'])}} \langle \mathbf{x}, \Sigma_{\mathcal{S}_{-i}^+([m'])}^Z \mathbf{x} \rangle.$$

Then  $\langle \mathbf{x}_*, \Sigma_{\mathcal{S}_{-i}^+([m])}^Z \mathbf{x}_* \rangle > \langle \mathbf{x}'_*, \Sigma_{\mathcal{S}_{-i}^+([m'])}^Z \mathbf{x}'_* \rangle$ . Since  $\mathcal{S}_{-i}^+([m]) \subseteq \mathcal{S}_{-i}^+([m'])$ , let  $\tilde{\mathbf{x}}_*$  be the elements in  $\mathbf{x}'_* \in \mathbb{R}^{|\mathcal{S}_{-i}^+([m'])|}$  with indices corresponding to  $\mathcal{S}_{-i}^+([m])$ . Then we have

$$\langle \mathbf{x}_*, \Sigma_{\mathcal{S}_{-i}^+([m])}^Z \mathbf{x}_* \rangle > \langle \mathbf{x}'_*, \Sigma_{\mathcal{S}_{-i}^+([m'])}^Z \mathbf{x}'_* \rangle \geq \langle \tilde{\mathbf{x}}_*, \Sigma_{\mathcal{S}_{-i}^+([m])}^Z \tilde{\mathbf{x}}_* \rangle,$$

which contradicts to the optimality of  $\mathbf{x}_*$ . Therefore, (EC.2.18) holds. Then according to the definition of  $\mathcal{D}_i^\tau(m)$ , we can conclude that

$$\mathcal{D}_i^\tau(p) \geq \dots \geq \mathcal{D}_i^\tau(2) \geq \mathcal{D}_i^\tau(1), \quad \forall i \in \mathcal{P} \setminus \{\tau\}.$$

Additionally, since  $\mathcal{J}_i^\tau(m)$  is independent of the ranking  $m$ , it remains constant for all  $m$ .

(c)  $\forall i, j \in \mathcal{P} \setminus \{\tau\}$ , since  $d_i^\tau$  and  $d_j^\tau$  are independent of  $r_{ij}$ , we have

$$\begin{aligned} \frac{\partial \text{PCS}(\tau)}{\partial r_{ij}} &= \frac{\partial P(y_1^\tau > -d_1^\tau, \dots, y_p^\tau > -d_p^\tau)}{\partial r_{ij}} \\ &= 2 \cdot \frac{\partial \text{PCS}(\tau)}{\partial \tilde{r}_{i,j}^\tau} \frac{\partial \tilde{r}_{i,j}^\tau}{\partial r_{ij}}. \end{aligned} \tag{EC.2.19}$$

It is easy to verify that  $\frac{\partial \tilde{r}_{i,j}^\tau}{\partial r_{ij}} > 0$  and according to (EC.2.4),  $\frac{\partial \text{PCS}(\tau)}{\partial \tilde{r}_{i,j}^\tau} \geq 0$ . Therefore,  $\frac{\partial \text{PCS}(\tau)}{\partial r_{ij}} \geq 0$ .

As for the order of magnitude, we have  $\frac{\partial \text{PCS}(\tau)}{\partial r_{ij}} \sim \mathcal{O}(e^{-\mathcal{J}_{ij}^\tau N})$ . If  $\mathcal{J}_i^\tau > \mathcal{D}_i^\tau$  holds, then since  $\mathcal{J}_{ij}^\tau \geq \mathcal{J}_i^\tau$ , we have  $|\frac{\partial \text{PCS}(\tau)}{\partial r_{ij}}| \sim o(\frac{\partial \text{PCS}(\tau)}{\partial r_{i\tau}})$  ( $i, j \neq \tau$ ). The influence of  $\frac{\partial \text{PCS}(\tau)}{\partial r_{ij}}$  is negligible compared to  $\frac{\partial \text{PCS}(\tau)}{\partial r_{i\tau}}$ .  $\square$

## EC.2.2. Justification of Assumption 2

Assumption 2 implies that  $\tilde{r}_{i,j}^\tau$  is bounded and not too extreme. In this subsection, we explain why this assumption is easily satisfied for commonly used R&S strategies as long as the correlations between alternatives are moderate.

Notice that

$$\tilde{r}_{i,j}^\tau = \frac{\frac{\sigma_\tau^2}{N_\tau} - \frac{\text{cov}(X_\tau, X_i)}{N_{\tau,i}} - \frac{\text{cov}(X_\tau, X_j)}{N_{\tau,j}} + \frac{\text{cov}(X_i, X_j)}{N_{i,j}}}{\sqrt{\left(\frac{\sigma_\tau^2}{N_\tau} + \frac{\sigma_i^2}{N_i} - 2\frac{\text{cov}(X_\tau, X_i)}{N_{\tau,i}}\right)\left(\frac{\sigma_\tau^2}{N_\tau} + \frac{\sigma_j^2}{N_j} - 2\frac{\text{cov}(X_\tau, X_j)}{N_{\tau,j}}\right)}}.$$

Typically, the alternative  $\tau$  that users are interested in (for example, in  $\text{PCS}_{\text{trad}}$ ,  $\tau = [1]$ ; in  $\text{moPCS}$ ,  $\tau = \tau^*$ ) has a high mean, and in nearly all prominent R&S strategies,  $\tau$  is allocated a large sample

size. Therefore, we can assume that  $N_\tau$  is much larger than most of the other sample sizes  $N_i$  and  $N_j$ . Under this assumption, we have

$$\tilde{r}_{i,j}^\tau \approx r_{i,j} \frac{\sqrt{N_i N_j}}{N_{i,j}} \leq r_{i,j}.$$

The inequality holds due to  $N_i$  and  $N_j \leq N_{i,j}$ . Therefore, Assumption 2 means that the correlation  $r_{i,j}$  should not be too extreme, which is a mild assumption, and it holds true in the case of independence. For example, under equal sample size, equal mean ( $\mu_i = \mu_j$ ), equal variance, and equal correlation ( $r_{\tau,i} = r_{\tau,j}$ ), we have  $R_{i,j}^b = 1$  and  $R_{i,j}^c \approx 0.84$ . Note that  $|r_{i,j}| \leq 1$ , so the condition  $|r_{i,j}| < R_{i,j}^b$  and  $|r_{i,j}| < R_{i,j}^c$  are easily satisfied.

### EC.3. Proof of Theorem 3 and the Order of $\gamma$ in (3).

*Proof* We view  $\text{PCS}(\tau; \Sigma, N)$  as a function of the total sample size and covariance matrix. First, we consider the strategy  $\mathcal{R}$ : randomly assigning  $\frac{p}{k}$  alternatives to each processor. In the following analysis, we focus on calculating the expected sample complexity reduction for the first processor. By symmetry, multiplying the result by  $k$  gives the total sample complexity reduction. The index set of alternatives in the first processor is denoted as  $\mathcal{P}_1$ . The local best  $\tau_1$  of this processor is assumed to be from cluster  $\mathcal{G}_1$ . In this processor, besides  $\tau_1$ , there are  $\eta$  alternatives from cluster  $\mathcal{G}_1$  (the index set of those alternatives is denoted as  $\mathcal{J}_1 \subseteq \mathcal{P}_1$ ). The remaining  $\frac{p}{k} - \eta$  alternatives are from other clusters.  $\eta$  follows a hypergeometric distribution  $H(p, \frac{p}{k}, \frac{p}{k})$  and  $E(\eta) = \frac{(\frac{p}{k})^2}{p}$ . The covariance matrix of alternatives in this processor is  $\Sigma$ . Suppose the initialization sample size is  $N_0$  and the corresponding  $\text{PCS}(\tau_1; \Sigma, N_0)$  of this processor is  $1 - \alpha_0$  at this point. We continue sampling until PCS reaches  $1 - \alpha$ . The sample size is increased to  $N_R$ . According to mean value theorem,

$$\text{PCS}(\tau_1; \Sigma, N_R) - \text{PCS}(\tau_1; \Sigma, N_0) = \frac{\partial \text{PCS}(\tau_1; \Sigma, N_0 + \xi_R(N_R - N_0))}{\partial N} \cdot (N_R - N_0) = \alpha_0 - \alpha, \quad (\text{EC.3.1})$$

where  $\xi_R \in (0, 1)$ . This process is illustrated in the red line in Figure EC.1.

Next we consider the strategy  $\mathcal{C}$ . By using correlation-based clustering,  $\beta(\frac{p}{k})$  alternatives in the first processor are correctly clustered (i.e., from  $\mathcal{G}_1$ ), where  $\beta = \frac{\sum_{i \in \mathcal{P}_1 \setminus \{\tau_1\}} \mathbb{I}(G_n(i) = G(i))}{\frac{p}{k}}$  and  $n$  is the sample size used for learning correlation information. Since  $\text{PCC} = P(\Pi_n = \Pi) \leq P(G_n(i) = G(i))$ ,  $\forall i \in \mathcal{P}_1$ , and the cardinality  $|\mathcal{P}_1 \setminus \{\tau_1\}| = \frac{p}{k}$ , we have

$$E(\beta) = E\left(\frac{\sum_{i \in \mathcal{P}_1 \setminus \{\tau_1\}} \mathbb{I}(G_n(i) = G(i))}{\frac{p}{k}}\right) = \frac{\sum_{i \in \mathcal{P}_1 \setminus \{\tau_1\}} P(G_n(i) = G(i))}{\frac{p}{k}} \geq \frac{\frac{p}{k} \cdot \text{PCC}}{\frac{p}{k}} = \text{PCC}. \quad (\text{EC.3.2})$$

The transition from Strategy  $\mathcal{R}$  to Strategy  $\mathcal{C}$  is equivalent to increasing the number of alternatives belonging to cluster  $\mathcal{G}_1$  from  $\eta$  to  $\beta(\frac{p}{k})$ . Furthermore, this is equivalent to changing the correlation structure of this processor from  $\Sigma$  to  $\Sigma'$  while keeping the means and variances unchanged. Specifically, the change in the correlation structure is as follows:

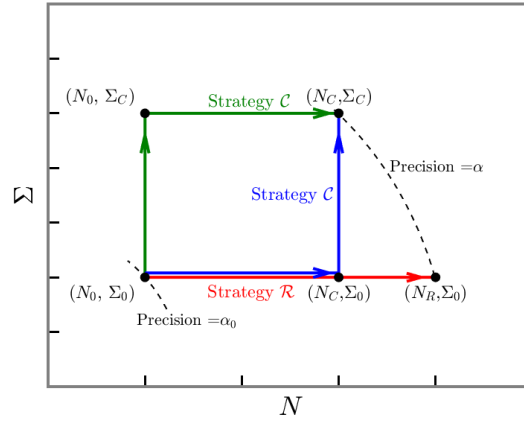


**Figure EC.1** Starting from the initialization, Strategy  $\mathcal{R}$  directly increases the total sample size, while Strategy  $\mathcal{C}$  is equivalent to first increasing the total sample size and then changing the covariance.

(i) The correlation coefficients between  $\beta(\frac{p}{k}) - \eta$  alternatives in  $\mathcal{P}_1 \setminus \mathcal{J}_1$  and alternative  $\tau_1$  are increased by  $\Delta r$  (the index set of those  $\beta(\frac{p}{k}) - \eta$  alternatives is denoted as  $\mathcal{J}_2$ ). For simplifying calculations, we assume that among the remaining  $\mathcal{J}_3 \triangleq \mathcal{P}_1 \setminus (\mathcal{J}_1 \cup \mathcal{J}_2 \cup \{\tau_1\})$ , there are no alternatives belonging to the same cluster as  $\mathcal{J}_2$ . This is reasonable, because according to Lemma 1, the impact of the correlation between  $\mathcal{J}_2$  and  $\mathcal{J}_3$  is a negligible lower-order term. (ii) As for the correlation coefficients  $\{r_{i,j}\}_{i,j \in \mathcal{P}_1 \setminus \{\tau_1\}}$  between two alternatives in  $\mathcal{P}_1 \setminus \{\tau_1\}$ ,  $\eta[\beta(\frac{p}{k}) - \eta]$  of them are increased by  $\Delta r$  (i.e., the correlations between the alternatives in  $\mathcal{J}_1$  and  $\mathcal{J}_2$ ). The remaining correlation coefficients remain unchanged.

Starting from the initialization  $N_0$  samples, we continue sampling until PCS reaches  $1 - \alpha$  and the total sample size is  $N_C$ . This process is depicted by the green line in Figure EC.1, where the correlation structure is first altered to  $\Sigma'$ , and then the total sample size is increased to  $N_C$ . This process is equivalent to the one illustrated by the blue line in Figure EC.1, which involves first increasing total sample size, keeping the correlation coefficients constant and then altering the correlation structure. Then by mean value theorem,

$$\begin{aligned} & \text{PCS}(\tau_1; \Sigma', N_C) - \text{PCS}(\tau_1; \Sigma, N_0) \\ &= \frac{\partial \text{PCS}(\tau_1)}{\partial N} \cdot (N_C - N_0) + \sum_{i \in \mathcal{J}_2} \frac{\partial \text{PCS}(\tau_1)}{\partial r_{i, \tau_1}} \Delta r + \sum_{i \in \mathcal{J}_1, j \in \mathcal{J}_2} \frac{\partial \text{PCS}(\tau_1)}{\partial r_{ij}} \Delta r \\ &= \alpha_0 - \alpha, \end{aligned} \quad (\text{EC.3.3})$$

where  $\frac{\partial \text{PCS}(\tau_1)}{\partial N}$  is evaluated at a point  $(\Sigma, N_0 + \xi_C(N_C - N_0))$  and  $\xi_C \in (0, 1)$ .  $\frac{\partial \text{PCS}(\tau_1)}{\partial r_{i, \tau_1}}$  and  $\frac{\partial \text{PCS}(\tau_1)}{\partial r_{ij}}$  are evaluated at a point  $(\Sigma + \xi'(\Sigma' - \Sigma), N_0 + \xi_C(N_C - N_0))$ , where  $\xi' \in (0, 1)$ .

With Lemma 1, we have

$$\sum_{i \in \mathcal{J}_1, j \in \mathcal{J}_2} \frac{\partial \text{PCS}(\tau_1)}{\partial r_{ij}} \Delta r > 0. \quad (\text{EC.3.4})$$

Since each PrOS has maximum mean, according to Theorem 2 and Assumption ??,  $\frac{\partial \text{PCS}(\tau_1)}{\partial r_{i,\tau_1}} \geq 0$  for any  $i \neq \tau_1$ , if we omit lower-order terms. As shown in Figure EC.1, the process of strategy  $\mathcal{R}$  and  $\mathcal{C}$  have the same starting ( $\alpha_0$ ) and ending points ( $\alpha$ ). With EC.3.1 and EC.3.3, the identical  $\alpha_0 - \alpha$  terms are canceled out, then we have

$$\begin{aligned} \sum_{i \in \mathcal{J}_2} \frac{\partial \text{PCS}(\tau_1)}{\partial r_{i,\tau_1}} \Delta r &\leq \sum_{i \in \mathcal{J}_2} \frac{\partial \text{PCS}(\tau_1)}{\partial r_{i,\tau_1}} \Delta r + \sum_{i \in \mathcal{J}_1, j \in \mathcal{J}_2} \frac{\partial \text{PCS}(\tau_1)}{\partial r_{ij}} \Delta r \\ &= \frac{\partial \text{PCS}(\tau_1; \Sigma, N_0 + \xi_R(N_R - N_0))}{\partial N} \cdot (N_R - N_0) - \\ &\quad \frac{\partial \text{PCS}(\tau_1; \Sigma, N_0 + \xi_C(N_C - N_0))}{\partial N} \cdot (N_C - N_0) \\ &\leq \frac{\partial \text{PCS}(\tau_1; \Sigma, N_0 + \xi_C(N_C - N_0))}{\partial N} \cdot (N_R - N_C) \end{aligned}$$

The “ $\leq$ ” in the last line arises because the PCS is a concave function that is increasing with respect to  $N$ , and  $N_R \geq N_C$ , thus  $\frac{\partial \text{PCS}(\tau_1; \Sigma, N_0 + \xi_R(N_R - N_0))}{\partial N} \leq \frac{\partial \text{PCS}(\tau_1; \Sigma, N_0 + \xi_C(N_C - N_0))}{\partial N}$ . Note that this is the only step where the concavity assumption is used. Without this assumption, the above inequality can be rewritten as  $\leq \max\left\{\frac{\partial \text{PCS}(\tau_1; \Sigma, N_0 + \xi_C(N_C - N_0))}{\partial N}, \frac{\partial \text{PCS}(\tau_1; \Sigma, N_0 + \xi_R(N_R - N_0))}{\partial N}\right\} \cdot (N_R - N_C)$ , and a similar final result can still be obtained.

Then, we have

$$(N_R - N_C) \geq \frac{\sum_{i \in \mathcal{J}_2} \frac{\partial \text{PCS}(\tau_1)}{\partial r_{i,\tau_1}} \Delta r}{\frac{\partial \text{PCS}(\tau_1; \Sigma, N_0 + \xi_C(N_C - N_0))}{\partial N}},$$

where

$$\sum_{i \in \mathcal{J}_2} \frac{\partial \text{PCS}(\tau_1)}{\partial r_{i,\tau_1}} \Delta r \geq \left(\beta \left(\frac{p}{k}\right) - \eta\right) \min_{i \in \mathcal{J}_2} \frac{\partial \text{PCS}(\tau_1)}{\partial r_{i,\tau_1}} \Delta r.$$

The derivative  $\frac{\partial \text{PCS}(\tau_1)}{\partial r_{i,\tau_1}}$  is evaluated at  $(\Sigma + \xi'(\Sigma' - \Sigma), N_0 + \xi_C(N_C - N_0))$ . By symmetry, for any  $i \in \mathcal{J}_2$ ,  $\frac{\partial \text{PCS}(\tau_1; \Sigma + \xi'(\Sigma' - \Sigma), N_0 + \xi_C(N_C - N_0))}{\partial r_{i,\tau_1}}$  are the same. Then

$$E(N_R - N_C) \geq \frac{\frac{\partial \text{PCS}(\tau_1; \Sigma + \xi'(\Sigma' - \Sigma), N_0 + \xi_C(N_C - N_0))}{\partial r_{i_0, \tau_1}}}{\frac{\partial \text{PCS}(\tau_1; \Sigma, N_0 + \xi_C(N_C - N_0))}{\partial N}} \Delta r \left( \frac{E(\beta) - \frac{1}{k}}{k} \right) p,$$

where  $i_0 \in \mathcal{J}_2$ . This is the sample savings on one processor. We scale up the result by  $k$  to obtain the total sample savings for all  $k$  processors:

$$\begin{aligned} E(N_R - N_C) &\geq \frac{\frac{\partial \text{PCS}(\tau_1; \Sigma + \xi'(\Sigma' - \Sigma), N_0 + \xi_C(N_C - N_0))}{\partial r_{i_0, \tau_1}}}{\frac{\partial \text{PCS}(\tau_1; \Sigma, N_0 + \xi_C(N_C - N_0))}{\partial N}} \Delta r \left( E(\beta) - \frac{1}{k} \right) p \\ &= \gamma \Delta r \left( E(\beta) - \frac{1}{k} \right) p \geq \gamma \Delta r \left( \text{PCC} - \frac{1}{k} \right) p. \end{aligned}$$

The “ $\geq$ ” in the last line is due to (EC.3.2). The proof of Theorem 3 concludes here. Next, we prove that the condition “ $\gamma$  is at least  $\mathcal{O}(1)$ ” is met for sampling strategies with lowest sample size growth rate  $\mathcal{O}(p)$ . According to Theorem 2 and Corollary 1, we have

$$\frac{\partial \text{PCS}(\tau_1)}{\partial r_{i,\tau_1}} = \tilde{I}_i^T + o(\tilde{I}_i^T). \quad (\text{EC.3.5})$$

Taking the derivative of PCS with respect to individual sample size  $N_i$ , we have (refer to the proof of Proposition 3 for details)

$$\frac{\partial \text{PCS}(\tau_1)}{\partial N_i} = I'_i + o(I'_i), \quad (\text{EC.3.6})$$

$$I'_i = \frac{\partial d_i^{\tau_1}}{\partial N_i} \int_{-d_1^{\tau_1}}^{\infty} \cdots \int_{-d_{i-1}^{\tau_1}}^{\infty} \int_{-d_{i+1}^{\tau_1}}^{\infty} \cdots \int_{-d_p^{\tau_1}}^{\infty} f_{y^{\tau_1}}(y_1, \dots, -d_i^{\tau_1}, \dots, y_p) dy_1 \cdots dy_p. \quad (\text{EC.3.7})$$

For any sampling strategy with lowest growth rate of total sample size  $N \sim \mathcal{O}(p)$ , according to Assumption 3 (all  $p$  alternatives have the same order), we can easily conclude that  $N_i \sim \mathcal{O}(1)$ ,  $\forall i \in \mathcal{P}$ . With (EC.2.15) and (EC.3.7), it is straightforward to verify

$$I'_i \sim \tilde{I}_i^\tau \sim \mathcal{O}(1). \quad (\text{EC.3.8})$$

Therefore, with EC.3.5, EC.3.6 and EC.3.8, we have

$$\frac{\partial \text{PCS}(\tau_1)}{\partial r_{i,\tau_1}} \sim \frac{\partial \text{PCS}(\tau_1)}{\partial N_i} \sim \mathcal{O}(1). \quad (\text{EC.3.9})$$

Given Assumption 3, there exists  $w_i \in (0, 1)$ , such that  $N_i = w_i N$ ,  $\forall i \in \mathcal{P}$ , then, according to the chain rule,

$$\frac{\partial \text{PCS}(\tau_1)}{\partial N} = \frac{\frac{\partial \text{PCS}(\tau_1)}{\partial N_i}}{\frac{\partial N}{\partial N_i}} = w_i \frac{\partial \text{PCS}(\tau_1)}{\partial N_i} < \frac{\partial \text{PCS}(\tau_1)}{\partial N_i}.$$

Therefore, with (EC.3.9),  $\frac{\partial \text{PCS}(\tau_1)}{\partial N}$  is *at most*  $\mathcal{O}(1)$ . Then we can conclude that  $\gamma$  is at least  $\mathcal{O}(1)$ .

□

## EC.4. The Gradient Analysis with respect to Sample Size

EC.4.1 presents the proof of Proposition 3 and EC.4.2 presents the proof of Proposition 4. EC.4.3 and EC.4.4 present the explicit form of  $\frac{\partial \text{moPCS}_B}{\partial N_i}$  and  $\tilde{I}_i^\tau$ , respectively, which are used in the GBA.

### EC.4.1. Proof of Proposition 3.

**Proposition 3:** (a) *The gradient of  $\text{PCS}(\tau)$  with respect to  $N_i$  is:  $\frac{\partial \text{PCS}(\tau)}{\partial N_i} = \tilde{D}_i^\tau + \tilde{I}_i^\tau$ ,  $\forall i \in \mathcal{P}$ , where  $|\tilde{D}_i^\tau| \sim \mathcal{O}(e^{-\mathcal{D}_i^\tau N})$  and  $|\tilde{I}_i^\tau| \sim \mathcal{O}(e^{-\mathcal{I}_i^\tau N})$ . For  $i \in \mathcal{P} \setminus \{\tau\}$ ,  $\mathcal{D}_i^\tau$  and  $\mathcal{I}_i^\tau$  are given by (1) and (2), respectively, and  $\mathcal{D}_\tau^\tau = \min_{i \in \mathcal{P} \setminus \{\tau\}} \mathcal{D}_i^\tau$ ,  $\mathcal{I}_\tau^\tau = \min_{i \in \mathcal{P} \setminus \{\tau\}} \mathcal{I}_i^\tau$ . (b)  $\forall i \in \mathcal{I}^+(\tau)$ , if “ $N_\tau \geq N_i$ ”, or “ $N_\tau < N_i$  and  $r_{\tau i} < \frac{\sigma_i}{2\sigma_\tau}$ ”, then it follows that  $\tilde{D}_i^\tau < 0$ .*

*Proof* Taking the derivative of  $\text{PCS}(\tau)$  with respect to  $N_i$ ,  $i \in \mathcal{P}$

Case (a):  $i \neq \tau$ . We have

$$\begin{aligned} & \frac{\partial \text{PCS}(\tau)}{\partial N_i} \\ &= \frac{\partial d_i^\tau}{\partial N_i} \int_{-d_1^\tau}^{\infty} \cdots \int_{-d_{i-1}^\tau}^{\infty} \int_{-d_{i+1}^\tau}^{\infty} \cdots \int_{-d_p^\tau}^{\infty} f_{y^\tau}(y_1, \dots, -d_i^\tau, \dots, y_p) dy_1 \cdots dy_p \\ &+ 2 \sum_{j \in \{1, \dots, p-1\} \setminus \{i\}} \frac{\partial \text{PCS}(\tau)}{\partial \tilde{r}_{i,j}^\tau} \frac{\partial \tilde{r}_{i,j}^\tau}{\partial N_i} \\ &= \tilde{D}_i^\tau + \tilde{I}_i^\tau. \end{aligned} \quad (\text{EC.4.1})$$

It is evident that the order of  $\tilde{D}_i^\tau$  and  $\tilde{I}_i^\tau$  matches that of  $D_i^\tau$  and  $I_i^\tau$  in Corollary 1, with polynomial-order terms omitted. Therefore, we have:  $|\tilde{D}_i^\tau| \sim \mathcal{O}(e^{-\mathcal{D}_i^\tau N})$  and  $|\tilde{I}_i^\tau| \sim \mathcal{O}(e^{-\mathcal{I}_i^\tau N})$ .

Next, we discuss the signs of  $\tilde{D}_i^\tau$  and  $\tilde{I}_i^\tau$ . If  $N_\tau \geq N_i$ , then

$$\frac{\partial d_i^\tau}{\partial N_i} = \frac{\mu_\tau - \mu_i}{2} \cdot \sigma_i^2 \left( \frac{\sigma_\tau^2}{N_\tau} + \frac{\sigma_i^2}{N_i} - 2 \cdot \frac{\text{cov}(X_\tau, X_i)}{N_\tau} \right)^{-\frac{3}{2}} N_i^{-\frac{1}{2}}. \quad (\text{EC.4.2})$$

If  $N_\tau < N_i$ , then

$$\frac{\partial d_i^\tau}{\partial N_i} = \frac{\mu_\tau - \mu_i}{2} \cdot \sigma_i \sigma_\tau \left( \frac{\sigma_i}{\sigma_\tau} - 2r_{\tau i} \right) \left( \frac{\sigma_\tau^2}{N_\tau} + \frac{\sigma_i^2}{N_i} - 2 \cdot \frac{\text{cov}(X_\tau, X_i)}{N_i} \right)^{-\frac{3}{2}} N_i^{-\frac{1}{2}}, \quad (\text{EC.4.3})$$

Therefore, if  $N_\tau \geq N_i$  or  $r_{\tau i} < \frac{\sigma_i}{2\sigma_\tau}$ , then we have “ $\tilde{D}_i^\tau > 0$  for  $i$  such that  $\mu_i < \mu_\tau$  and  $\tilde{D}_i^\tau < 0$  for  $i$  such that  $\mu_i > \mu_\tau$ .”

Case (b):  $i = \tau$ . Then we have

$$\begin{aligned} & \frac{\partial \text{PCS}(\tau)}{\partial N_\tau} \\ &= \sum_{i \in \{1, \dots, p\} \setminus \{\tau\}} \frac{\partial d_i^\tau}{\partial N_\tau} \int_{-d_1^\tau}^\infty \cdots \int_{-d_{i-1}^\tau}^\infty \int_{-d_{i+1}^\tau}^\infty \cdots \int_{-d_p^\tau}^\infty f_{y^\tau}(y_1, \dots, -d_i^\tau, \dots, y_p) dy_1 \cdots dy_p \\ &+ 2 \sum_{i \in \{1, \dots, p\} \setminus \{\tau\}} \sum_{j \in \mathcal{P} \setminus \{i, \tau\}} \frac{\partial \text{PCS}(\tau)}{\partial \tilde{r}_{i,j}^\tau} \frac{\partial \tilde{r}_{i,j}^\tau}{\partial N_\tau} \\ &= \tilde{D}_\tau^\tau + \tilde{I}_\tau^\tau. \end{aligned} \quad (\text{EC.4.4})$$

As for the order of  $\tilde{D}_\tau^\tau$  and  $\tilde{I}_\tau^\tau$ , we have

$$\tilde{D}_\tau^\tau \sim \mathcal{O}(e^{-\mathcal{D}^\tau N}),$$

$$\tilde{I}_\tau^\tau \sim \mathcal{O}(e^{-\mathcal{I}^\tau N}),$$

where  $\mathcal{D}^\tau = \min_{i \in \mathcal{P} \setminus \{\tau\}} \mathcal{D}_i^\tau$  and  $\mathcal{I}^\tau = \min_{i \in \mathcal{P} \setminus \{\tau\}} \mathcal{I}_i^\tau$ .

#### EC.4.2. Proof of Proposition 4.

**Proposition 4:**  $\text{sign}\left(\frac{\partial \text{moPCS}_B}{\partial N_i}\right) = \text{sign}(\tilde{D}_i^{\tau*}), \forall i \in \mathcal{P} \setminus \{\tau^*\}$ .

*Proof* Since  $\text{moPCS}_B \triangleq \sum_{i \in \mathcal{P} \setminus \{\tau^*\}} \Phi\left(d_i^{\tau*}\right) - (p-2)$ , we have

$$\frac{\partial \text{moPCS}_B}{\partial N_i} = \frac{\partial d_i^{\tau*}}{\partial N_i} \phi(d_i^{\tau*}), \forall i \in \mathcal{P} \setminus \{\tau^*\},$$

where  $\phi$  is the probability density function of the standard Gaussian distribution. Therefore,  $\phi(d_i^{\tau*}) > 0$ . Comparing with Equation (EC.4.1), it is straightforward to verify that

$$\text{sign}\left(\frac{\partial \text{moPCS}_B}{\partial N_i}\right) = \text{sign}(\tilde{D}_i^{\tau*}).$$

**EC.4.3. The Gradient of moPCS<sub>B</sub>**

The gradient of moPCS<sub>B</sub> with respect to  $N_i$ ,  $i \neq \tau^*$ :

$$\frac{\partial \text{moPCS}_B}{\partial N_i} = \frac{\partial}{\partial N_i} \Phi(d_i^{\tau^*}) = \phi(d_i^{\tau^*}) \cdot \left( -\frac{\mu_{\tau^*} - \mu_i}{2(\lambda_i^{\tau^*})^{3/2}} \left( -\frac{\sigma_i^2}{N_i^2} + 2 \frac{\text{cov}(X_{\tau^*}, X_i)}{N_i^2} \cdot \mathbf{1}_{N_i \geq N_{\tau^*}} \right) \right).$$

The gradient of moPCS<sub>B</sub> with respect to  $N_{\tau^*}$ :

$$\begin{aligned} \frac{\partial \text{moPCS}_B}{\partial N_{\tau^*}} &= \sum_{i \in \mathcal{P} \setminus \{\tau^*\}} \frac{\partial}{\partial N_{\tau^*}} \Phi(d_i^{\tau^*}) \\ &= \sum_{i \in \mathcal{P} \setminus \{\tau^*\}} \phi(d_i^{\tau^*}) \cdot \left( -\frac{\mu_{\tau^*} - \mu_i}{2(\lambda_i^{\tau^*})^{3/2}} \left( -\frac{\sigma_{\tau^*}^2}{N_{\tau^*}^2} + 2 \frac{\text{cov}(X_{\tau^*}, X_i)}{N_{\tau^*}^2} \cdot \mathbf{1}_{N_{\tau^*} \geq N_i} \right) \right). \end{aligned} \quad (\text{EC.4.5})$$

**EC.4.4. Calculation of  $\tilde{I}_i^\tau$** 

According to the Equation (EC.4.1),

$$\tilde{I}_i^\tau = \sum_{j \in \{1, \dots, p-1\} \setminus \{i\}} \frac{\partial \text{PCS}(\tau)}{\partial \tilde{r}_{i,j}^\tau} \frac{\partial \tilde{r}_{i,j}^\tau}{\partial N_i}.$$

First, we present the specific expression of  $\frac{\partial \tilde{r}_{i,j}^\tau}{\partial N_i}$ . If  $N_i \geq N_\tau$ ,  $N_i > N_j$

$$\frac{d\tilde{r}_{i,j}^\tau}{dN_i} = \frac{1}{N_i^2} \left[ \frac{(r_{\tau,i}\sigma_\tau\sigma_i - r_{i,j}\sigma_i\sigma_j)}{\sqrt{AB}} + \frac{C(\sigma_i^2 - 2r_{\tau,i}\sigma_\tau\sigma_i)}{2A^{\frac{3}{2}}B^{\frac{1}{2}}} \right],$$

If  $N_i \geq N_\tau$ ,  $N_i < N_j$

$$\frac{d\tilde{r}_{i,j}^\tau}{dN_i} = \frac{1}{N_i^2} \left[ \frac{r_{\tau,i}\sigma_\tau\sigma_i}{\sqrt{AB}} + \frac{C(\sigma_i^2 - 2r_{\tau,i}\sigma_\tau\sigma_i)}{2A^{\frac{3}{2}}B^{\frac{1}{2}}} \right],$$

If  $N_i < N_\tau$ ,  $N_i < N_j$

$$\frac{d\tilde{r}_{i,j}^\tau}{dN_i} = \frac{1}{N_i^2} \frac{C\sigma_i^2}{2A^{\frac{3}{2}}B^{\frac{1}{2}}},$$

If  $N_i < N_\tau$ ,  $N_i > N_j$

$$\frac{d\tilde{r}_{i,j}^\tau}{dN_i} = \frac{1}{N_i^2} \left[ -\frac{r_{i,j}\sigma_i\sigma_j}{\sqrt{AB}} + \frac{C\sigma_i^2}{2A^{\frac{3}{2}}B^{\frac{1}{2}}} \right],$$

where

$$\begin{aligned} A &= \frac{\sigma_\tau^2}{N_\tau} + \frac{\sigma_i^2}{N_i} - 2 \frac{r_{\tau,i}\sigma_\tau\sigma_i}{N_{\tau i}}, \\ B &= \frac{\sigma_\tau^2}{N_\tau} + \frac{\sigma_j^2}{N_j} - 2 \frac{r_{\tau,j}\sigma_\tau\sigma_j}{N_{\tau j}}, \\ C &= \frac{\sigma_\tau^2}{N_\tau} - \frac{r_{\tau,i}\sigma_\tau\sigma_i}{N_{\tau i}} - \frac{r_{\tau,j}\sigma_\tau\sigma_j}{N_{\tau j}} + \frac{r_{i,j}\sigma_i\sigma_j}{N_{ij}}. \end{aligned}$$

Then,  $\frac{\partial \text{PCS}(\tau)}{\partial \tilde{r}_{i,j}^\tau}$  can be approximated by (EC.2.4).

## EC.5. Sample Optimality of P3C

This section discusses the sample optimality of P3C under both fixed-precision and fixed-budget formulations, in EC.5.1 and EC.5.2, respectively. As  $p \rightarrow \infty$ , the multi-round mechanism of P3C resembles that of KT (under fixed-precision) and FBKT (under fixed-budget). Intuitively, the key distinction is that, in each round of P3C, instead of only two alternatives competing, up to  $p_m < \infty$  alternatives are considered. Therefore, the proof framework in this section is largely consistent with those in Zhong and Hong (2022) and Hong et al. (2022). Below, we only present the modifications needed in the proofs compared to the existing literature. In the following proof, we maintain the same assumptions as in Zhong and Hong (2022) and Hong et al. (2022). Additionally, we adopt the same asymptotic setup as in Li et al. (2024): the covariance between any pair of alternatives  $i$  and  $j$  is bounded above by  $\sigma_{\text{upper}}^2$ , and  $\mu_{[1]} > \mu_i + \delta$ ,  $\forall i \neq [1]$ , where  $\delta > 0$ . Furthermore, any technical issues related to non-integer sample sizes, number of alternatives and number of rounds are disregarded, as they do not affect the analysis of the rate.

### EC.5.1. Sample Optimality in Fixed-precision R&S: Proof of Proposition 2

**Proposition 2:** *Let  $N_{KN}$  and  $N_{KT}$  denote the required total sample size to achieve  $\text{moPCS} \geq \text{PCS}_{\text{trad}} \geq 1 - \alpha$  using P3C – KN and P3C – KT, respectively. If the number of alternatives within each cluster is upper bounded by a constant  $p_m < \infty$ , then  $\mathbb{E}(N_{KN}) \sim \mathbb{E}(N_{KT}) \sim \mathcal{O}(p)$  as  $p \rightarrow \infty$ .*

*proof* This proof is based on the proof Theorem 3 in Zhong and Hong (2022). In the following, we only present the modifications made to the original proof. The number of alternatives in contention at the beginning of round  $r$  changes to  $\frac{p}{p_m^{r-1}}$  and the total number of rounds changes to  $\log_{p_m} p$ . If we apply KN family at each cluster  $\mathcal{G}_j$ ,  $j = 1, \dots, k$  to select the local best, for each alternative, at round  $r$ , it takes at most

$$N_r = \max_{i \in \mathcal{G}_j} \max_{m \neq i} \frac{(n_0 - 1)S_{i,k}^2}{\delta^2} \left[ \left( \frac{\alpha}{2^{r-1}(|\mathcal{G}_j| - 1)} \right)^{-\frac{2}{n_0-1}} - 1 \right] \quad (\text{EC.5.1})$$

observations. Taking expectation on both sides, since  $|\mathcal{G}_j| \leq p_m$ , the expectation of (EC.5.1) is upper bounded by

$$\mathbb{E}(N_r) \leq \frac{(n_0 - 1)\sigma_{\text{upper}}^2}{\delta^2} \left[ \left( \frac{\alpha}{2^{r-1}(p_m - 1)} \right)^{-\frac{2}{n_0-1}} - 1 \right]. \quad (\text{EC.5.2})$$

Then

$$\begin{aligned} \mathbb{E}(N_{KN}) &\leq \sum_{r=1}^{\log_{p_m} p} \frac{p}{p_m^r} \times \frac{(n_0 - 1)\sigma_{\text{upper}}^2}{\delta^2} \left[ \left( \frac{\alpha}{2^{r-1}(p_m - 1)} \right)^{-\frac{2}{n_0-1}} - 1 \right] \\ &\leq \frac{p(n_0 - 1)\sigma_{\text{upper}}^2}{\delta^2} \left\{ \left( \frac{\alpha}{p_m - 1} \right)^{-\frac{2}{n_0-1}} \sum_{r=1}^{\infty} \frac{2^{\frac{2(r-1)}{n_0-1}}}{p_m^r} - \sum_{r=1}^{\infty} \frac{1}{p_m^r} \right\} \\ &= \frac{p(n_0 - 1)\sigma_{\text{upper}}^2}{\delta^2} \left\{ \frac{\left( \frac{\alpha}{p_m - 1} \right)^{-\frac{2}{n_0-1}}}{p_m - 2^{\frac{2}{n_0-1}}} - \frac{1}{p_m - 1} \right\}. \end{aligned} \quad (\text{EC.5.3})$$

The last equality uses the fact  $n_0 \geq 3$  and  $p_m \geq 2 \geq 2^{\frac{2}{n_0-1}}$ .

Therefore,  $\mathbb{E}(N_{KN}) \sim \mathcal{O}(p)$ . According to Zhong and Hong (2022), KT is proven to be sample optimal, whereas KN is not. Therefore, KT is more sample-efficient than KN in rate. Given that P3C-KN achieves sample optimality, it is straightforward to conclude that P3C-KT also achieves optimal sample efficiency.

### EC.5.2. Sample Optimality in Fixed-budget R&S

First, we provide a detailed description of the P3C procedure under the fixed-budget setting. Similar to Hong et al. (2022), the fixed-budget P3C procedure proceeds with  $r$  rounds of “clustering and conquering” until the number of remaining alternatives is less than  $p_m$ . The sample size allocated to the  $r$ -th round is  $N^r = \frac{r}{\phi(\phi-1)} \left(\frac{\phi-1}{\phi}\right)^r N$ , where  $\phi \geq 2$  and  $N$  is the total sample size (It is easy to verify that the total sample size across all rounds sums to  $N$ ). Next, we allocate  $N^r$  among all clusters in proportion to the number of alternatives within each cluster. Within each cluster, we can apply budget allocation strategies such as EA, OCBA, or GBA. The sample optimality of P3C using the equal allocation (EA) strategy can be stated as the following Proposition EC.1. Consequently, any sample allocation strategy that outperforms EA, when combined with P3C, can also achieve sample optimality. While the proof that GBA outperforms EA remains an open problem, numerical experiments clearly demonstrate this superiority.

**PROPOSITION EC.1.** *Suppose that we apply EA within each cluster in P3C and the number of alternatives in each cluster is upper bounded by  $p_m < \infty$ . For any positive constant  $\eta_1 \geq 2\phi^2$ , if  $N > p\eta_1$ , the moPCS and PCS of the P3C procedure satisfy that*

$$\text{moPCS} \geq \text{PCS} \geq \left( -\frac{p_m \pi^2 \phi^2 \sigma_{\text{upper}}^2}{3\eta_1 \delta^2} \right).$$

*Proof* This proof is based on the proof Theorem 2 in Hong et al. (2022). In the following, we only present the modifications made to the original proof. First, we modify the definition of the event to  $\mathcal{Q}_r = \{\bar{x}_{[1]} \geq \bar{x}_{[j]} : j \in \mathcal{G}^r\}$ , where  $\mathcal{G}^r$  is the cluster to which [1] is assigned ( $|\mathcal{G}^r| \leq p_m$ ) and  $\bar{x}_j^r$  is the sample average of the alternative  $j$  at the  $r$ -th round.

Then, Equation (8) of Hong et al. (2022) is modified to

$$\text{PCS} = (1 - \mathbb{P}(\max_{j \in \mathcal{G}^1} \bar{x}_j^1 > \bar{x}_{[1]}^1)) \prod_{r=2}^{\log_{p_m} p} (1 - \mathbb{P}(\max_{j \in \mathcal{G}^r} \bar{x}_j^r > \bar{x}_{[1]}^r | \mathcal{Q}_1, \dots, \mathcal{Q}_{r-1})). \quad (\text{EC.5.4})$$

The sample size allocated to each alternative at round  $r$  is modified to

$$\mathcal{N}_r = \frac{r}{\phi(\phi-1)} \left(\frac{\phi-1}{\phi}\right)^r \frac{\eta_1 p}{\frac{p}{p_m^{r-1}}} \geq r \left(\frac{\eta_1 p_m^{r-1}}{\phi(\phi-1)} \left(\frac{\phi-1}{\phi}\right)^r\right).$$

Then, by Slepian (1962) (which is applicable due to the same assumptions as in Hong et al. (2022) in this proof), we have

$$\begin{aligned}
1 - \mathbb{P}(\max_{j \in \mathcal{G}^r} \bar{x}_j^1 > \bar{x}_{[1]}^r | \mathcal{Q}_1, \dots, \mathcal{Q}_{r-1}) &\geq \prod_{j \in \mathcal{G}^r} (1 - \mathbb{P}(\bar{x}_j^1 > \bar{x}_{[1]}^r | \mathcal{Q}_1, \dots, \mathcal{Q}_{r-1})) \\
&\geq \left( 1 - \mathbb{P}\left( Z > \sqrt{r \left( \frac{\eta_1 p_m^{r-1}}{\phi(\phi-1)} \left( \frac{\phi-1}{\phi} \right)^r \right) \frac{\delta}{\sigma_{upper}^2}} \right) \right)^{|\mathcal{G}^r|} \\
&\geq \left( 1 - \mathbb{P}\left( Z > \sqrt{r \left( \frac{\eta_1}{\phi^2} \right) \frac{\delta}{\sigma_{upper}^2}} \right) \right)^{p_m} \\
&\geq \left( 1 - \exp\left( -\frac{\eta_1 \delta^2}{2\phi^2 \sigma_{upper}^2} r \right) \right)^{p_m},
\end{aligned} \tag{EC.5.5}$$

where the last inequality holds due to the Lemma 3 of Hong et al. (2022). Then the Equation (10) of Hong et al. (2022) is modified to

$$\begin{aligned}
(10) &\geq \prod_{r=1}^{\infty} \left( 1 - \mathbb{P}\left( Z > \sqrt{r \left( \frac{\eta_1}{\phi^2} \right) \frac{\delta}{\sigma_{upper}^2}} \right) \right)^{p_m} \\
&\geq \prod_{r=1}^{\infty} \left( 1 - \exp\left( -\frac{\eta_1 \delta^2}{2\phi^2 \sigma_{upper}^2} r \right) \right)^{p_m} \\
&\geq \exp\left( -\frac{p_m \pi^2 \phi^2 \sigma_{upper}^2}{3\eta_1 \delta^2} \right),
\end{aligned} \tag{EC.5.6}$$

which concludes the proof. The last inequality holds due to the Lemma 2 in Hong et al. (2022).

## EC.6. Alternative Clustering Algorithm and Its Theoretical Analysis

In EC.6.1, the pseudo-codes of  $\mathcal{AC}$  is provided in the Algorithm 3. EC.6.2 presents a covariance estimator tailored for large-scale problem. EC.6.3 calculates the PCC of the  $\mathcal{AC}$  algorithm and presents the proof of Proposition 5.

### EC.6.1. The Pseudo-code of Algorithm $\mathcal{AC}$ .

### EC.6.2. Large-dimensional Covariance Matrix Estimator

We adopt the naive Equal Allocation (EA) policy for covariance estimation. The reason is that by using EA, we simulate the complete vector  $(X_1, X_2, \dots, X_p)$  at one time, generating a complete data matrix  $\mathcal{X}_n^T = (x_{ij}) \in \mathbb{R}^{p \times n}$  after sampling  $n$  times. Otherwise, if the sample sizes are unequal, it becomes a statistically challenging problem known as ‘‘covariance estimation with missing data’’ (Pavez and Ortega 2020, Gorder and Kolonko 2019).

In large-scale situation, the traditional estimator is given by  $S_n = \frac{\tilde{\mathcal{X}}_n^T \tilde{\mathcal{X}}_n}{n-1}$ , where  $\tilde{\mathcal{X}}_n$  is obtained from  $\mathcal{X}_n$  by subtracting the mean of each column. The analytical nonlinear shrinkage estimator (Ledoit and Wolf 2020), originally from the study of the spectral distribution of quantum energy levels in physics, is given by

$$\hat{\Sigma}_n = \sum_{i=1}^p \hat{\lambda}_{n,i} \cdot u_{n,i} u_{n,i}^T, \tag{EC.6.1}$$

**Algorithm 3** Linkage Alternative Clustering ( $\mathcal{AC}$ )

**Input:** estimated covariance matrix  $\hat{\Sigma}_n$ , the number of clusters  $k$ , maximum size  $p_m$  of each cluster

**Initialization:** Compute estimated correlation coefficient  $r_{ab}$ ,  $a, b \in \mathcal{P}$  from covariance matrix  $\hat{\Sigma}_n$ . Initialize the collection of clusters  $\mathcal{C}$  as  $\{\{1\}, \dots, \{p\}\}$  and the number of clusters  $N_{\mathcal{C}}$  as  $p$ .

**While**  $N_{\mathcal{C}} > k$  **do**

(i) Compute  $R_{XY}$  for each cluster pair  $(X, Y) \in \mathcal{C}$ . (ii) Sort cluster pairs in descending order of  $R_{XY}$ . (iii) Iterate through sorted pairs and find the first pair  $(A, B)$  such that  $|A \cup B| \leq p_m$ . Let  $M(A, B) = \{i | i \in A \cup B\}$ . (iv)  $\mathcal{C} \leftarrow \mathcal{C} - A - B + M(A, B)$ . (v)  $N_{\mathcal{C}} \leftarrow N_{\mathcal{C}} - 1$ .

**end while**

Return the partition  $\mathcal{C}$  and label the clusters in  $\mathcal{C}$  with index  $1, 2, \dots, k$ .

where

$$\begin{aligned} \hat{\lambda}_{n,i} &= \frac{\lambda_{n,i}}{\left[ \pi \frac{p}{n} \lambda_{n,i} f_n(\lambda_{n,i}) \right]^2 + \left[ 1 - \frac{p}{n} - \pi \frac{p}{n} \lambda_{n,i} \mathcal{H}(\lambda_{n,i}) \right]^2}, \\ f_n(\lambda_{n,i}) &= \frac{1}{p} \sum_{j=1}^p \frac{3}{4\sqrt{5}\lambda_{n,j}n^{-\frac{1}{3}}} \left[ 1 - \frac{1}{5} \left( \frac{\lambda_{n,i} - \lambda_{n,j}}{\lambda_{n,j}n^{-\frac{1}{3}}} \right)^2 \right]^+, \\ \mathcal{H}(\lambda_{n,i}) &= \frac{1}{p} \sum_{j=1}^p \left\{ -\frac{3(\lambda_{n,i} - \lambda_{n,j})}{10\pi\lambda_{n,j}^2n^{-\frac{2}{3}}} + \frac{3 \left[ 1 - \frac{1}{5} \left( \frac{\lambda_{n,i} - \lambda_{n,j}}{\lambda_{n,j}n^{-\frac{1}{3}}} \right)^2 \right]}{4\sqrt{5}\pi\lambda_{n,j}n^{-\frac{1}{3}}} \cdot \log \left| \frac{\sqrt{5}\lambda_{n,j}n^{-\frac{1}{3}} - \lambda_{n,i} + \lambda_{n,j}}{\sqrt{5}\lambda_{n,j}n^{-\frac{1}{3}} + \lambda_{n,i} - \lambda_{n,j}} \right| \right\}. \end{aligned}$$

$\lambda_{n,i}$  ( $i = 1, 2, \dots, p$ ) is the eigenvalue of  $S_n$  and  $u_{n,i}$  is the corresponding eigenvector, which are obtained by performing matrix spectral decomposition on  $S_n$ . Notably, as  $n$  approaches infinity with a fixed  $p$ , the  $\hat{\Sigma}_n$  will approach the sample covariance matrix  $S_n$ . This estimator has closed-form, which only requires matrix decomposition of  $S_n$  one time.

**EC.6.3. Computation of  $\text{PCC}_{\mathcal{AC}}$  and Proof of Proposition 5**

In this section, we calculate the PCC of the  $\mathcal{AC}$  algorithm and present the proof of Proposition 5. Finally, we discuss the required sample size for achieving a given clustering precision.

First, we calculate the  $\text{PCC}_{\mathcal{AC}}$ . Consider the following partition of the correlation matrix:

$$\Sigma = \begin{pmatrix} \Sigma_{11} & \Sigma_{12} & \cdots & \Sigma_{1k} \\ \Sigma_{12} & \Sigma_{22} & \cdots & \Sigma_{2k} \\ \vdots & \vdots & \ddots & \vdots \\ \Sigma_{1k} & \Sigma_{12} & \cdots & \Sigma_{kk} \end{pmatrix}, \quad (\text{EC.6.2})$$

where diagonal block  $\Sigma_{jj}$  ( $j \in \{1, \dots, k\}$ ) is the  $p_j \times p_j$  correlation matrix of cluster  $\mathcal{G}_j$ , and off-diagonal block  $\Sigma_{ij}$  ( $i \neq j$ ) is the  $p_i \times p_j$  correlation matrix between  $\mathcal{G}_i$  and  $\mathcal{G}_j$ . According to Assumption 1, each element in  $\Sigma_{jj}$  ( $j \in \{1, \dots, k\}$ ) should be greater than the elements in  $\Sigma_{ij}$  ( $i \neq j$ ).

Accurate clustering necessitates a sufficiently precise estimation of the correlation matrix to correctly identify this relationship. We define  $\Gamma = \{(ab, ac) | G(a) = G(b), G(a) \neq G(c), a, b, c \in \mathcal{P}, a \neq b\}$  and  $\Gamma' = \{(ab, cd) | G(a) = G(b), G(c) \neq G(d), G(c) \neq G(a), G(d) \neq G(a), a, b, c, d \in \mathcal{P}\}$ .  $\Gamma$  represents the comparison between an element  $r_{ab}$  from diagonal block  $\Sigma_{jj}$  and an element  $r_{ac}$  from off-diagonal block  $\Sigma_{ij}$ , sharing a common  $a$ .  $\Gamma'$  represents the comparison between an element  $r_{ab}$  from diagonal block  $\Sigma_{jj}$  and an element  $r_{cd}$  from an off-diagonal block that are not in the same row or column as  $\Sigma_{jj}$ . With Assumption 1, we have  $r_{ab} > r_{cd}$ ,  $\forall (ab, cd) \in \Gamma \cup \Gamma'$ . We have the following lemma.

LEMMA EC.1.  $\text{PCC}_{\mathcal{AC}} \geq P\left(\bigcap_{(ab, cd) \in \Gamma \cup \Gamma'} \{\hat{r}_{ab}^n > \hat{r}_{cd}^n\}\right)$ , and if all clusters have equal sizes,  $\text{PCC}_{\mathcal{AC}} \geq P\left(\bigcap_{(ab, ac) \in \Gamma} \{\hat{r}_{ab}^n > \hat{r}_{ac}^n\}\right)$ .

This lemma can be proved by induction. In Step 1 of  $\mathcal{AC}$ , if event  $\bigcap_{(ab, ac) \in \Gamma} \{\hat{r}_{ab}^n > \hat{r}_{ac}^n\}$  occurs, it can be easily verified that two alternatives belonging to the same cluster are merged together. Suppose that at the end of Step  $s - 1$ , each group contains alternatives from the same cluster. In Step  $s$ , assuming  $A$  and  $B$  represents two groups maximizing the empirical similarity  $R$ , they will be merged into one in this step. If event  $\bigcap_{(ab, cd) \in \Gamma \cup \Gamma'} \{\hat{r}_{ab}^n > \hat{r}_{cd}^n\}$  occurs, we can prove that  $A$  and  $B$  must come from the same cluster by contradiction. Assuming  $A$  and  $B$  do not come from the same cluster: (i) If there are still other groups from the same cluster as  $A$  (or  $B$ ), denoted as  $A'$ , then according to  $\bigcap_{(ab, ac) \in \Gamma} \{\hat{r}_{ab}^n > \hat{r}_{ac}^n\}$ , there exist  $a_0 \in A$ ,  $b_0 \in B$  and  $a'_0 \in A'$  such that  $R(A, B) = \hat{r}_{a_0, b_0}^n < \hat{r}_{a_0, a'_0}^n \leq R(A, A')$ , which contradicts the maximization of  $R(A, B)$ ; (ii) If there are no other groups remaining that come from the same cluster as  $A$  and  $B$ , then, since the algorithm has not yet stopped, there still exist two groups belonging to the same cluster that have not been merged, denoted as  $C$  and  $C'$ . With  $\bigcap_{(ab, cd) \in \Gamma'} \{\hat{r}_{ab}^n > \hat{r}_{cd}^n\}$ , we have  $R(A, B) < R(C, C')$ , which contradicts the maximization of  $R(A, B)$ . Therefore,  $A$  and  $B$  must come from the same cluster. Additionally, if all clusters have the same size, then each cluster's size is known to be  $\frac{p}{k}$ . In the aforementioned scenario (ii), both group  $A$  and  $B$  reach maximum size  $\frac{p}{k}$ . The algorithm will not merge them but will consider the two groups with the second-largest  $R$ . Therefore, in this case, correct clustering does not rely on ensuring the occurrence of event  $\bigcap_{(ab, cd) \in \Gamma'} \{\hat{r}_{ab}^n > \hat{r}_{cd}^n\}$ . Finally, by induction, algorithm  $\mathcal{AC}$  stops when only  $k$  groups remain, and each group contains alternatives from the same cluster. Therefore, the clustering is correct, and thus,  $\text{PCC}_{\mathcal{AC}} \geq P\left(\bigcap_{(ab, cd) \in \Gamma \cup \Gamma'} \{\hat{r}_{ab}^n > \hat{r}_{cd}^n\}\right)$ . If all clusters have equal sizes,  $\text{PCC}_{\mathcal{AC}} \geq P\left(\bigcap_{(ab, ac) \in \Gamma} \{\hat{r}_{ab}^n > \hat{r}_{ac}^n\}\right)$ .

Following the same proof technique, the convergence of algorithm  $\mathcal{AC}^+$  can be similarly demonstrated. For simplicity, we state without proof that the PCC of  $\mathcal{AC}^+$  is lower bounded by

$$\text{PCC}_{\mathcal{AC}^+} \geq P(D) \text{PCC}_{\mathcal{AC}}^{(\mathcal{P}_s)} P\left(\bigcap_{(ab, ac) \in \Gamma_q} \{\hat{r}_{ab}^n > \hat{r}_{ac}^n\}\right), \quad (\text{EC.6.3})$$

where  $D \triangleq \bigcap_{j \in \{1, \dots, k\}} \{\sum_{i \in \mathcal{P}_s} \mathbb{I}(G(i) = j) \geq 1\}$  and  $\text{PCC}_{\mathcal{AC}}^{(\mathcal{P}_s)}$  being the PCC of  $\mathcal{P}_s$  by using algorithm  $\mathcal{AC}$ . The three terms on the right-hand side of (EC.6.3) represent the events of “in the support set, there is at least one alternative belonging to  $\mathcal{G}_j$  for any  $j \in 1, 2, \dots, k$ ,” “alternatives in the support set are correctly clustered,” and “alternatives in the query set are matched to the correct prototypes”, respectively. If all clusters have equal sizes, the event  $D$  can be modeled as the occupancy problem which involves randomly distributing  $p_s$  “balls” to  $k$  “boxes” (see Example 2.2.10 of Durrett (2019)), and  $P(D) \geq 1 - k(1 - 1/k)^{p_s}$ . Moreover, with Lemma EC.1, the lower bound of  $\text{PCC}_{\mathcal{AC}}^{(\mathcal{P}_s)}$  is given by

$$\text{PCC}_{\mathcal{AC}}^{(\mathcal{P}_s)} \geq P\left(\bigcap_{(ab, cd) \in \Gamma_s \cup \Gamma'_s} \{\hat{r}_{ab}^n > \hat{r}_{cd}^n\}\right),$$

where  $\Gamma_s \triangleq \{(ab, ac) \in \Gamma \mid a, b, c \in \mathcal{P}_s\}$  and  $\Gamma'_s \triangleq \{(ab, cd) \in \Gamma' \mid a, b, c, d \in \mathcal{P}_s\}$ . If all clusters have equal sizes,

$$\text{PCC}_{\mathcal{AC}}^{(\mathcal{P}_s)} \geq P\left(\bigcap_{(ab, ac) \in \Gamma_s} \{\hat{r}_{ab}^n > \hat{r}_{ac}^n\}\right).$$

Next, we will proceed with the specific calculation of  $P\left(\bigcap_{(ab, ac) \in \Gamma} \{\hat{r}_{ab}^n > \hat{r}_{ac}^n\}\right)$  and  $P\left(\bigcap_{(ab, cd) \in \Gamma'} \{\hat{r}_{ab}^n > \hat{r}_{cd}^n\}\right)$ . First, we consider the former, which involves comparing two overlapping correlation coefficients  $\hat{r}_{ab}^n$  and  $\hat{r}_{ac}^n$ . As shown by Meng et al. (1992), the two overlapping correlations satisfy:

$$\frac{z(\bar{r}_{ab}^n) - z(\bar{r}_{ac}^n) - (z(r_{ab}) - z(r_{ac}))}{\sqrt{\frac{2(1-\bar{r}_{bc}^n)h(a,b,c)}{n-3}}} \sim N(0, 1),$$

where  $h(a, b, c) = \frac{1-f \cdot \bar{R}^2}{1-\bar{R}^2}$  and  $f = \frac{1-\bar{r}_{bc}^n}{2(1-\bar{R}^2)}$ ,  $\bar{R}^2 = \frac{(\bar{r}_{ab}^n)^2 + (\bar{r}_{bc}^n)^2}{2}$ .  $f$  must be  $\leq 1$ , and should be set to 1 if  $\frac{1-\bar{r}_{bc}^n}{2(1-\bar{r}^2)} > 1$ . Then if the assumption “ $r_{ab} \geq r_{ac} + \delta_c$ ” holds for  $(ab, ac) \in \Gamma$ , we have

$$P(\{\hat{r}_{ab}^n > \hat{r}_{ac}^n\}) \approx P(\bar{r}_{ab}^n > \bar{r}_{ac}^n) = P(z(\bar{r}_{ab}^n) > z(\bar{r}_{ac}^n)) = \Phi\left(\frac{z(r_{ab}) - z(r_{ac})}{\sqrt{\frac{2(1-\bar{r}_{bc}^n)h}{n-3}}}\right) \geq \Phi\left(\frac{\delta_c}{\sqrt{\frac{2(1-\bar{r}_{bc}^n)h}{n-3}}}\right).$$

The “ $\approx$ ” here arises from replacing  $\hat{r}_{ab}^n$  with sample correlation coefficient  $\bar{r}_{ab}^n$  (the new large-scale estimator (EC.6.1) is equivalent to the sample correlation as  $n$  approaches infinity). Then with Bonferroni lower bound, we have

$$P\left(\bigcap_{(ab, ac) \in \Gamma_\star} \{\hat{r}_{ab}^n > \hat{r}_{ac}^n\}\right) \approx \sum_{(ab, ac) \in \Gamma_\star} \Phi\left(\frac{\delta_c}{\sqrt{\frac{2(1-\bar{r}_{bc}^n)h(a,b,c)}{n-3}}}\right) - (|\Gamma_\star| - 1), \quad (\text{EC.6.4})$$

where  $\Gamma_\star$  can be  $\Gamma$ ,  $\Gamma_s$  or  $\Gamma_q$ . As for  $(ab, cd) \in \Gamma'$ ,  $r_{ab}$  and  $r_{cd}$  can be approximated as two independent correlations. Then we have (Asuero et al. 2006)

$$\frac{z(\bar{r}_{ab}^n) - z(\bar{r}_{cd}^n) - (z(r_{ab}) - z(r_{cd}))}{\sqrt{\frac{2}{n-3}}} \sim N(0, 1).$$

If the assumption “ $r_{ab} \geq r_{cd} + \delta_c$ ” holds for  $(ab, cd) \in \Gamma'$ , we have

$$P\left(\bigcap_{(ab,cd) \in \Gamma'_*} \{\hat{r}_{ab}^n > \hat{r}_{cd}^n\}\right) \approx \sum_{(ab,cd) \in \Gamma'_*} \Phi\left(\frac{\delta_c}{\sqrt{\frac{2}{n-3}}}\right) - (|\Gamma'_*| - 1) = 1 - |\Gamma'_*| \left(1 - \Phi\left(\frac{\delta_c}{\sqrt{\frac{2}{n-3}}}\right)\right), \quad (\text{EC.6.5})$$

where  $\Gamma'_*$  can be  $\Gamma'$  or  $\Gamma'_s$ .

Finally, with (EC.6.3), (EC.6.4) and (EC.6.5), one can easily calculate the required sample size to achieve a given PCC level. For example, if we want to guarantee that the term  $P\left(\bigcap_{(ab,ac) \in \Gamma_q} \{\hat{r}_{ab}^n > \hat{r}_{ac}^n\}\right)$  in Equation (EC.6.3) exceeds  $\alpha_q$ , then the required sample size is

$$N(\alpha_q) = \max\left\{0, \left\lfloor \frac{2z_{\alpha_q}^2}{\delta_c^2} \max_{(ab,ac) \in \Gamma_q} (1 - \bar{r}_{bc}^{N_0})h(a, b, c) + 3 - N_0 \right\rfloor\right\},$$

where  $z_{\alpha}$  is the  $\alpha$  quantile of the standard normal distribution.

## References in Online Appendices

- Asuero AG, Sayago A, González AG (2006) The correlation coefficient: An overview. *Critical Reviews in Analytical Chemistry* 36:41 – 59, URL <https://api.semanticscholar.org/CorpusID:39213560>.
- Azaïs JM, Wschebor M (2009) *Level sets and extrema of random processes and fields* (John Wiley & Sons).
- Durrett R (2019) *Probability: theory and examples*, volume 49 (Cambridge university press).
- Görder B, Kolonko M (2019) Ranking and selection: A new sequential bayesian procedure for use with common random numbers. *ACM Transactions on Modeling and Computer Simulation (TOMACS)* 29(1):1–24.
- Hashorva E, Hüsler J (2003) On multivariate gaussian tails. *Annals of the Institute of Statistical Mathematics* 55:507–522.
- Hong LJ, Jiang G, Zhong Y (2022) Solving large-scale fixed-budget ranking and selection problems. *INFORMS Journal on Computing* 34(6):2930–2949.
- Ledoit O, Wolf M (2020) Analytical nonlinear shrinkage of large-dimensional covariance matrices .
- Meng XL, Rosenthal R, Rubin DB (1992) Comparing correlated correlation coefficients. *Psychological bulletin* 111(1):172.
- Pavez E, Ortega A (2020) Covariance matrix estimation with non uniform and data dependent missing observations. *IEEE Transactions on Information Theory* 67(2):1201–1215.
- Slepian D (1962) The one-sided barrier problem for gaussian noise. *Bell System Technical Journal* 41(2):463–501.
- Zhong Y, Hong LJ (2022) Knockout-tournament procedures for large-scale ranking and selection in parallel computing environments. *Operations Research* 70(1):432–453.